Er doped silicon structures for photonic applications

M. Stepikhova

Institute for Physics of Microstructures RAS,
Nizhny Novgorod, Russia

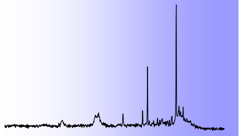

OUTLINE

1. Si-based photonics. Motivation.
2. Doping with the rare earth elements. An introduction.
3. Er doped Si and SiGe structures grown by the sublimation MBE technique
    - Structure growth & characterization
    - Luminescent properties of Si:Er and SiGe:Er structures
4. Applications
    - Light-emitting diodes
    - Structures for laser realization
5. Conclusions

Si-based photonics. Motivation.

Photonics is the technology associated with signal generation, processing, transmission and detection, where the signal is carried by photons (i.e. light).

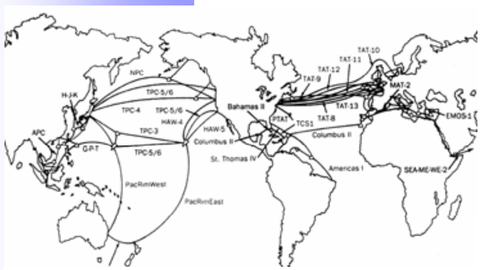

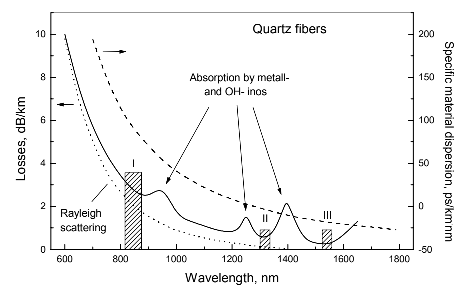

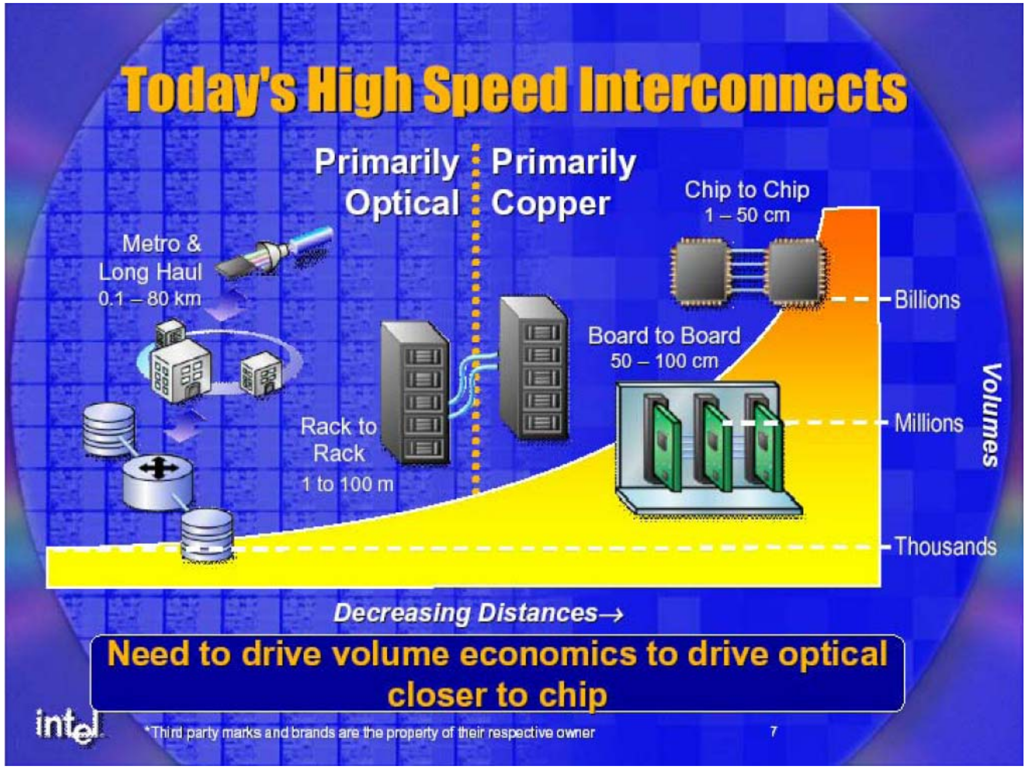

<u>Motivation to Si-based photonics:</u>

- Emerging problems of modern microelectronics – "intra- and interconnects bottleneck"
- Rapid development of fiber-optic communication systems

Si-based photonics. Motivation.

Power density required to operate a chip

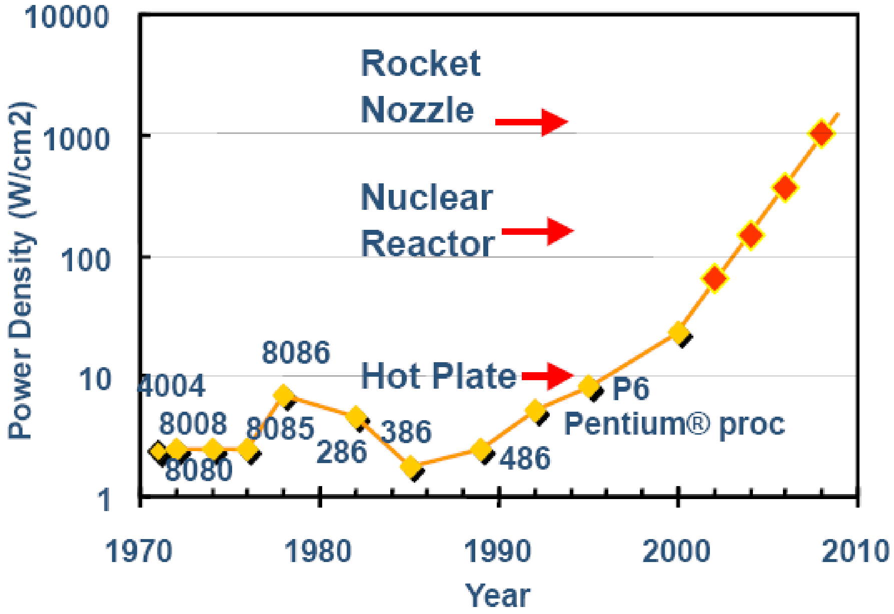

Emerging problems of modern microelectronics:

Electrical intra- and interconnects bottleneck:

- limiting speed and signal integrity
- increasing power density and heat dissipation problem

Interconnects length on a chip

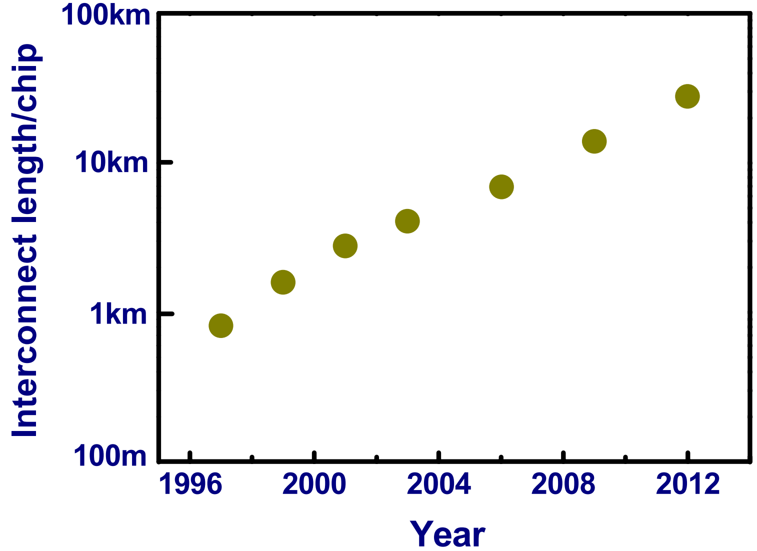

Si-based photonics. Motivation.

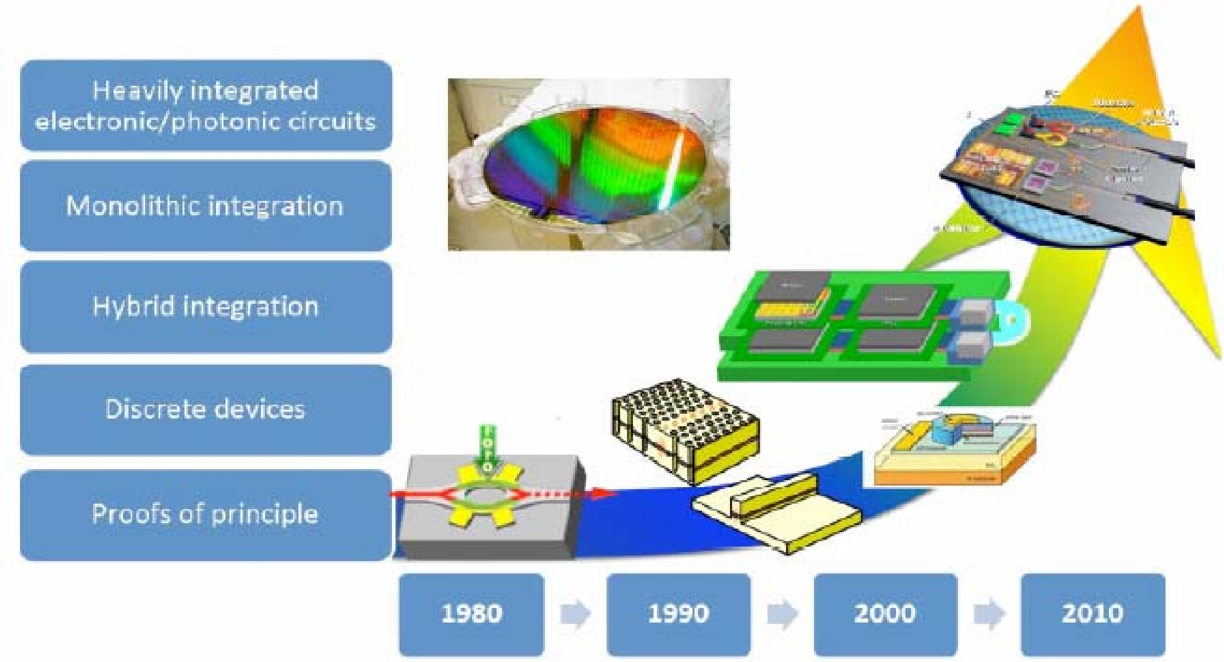

Figure 1 (online color at: www.lpr-journal.org) Schematic evolution of silicon photonics versus years. The various diagrams are courtesy of Ghent University and Intel Corp.

N. Daldosso et al. Laser & Photon. Rev. (2009)

The first end-to-end Si photonic integrated link (INTEL 2010)

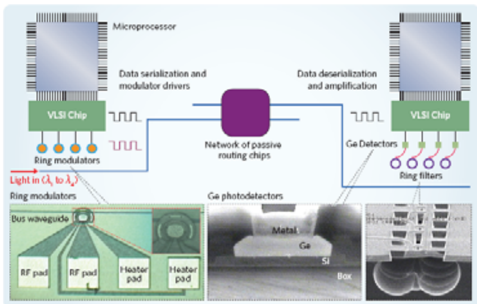

Sub-μm waveguide technology for chip-scale communication (Kotura 2011)

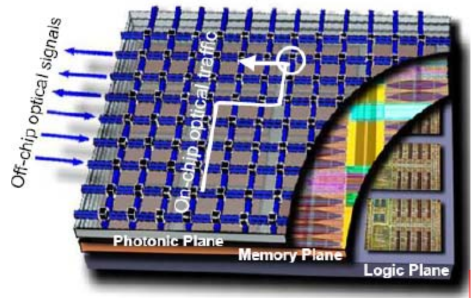

Vision for 2018 – optically connected 3D supercomputer chip (IBM)

Si-based photonics. Motivation.

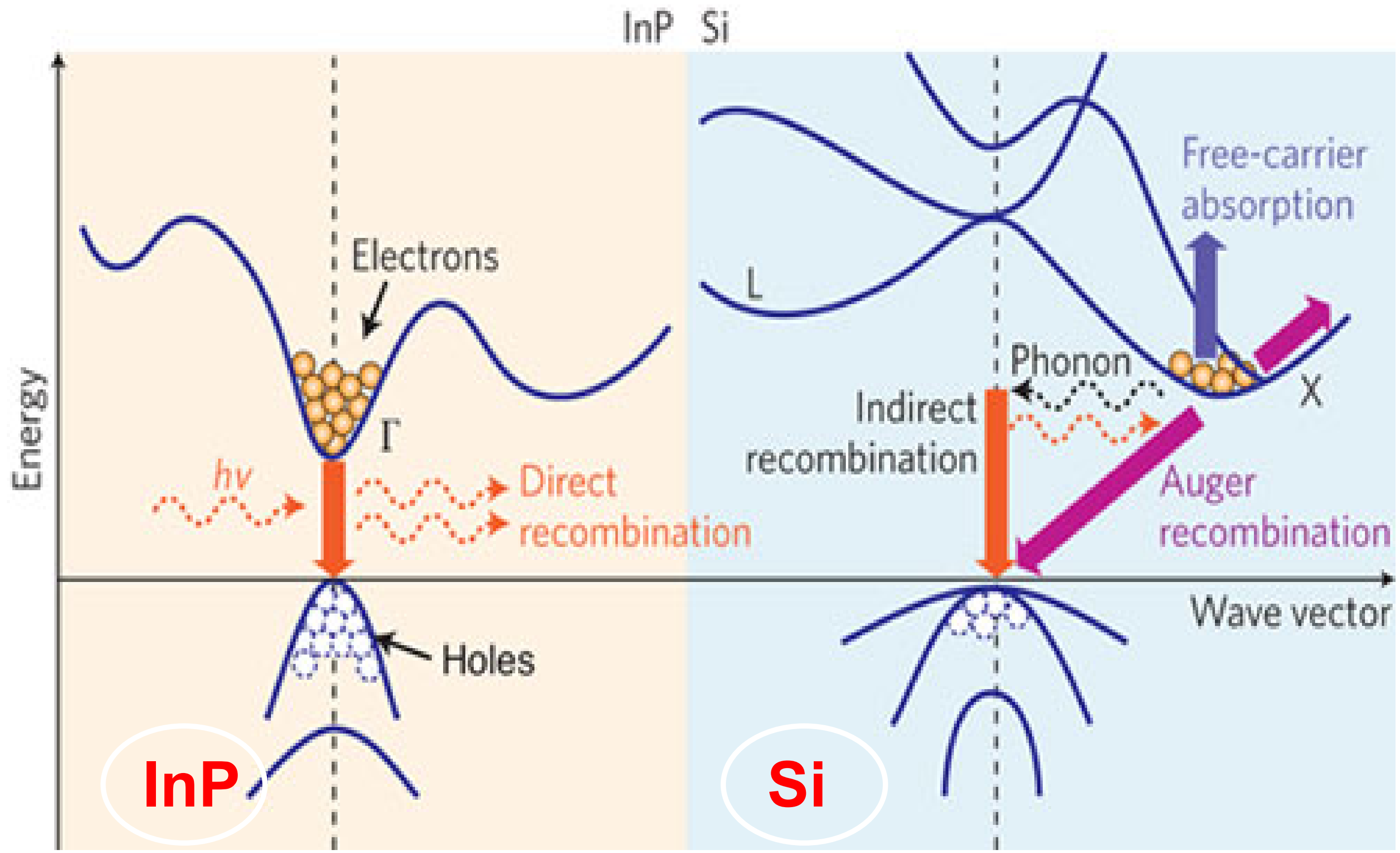

Di Liang, J.E. Bowers, Nature Photonics, 4, 511 (2010)

Energy band diagrams and major carrier transition processes in InP and silicon crystals. In a direct band structure (such as InP, left), electron-hole recombination almost always results in photon emission, whereas in an indirect band structure (such as Si, right), free-carrier absorption, Auger recombination and indirect recombination exist simultaneously resulting in little photon emission.

Light-emitting structures on Si basis

Hybrid A_3B_5/Si structures

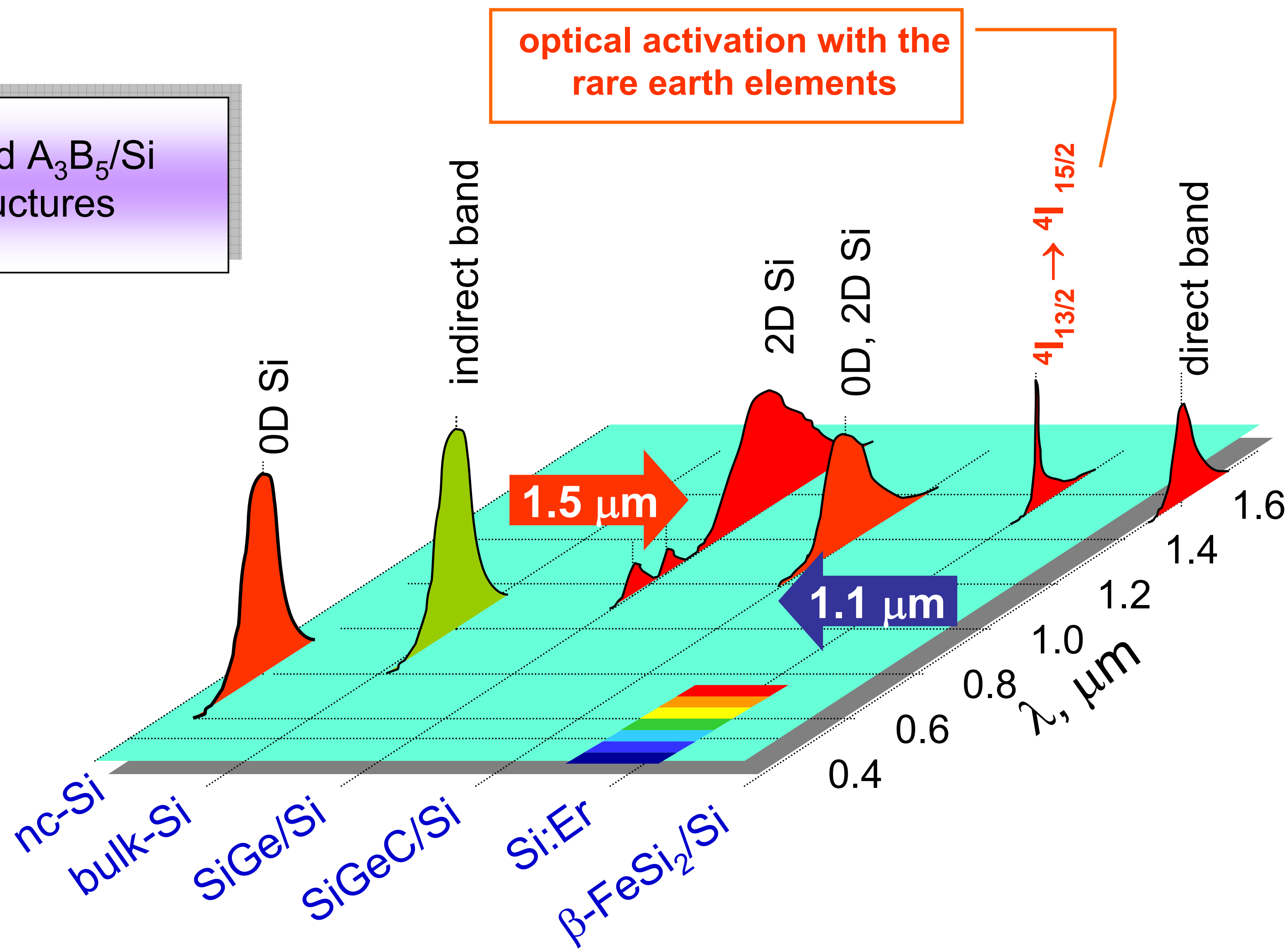

Optical activation of Si by the rare earths elements

Rare earths elements		Silicon
Effective optical transitions	⇄	Advanced electrical properties

$\varepsilon_{g,Si}$ = 1,12 eV

at T=300 K

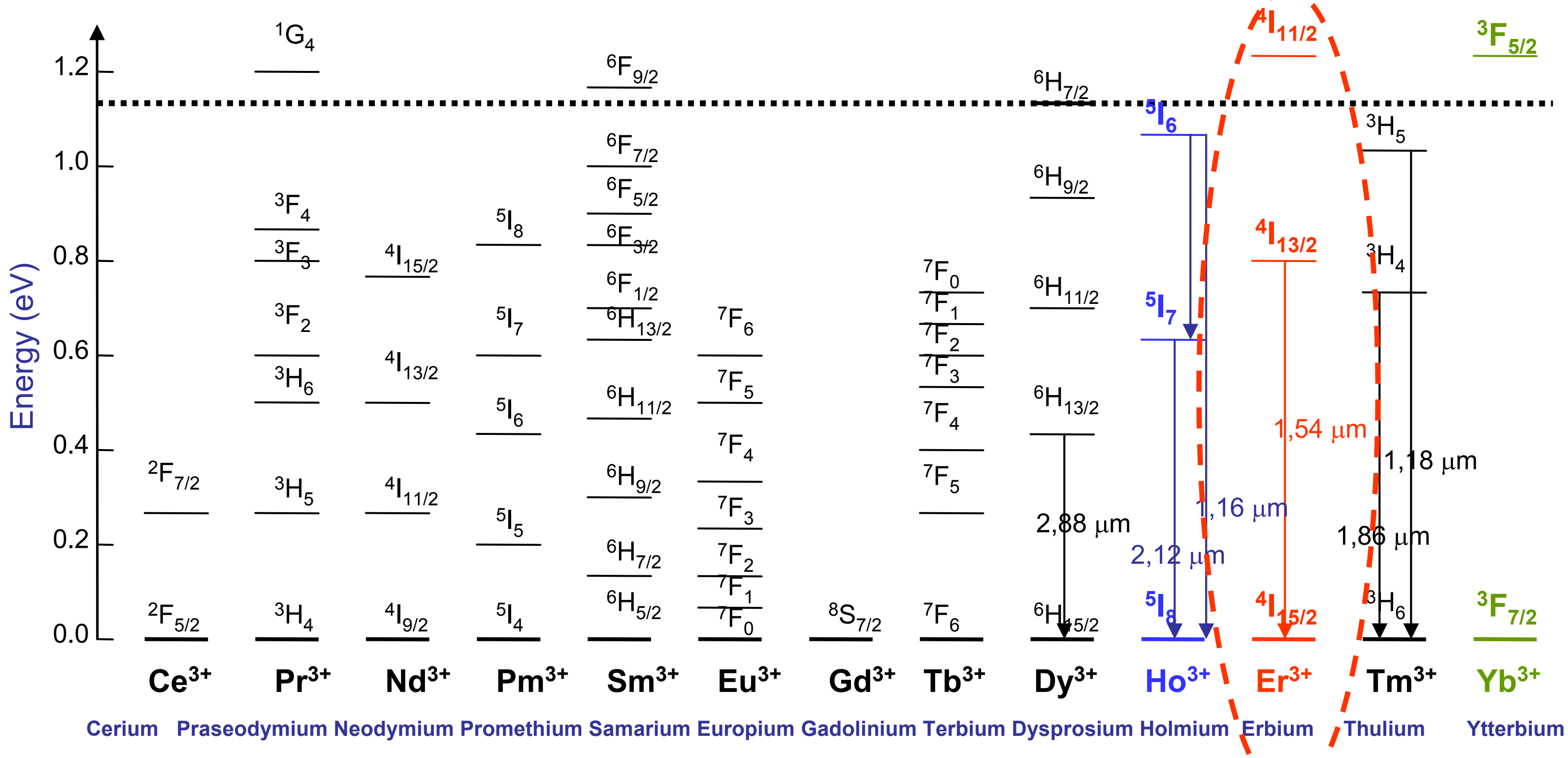

In the majority, the rare earths elements are characterized by the high efficiency of their intrashell optical transitions. The diagram shows the energies of 4f-shell transitions for rare earth elements in comparison with the Si bandgap energy.

H. Ennen et al. Appl. Phys. Lett., vol. 43, p. 943, 1983.

Energy level diagram of Er^{3+} ions in the crystal and magnetic fields

The energy levels of the rare earth ions split in the crystal and magnetic fields. The crystal field splitting depends on the crystal field symmetry.

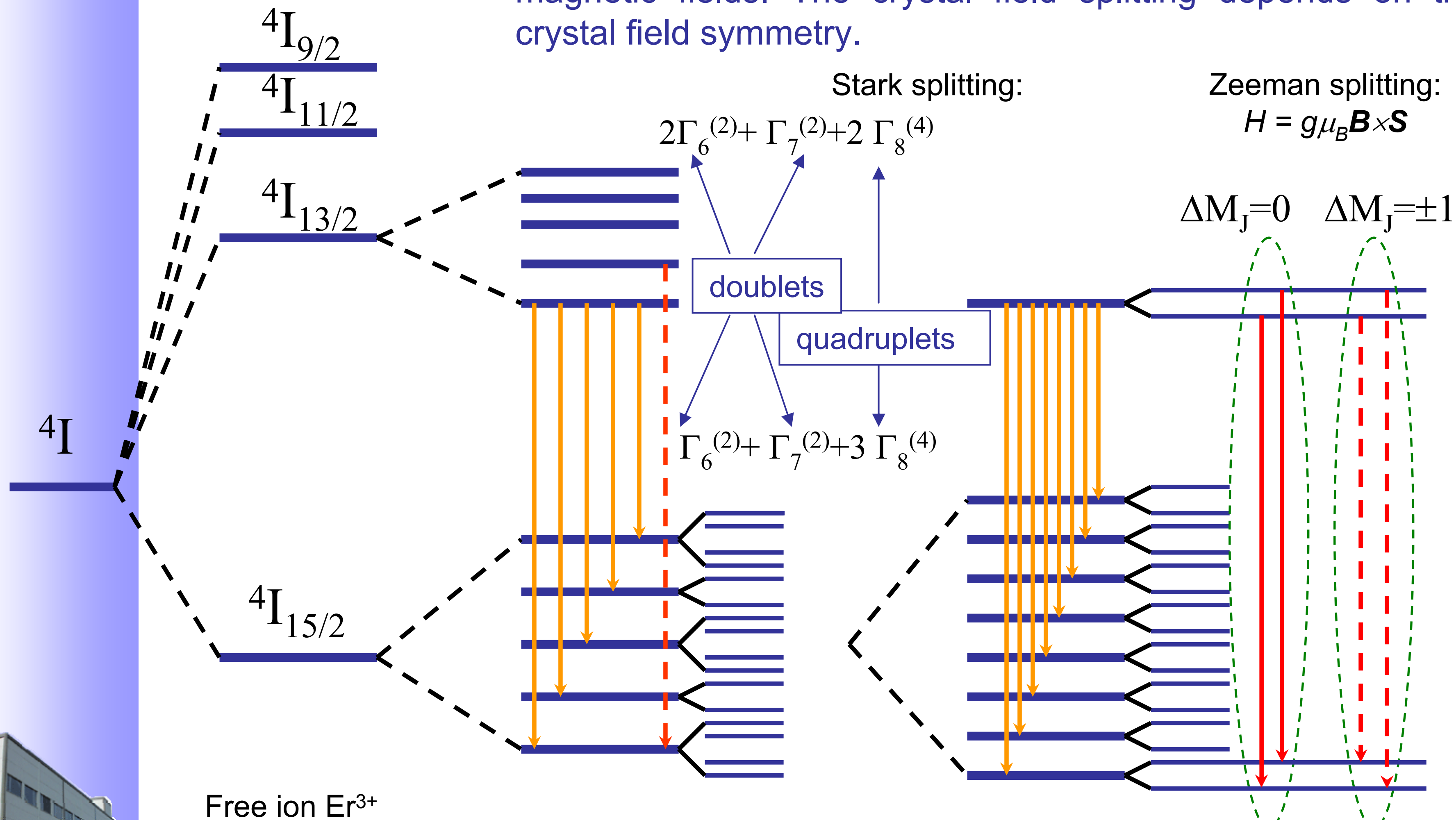

Energy position of the rare-earth impurity 4f levels in semiconductors

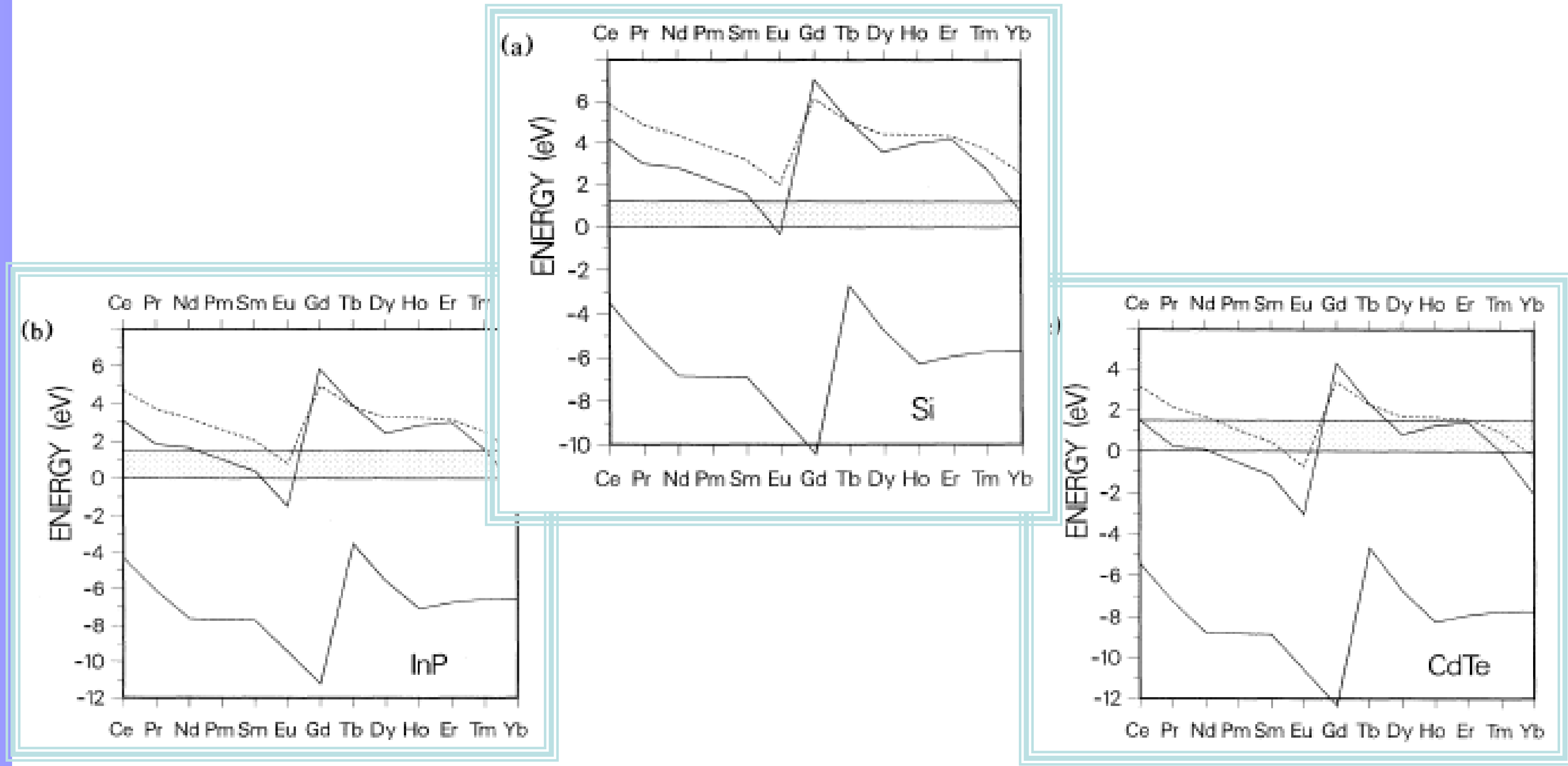

FIG. 1. (a) 4f levels for substitutional rare-earth impurities in silicon. These levels are positioned with respect to the band gap (horizontal lines), the top of the valence band being at the origin of these energies. The lowest level and the highest level plotted with a continuous line are, respectively, the $\epsilon_{4f}(3.5)$ and $\epsilon_{4f}(2.5)$ levels calculated with the Hartree-Fock data of Ref. [18a] for rare-earth atoms. The level plotted with a dashed line is the $\epsilon_{4f}(2.5)$ level calculated with the experimental data of the same reference to account for the correlation energy. (b) Same as (a) for InP. (c) Same as (a) for CdTe.

C. Delerue, M. Lannoo, Phyis. Rev. Lett., vol. 67, p. 3006, 1991.

Energy transfer processes in Er doped silicon

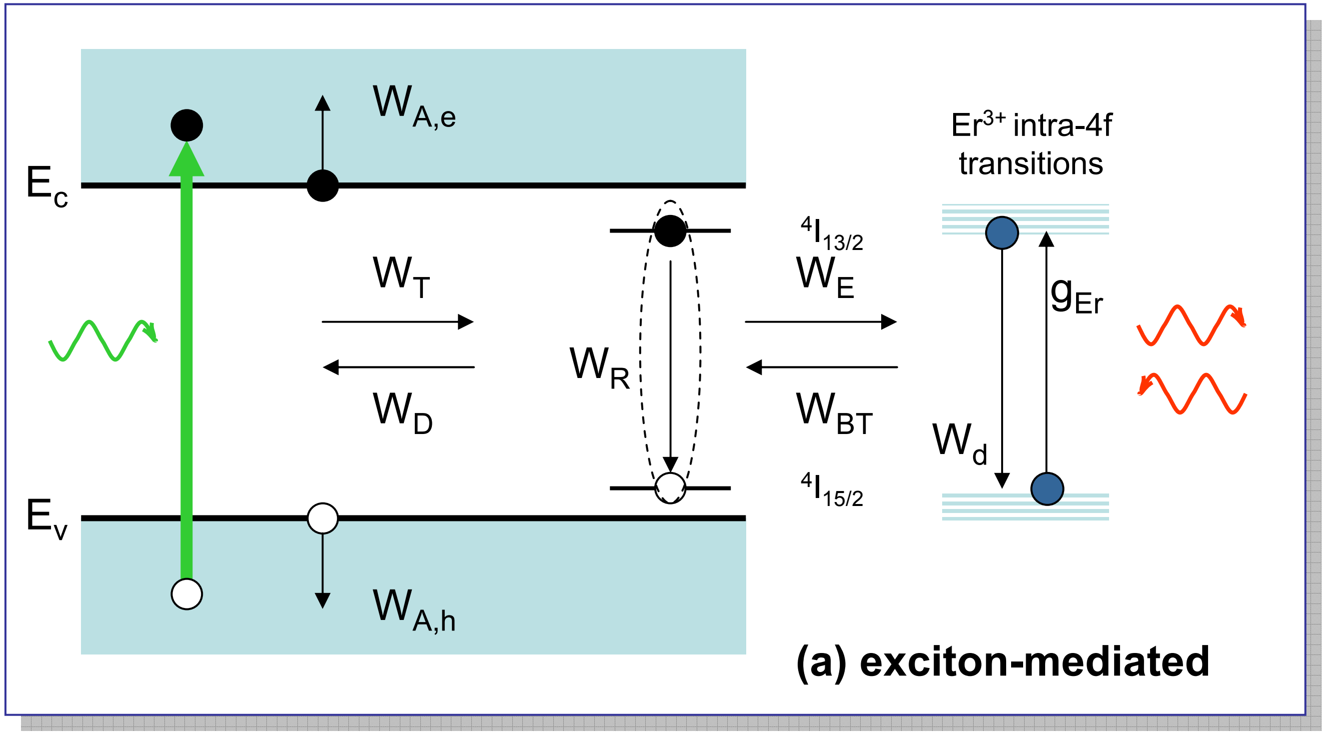

The excitation mechanism of Er^{3+} ions in Si under optical pumping is the exciton-mediated mechanism, where an optically generated electron-hole pair forms an exciton that can be trapped by the Er-related level in Si bandgap and then recombine nonradiatively transferring their energy to Er^{3+} ion. In the reverse process, an optically excited Er^{3+} ion decays nonradiatively creating a bound exciton, which can dissociate with the formation of free electron-hole pair. Exciton trapping (W_T) and dissociation (W_D), Er^{3+} excitation (W_E) and energy backtransfer (W_{BT}) mechanisms are shown on the scheme by horizontal arrows.

Auger quenching and impact excitation of Er ions

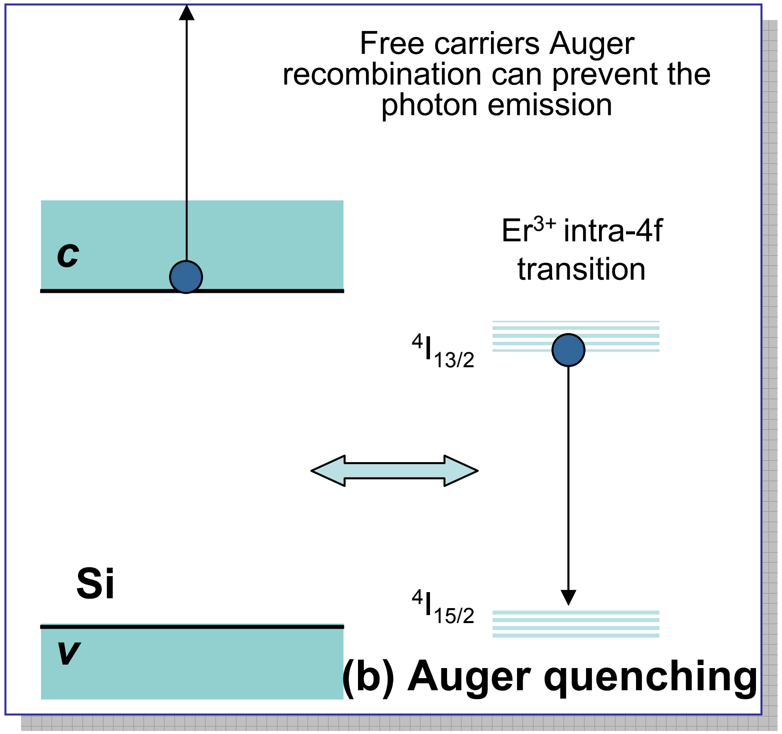

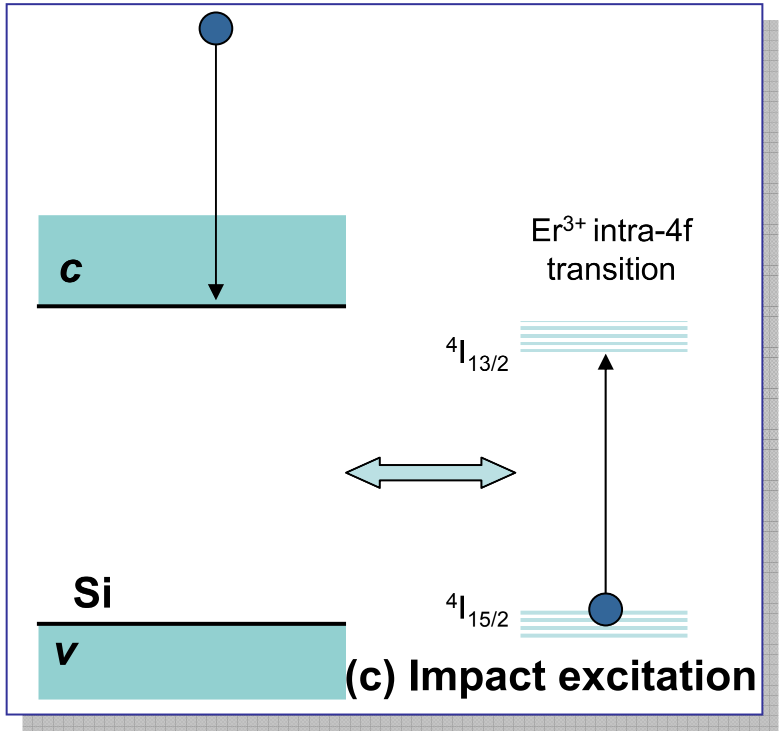

Free carriers Auger recombination is the main de-excitation mechanism of Er^{3+} ions in Si structures under high excitation conditions, though the impact excitation can be successfully used in devices.

Er incorporation in Si

Solid solubility of Er in Si ~ 10^{16} cm^{-3} at 1300°C → nonequilibrium incorporation methods (ion implantation, MBE, CVD) have to be used.

Concentration limit set by the onset of Er precipitation in ion implanted structures - $5 \cdot 10^{17}$ cm^{-3}

[D.J. Eaglesham et al. APL. 58, 2797 (1991)]

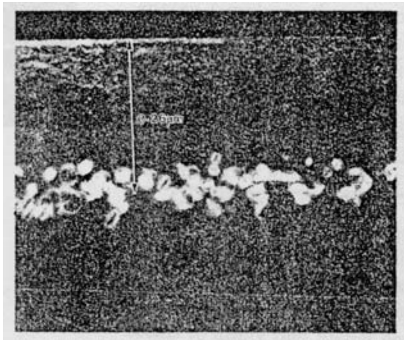

Er implanted Si: implantation dose – $1.2 \cdot 10^{14} cm^{-2}$, energy 500keV, implantation was carried out at 130ºC, annealing at 900ºC, 30min.

Strong interaction of Er impurity with O within the Si matrix:

(i) increases the effective solubility of Er in Si

[S. Coffa et al., Phys.Rev.B 48, 11782 (1993)]

(ii) inhibits Er segregation during solid phase and molecular beam epitaxy

[J.S. Custer et al., JAP 75, 2809 (1994), R. Serna et al., APL 66, 1385 (1995)]

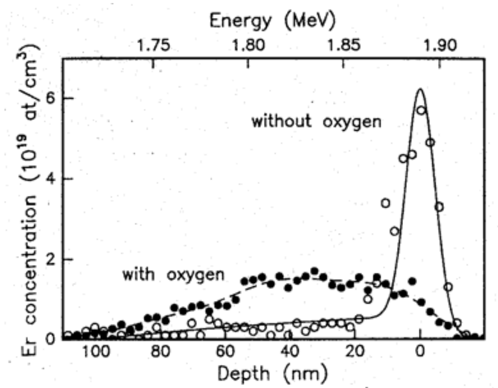

"Coimplantation of Er and O in the ratio of 1:10 enable to incorporate up to <u>10^{20} Er cm^{-3}</u> in crystalline Si" [S. Coffa et al., MRS Bull. **23**, 25 (1998)]

Concentration of the optically active Er centers ~ 10% of the total amount of Er

Er doped Si structures grown by the sublimation MBE technique

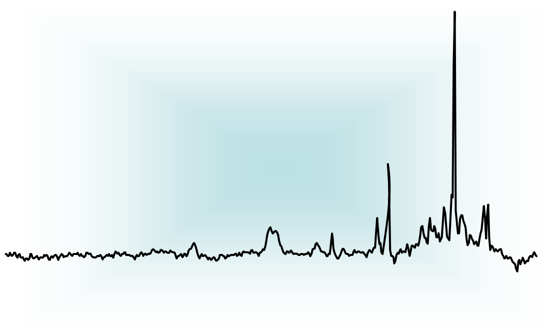

Sublimation molecular beam epitaxy

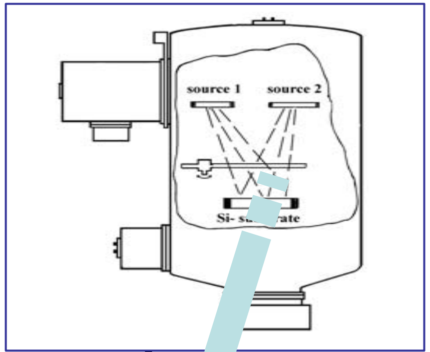

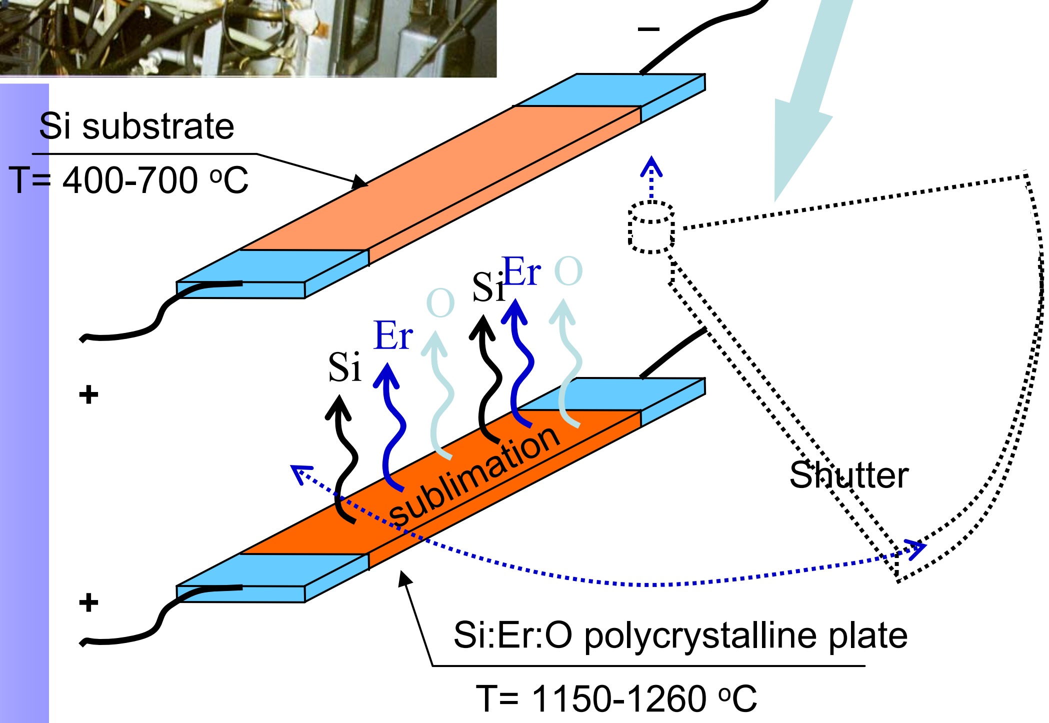

All structures were grown by the SMBE method, designed and applied for the first time in Nizhny Novgorod. Today we may be a unique group which grows structures by such a method.

Advantages of
Sublimation MBE method:

- High doping level ($\leq 10^{21}$ cm^{-3});
- Precise control of the doping profiles;
- Capability to grow the uniformly doped structures as well as the structures with the desired impurity profiles;
- Growth of the high-pure Si layers with the residual doping level < $2 \cdot 10^{13}$ cm^{-3};
- Fast and variable growth rate - 0.2-5 μm/h;
- Inexpensive installation.

M. Stepikhova et al., Acta Physica Polonica A (1998)

Sublimation MBE in germane gas atmosphere: growth of Si/SiGe:Er structures

The specificity of the growth method in germane (GeH_4) gas atmosphere consists in the combination of the standard SMBE procedure with the elements of CVD. In this method, the fluxes of Si and Er are produced by the sublimation of the appropriate Er-doped and Si sources, where Ge doping occurs through the pyrolysis reaction of the GeH_4 gas nearby the current-heated Si substrate.

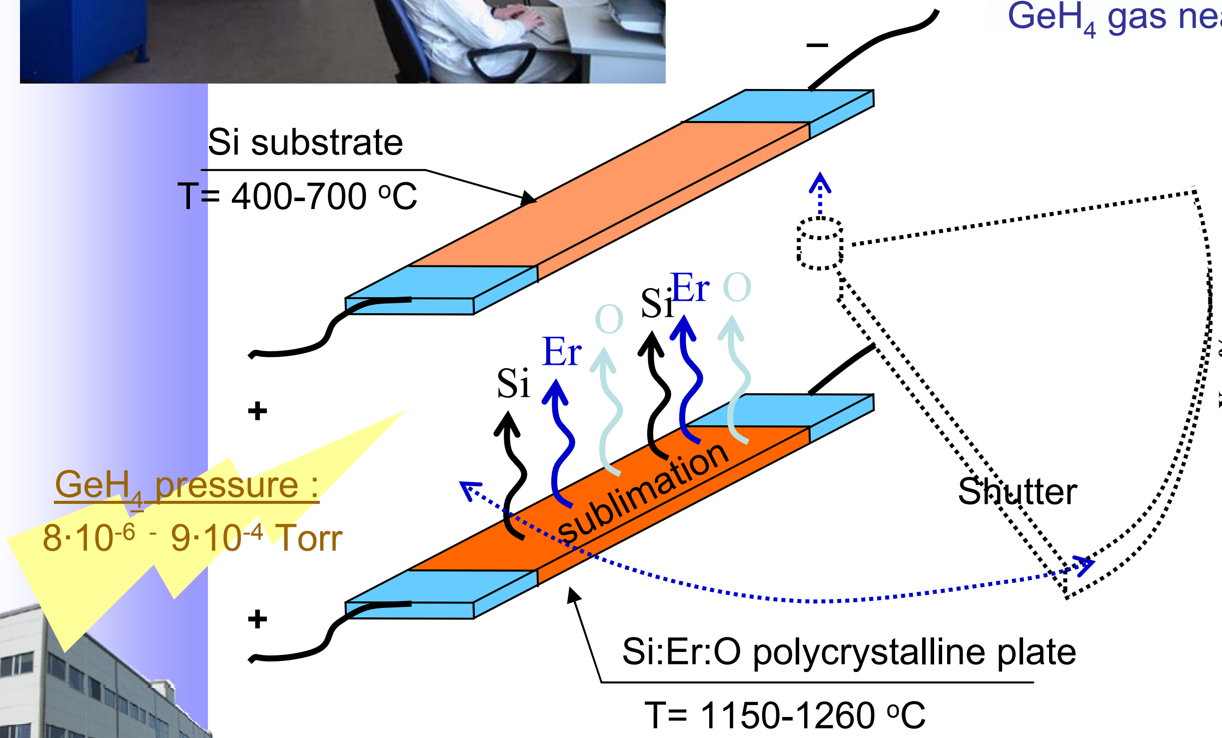

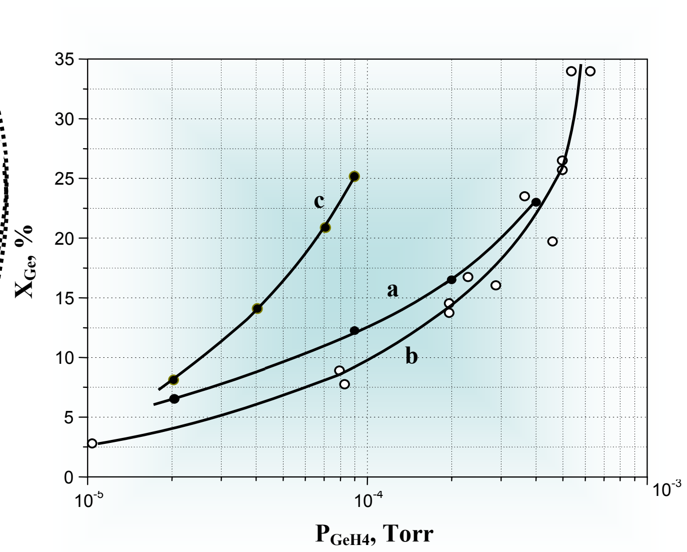

a) T_{sub}=500°C, V_{growth}=5 nm/min (T_{source}=1300°C),
b) T_{sub}=500°C, V_{growth}=1 nm/min (T_{source}=1220°C),
c) T_{sub}=550°C, V_{growth}=1 nm/min (T_{source}=1220°C).

V.G. Shengurov et al., Semiconductors (2002)

Parameters of Si:Er and SiGe:Er structures grown by sublimation MBE

⇨ ***source:***	polycrystalline Si:Er (Er - up to 10^{21} cm $^{-3}$)
⇨ ***growth conditions:***	substrates – CZ-Si (100), T_{gr}= 300-700 °C, growth rate – 0.2- 5 μm/h
⇨ ***post annealing:***	T_{ann}= 700-900° C (in H_2 or in vacuum)

Layer parameters:

⇨ ***Si/Si:Er structures:***	$d_{Si:Er}$ = 2 nm - 3 μm [Er] ~ (0.5-5)·10^{18} cm $^{-3}$ - SIMS data [O] ~ (1-10)·10^{19} cm $^{-3}$ - SIMS data $n_{300K} \leq 10^{18}$ cm $^{-3}$ - C-V, Hall data $\chi_{min<100>}$ = 3-5% - RBS data
⇨ ***Si/SiGe:Er structures:***	$d_{SiGe:Er}$ = 10 nm - 2.5 μm Ge content ≤ 40% - XRD data [Er] ~ (0.1-5)·10^{18} cm $^{-3}$ - SIMS data [O] ~ (2-20)·10^{18} cm $^{-3}$ - SIMS data

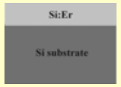

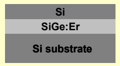

Z.F. Krasilnik et al. *in Towards the First Silicon Laser,* NATO Science Series (2003).
L. Krasilnikova, et al., Phys. Stat. Sol. (c), vol. 8, pp. 1044 (2011).

Periodic Er-doped Si and Si/SiGe structures

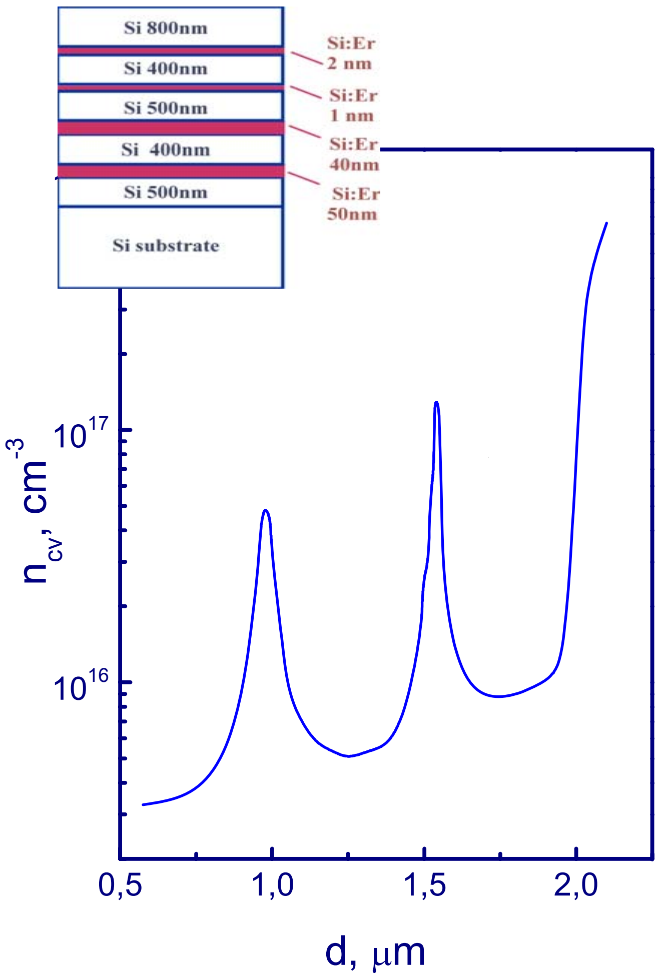

CV-profile of the selectively doped Si:Er structure # 990.
The thicknesses of Er doped layers: 20 Å, 10 Å, 400 Å, 500 Å.

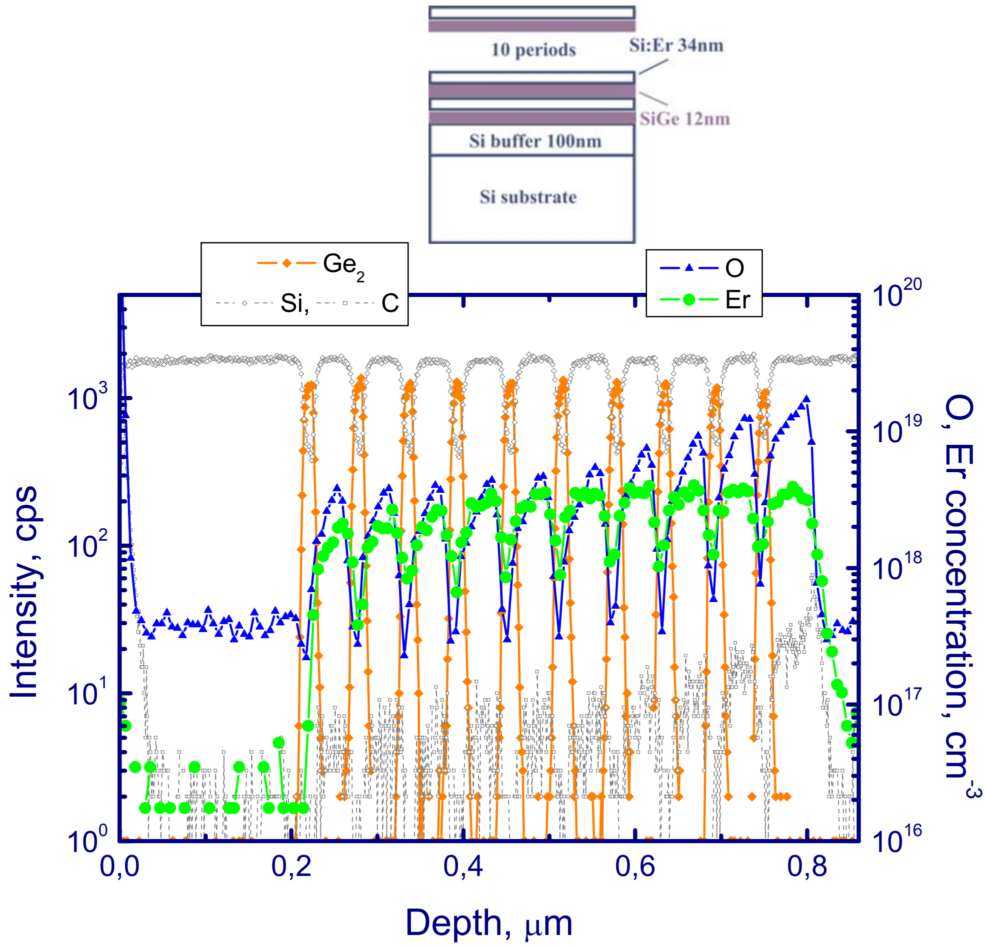

SIMS-profile of periodic Si:Er/SiGe structure # 619.
The thicknesses of Si:Er and SiGe layers: 34 nm, 12 nm.

Optically active Er centers in PL response of Si:Er structures grown by the sublimation MBE

"As grown" structures:

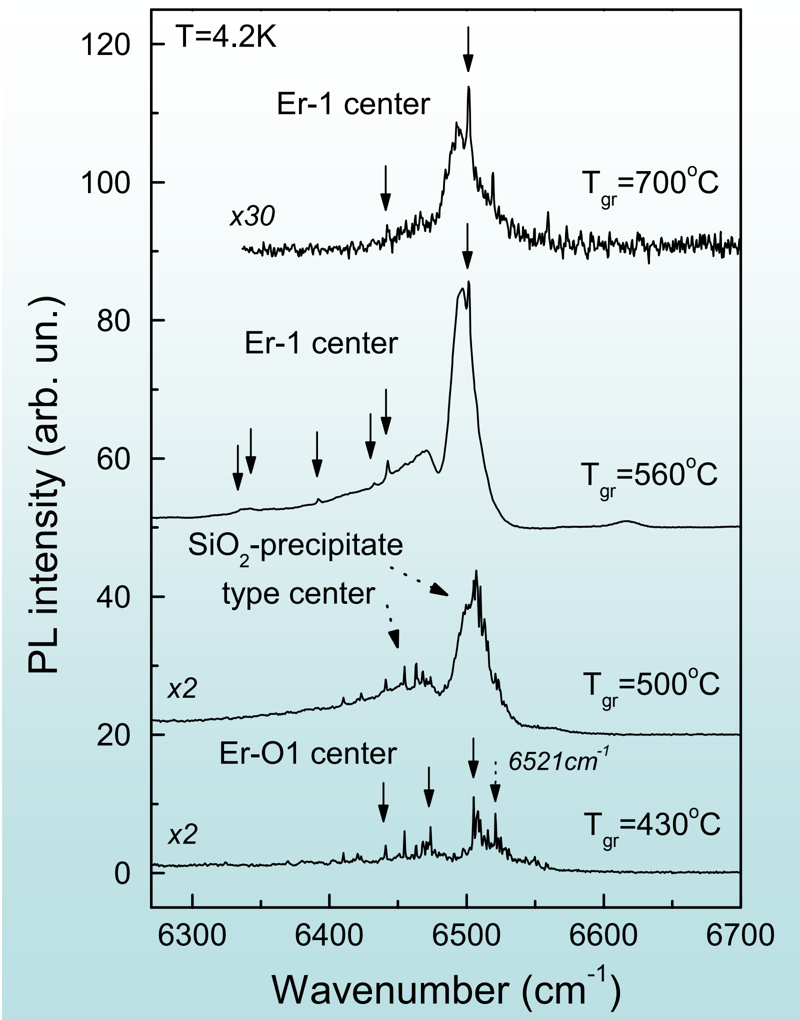

The center formation depends on the growth temperature and annealing conditions.

Formation of the centers identical to those identified in Er implanted Si has been observed.

The novel optically active center, namely the center Er-1, was observed in the sublimation MBE grown structures. This center starts to form in Si:Er layers at the growth temperature of approx. 560°C.

A.Yu. Andreev et al., J. of Cryst. Growth (1999)
M.V. Stepikhova et al., Thin Solid Films (2001)

Optically active Er centers in PL response of Si:Er structures grown by the sublimation MBE

The role of an annealing procedure:

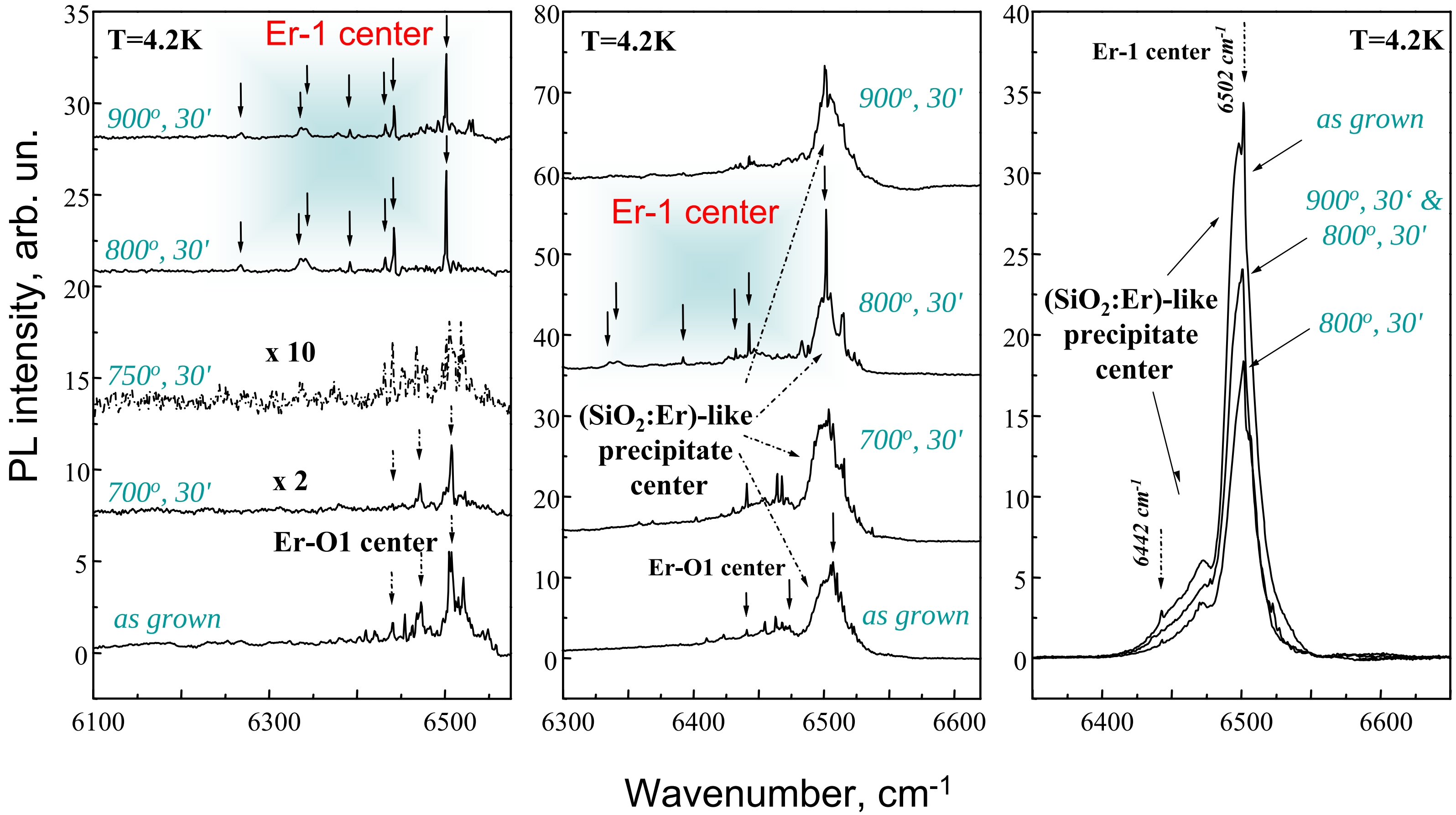

a) T_{gr}= 430°C   b) T_{gr}= 500°C   c) T_{gr}= 560°C

M. Stepikhova et al., Mat. Sci. & Eng. (2001)
Z.F. Krasilnik et al. in Towards the First Silicon Laser, NATO Science Series (2003)

Er-1 center in Si:Er/Si structures grown by the sublimation MBE

Preferential formation of a single type centers in SMBE structures - optically active center Er-1

T = 4.2 K

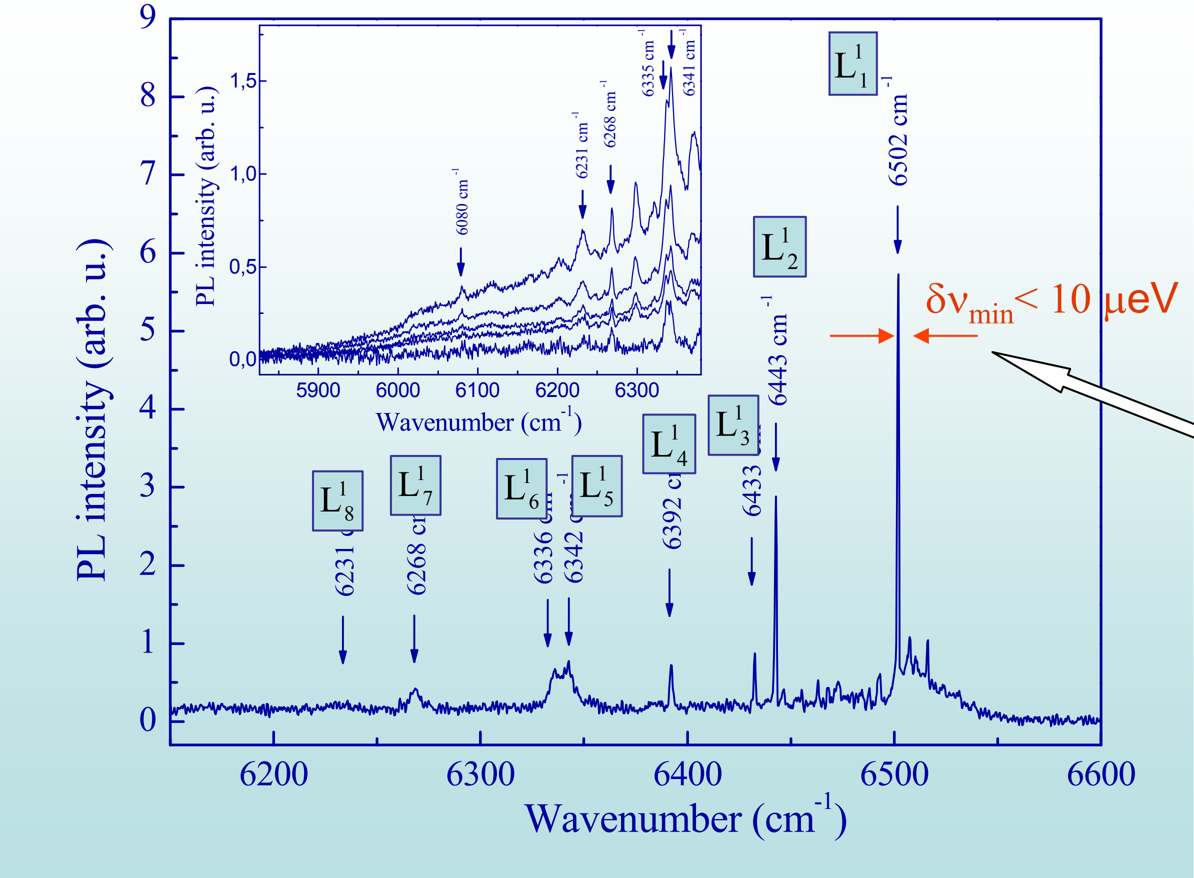

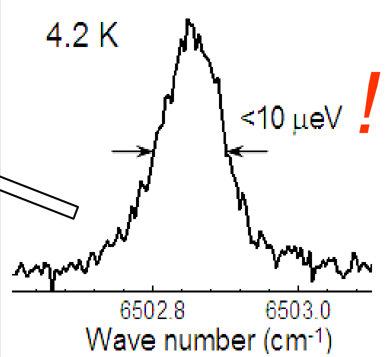

High-resolution scan of the most intense L^1_1 line in the Er-1 series.

It is the least value of the PL peak width, which was observed in silicon.

B.A. Andreev et al., Bulletin RAS, Ser. Phys. (2000)
N.Q.Vinh et al., Physica B (2001)

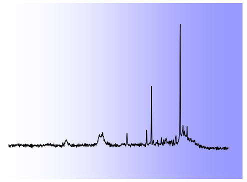

Position and intensity ratio of PL lines in Er-1 series

We have every reason to believe that all peaks in Er-1 series relate to one center:

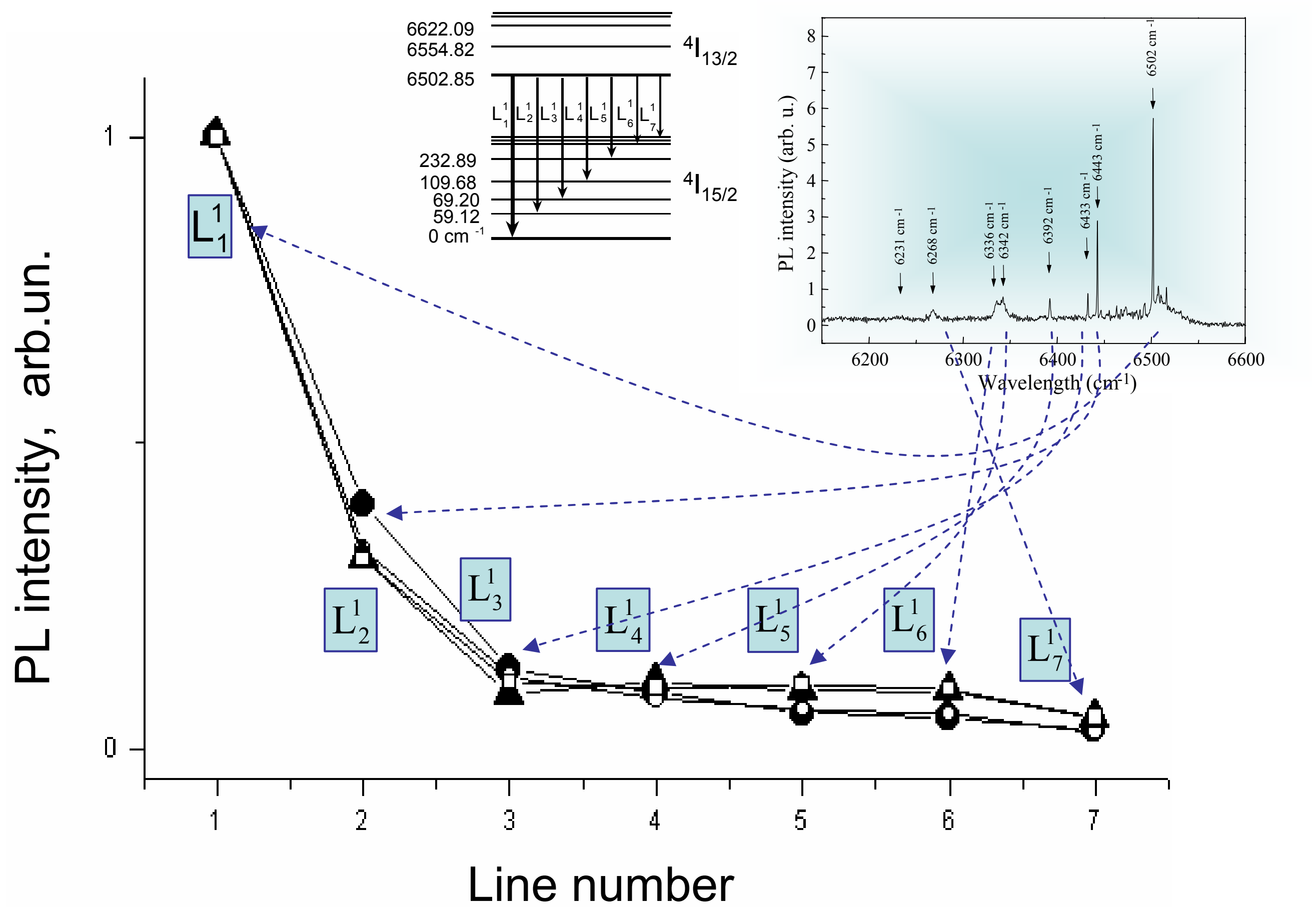

1. The position and intensity ratio of PL lines are well reproducible in various samples obtained under different growth conditions.

Dependence of Er-1 lines intensity on the excitation power

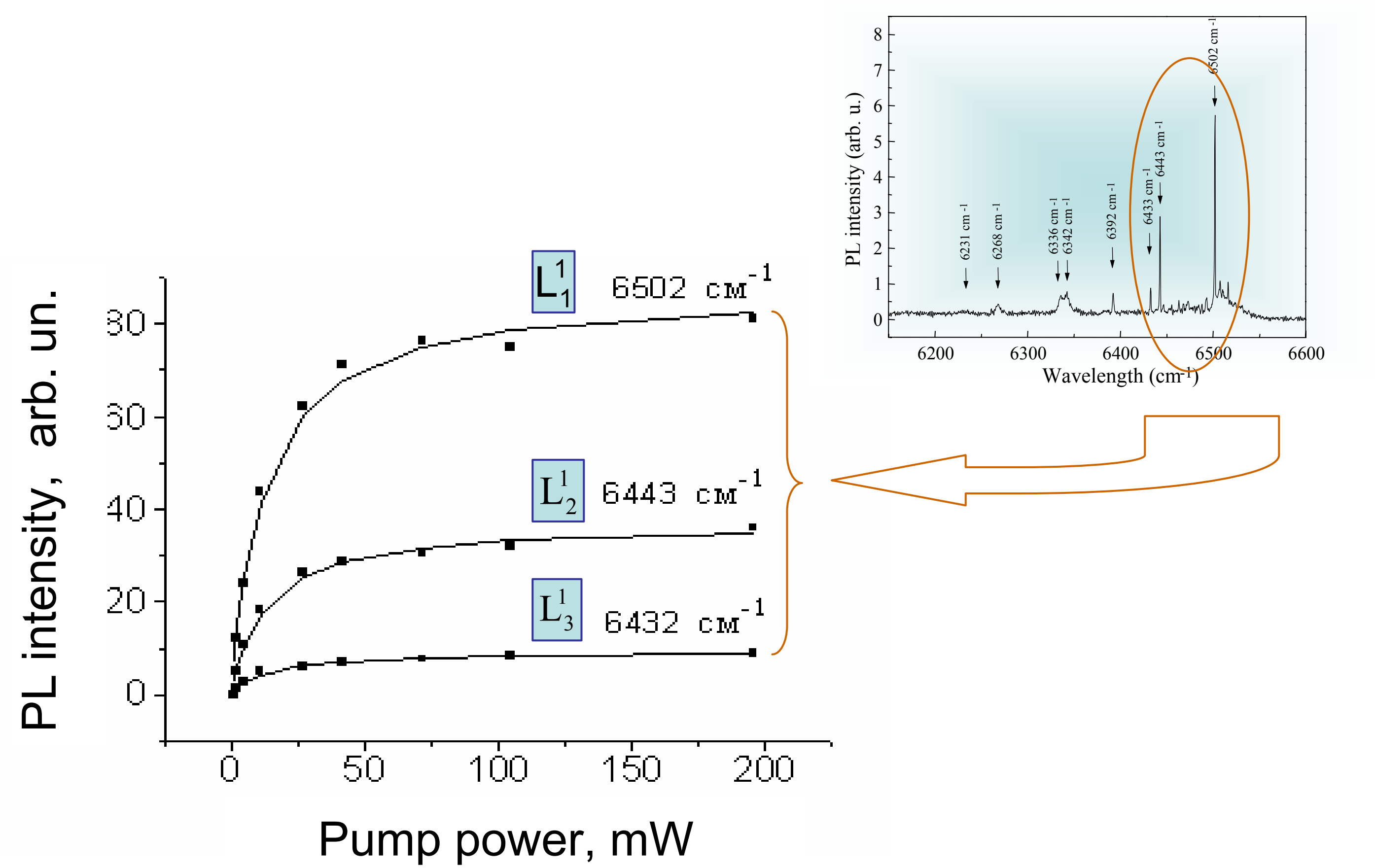

2 Identical dependence of the luminescence intensity on the excitation power has been obtained for all lines in Er-1 series.

Temperature dependence of Er-1 lines

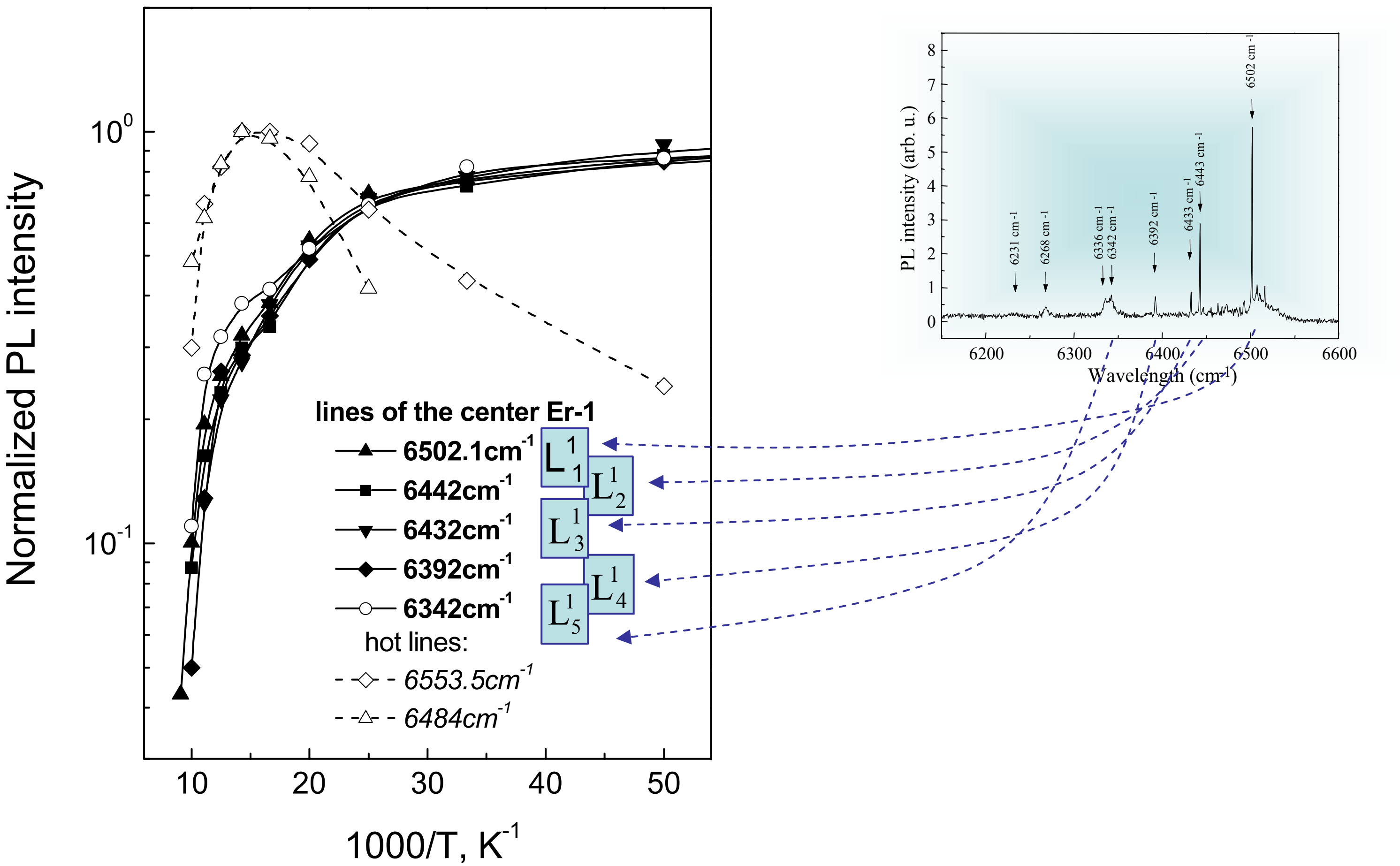

3 Identical temperature behavior has been observed for all lines in Er-1 series.

Satellite “hot lines” at elevated temperatures

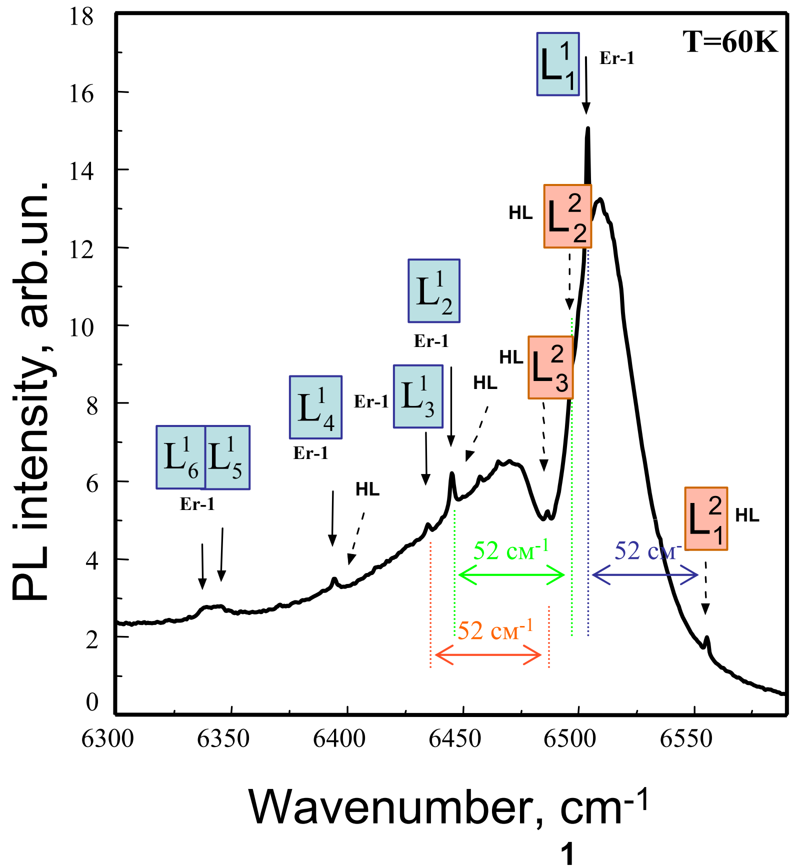

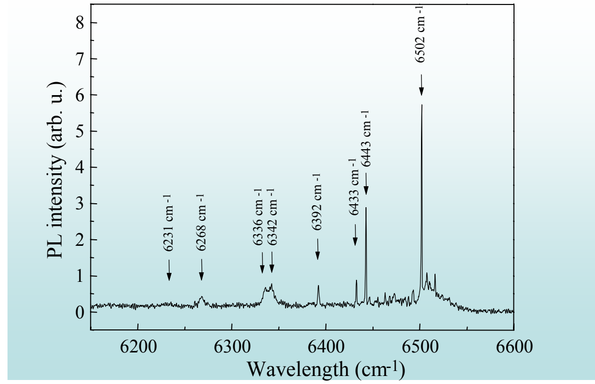

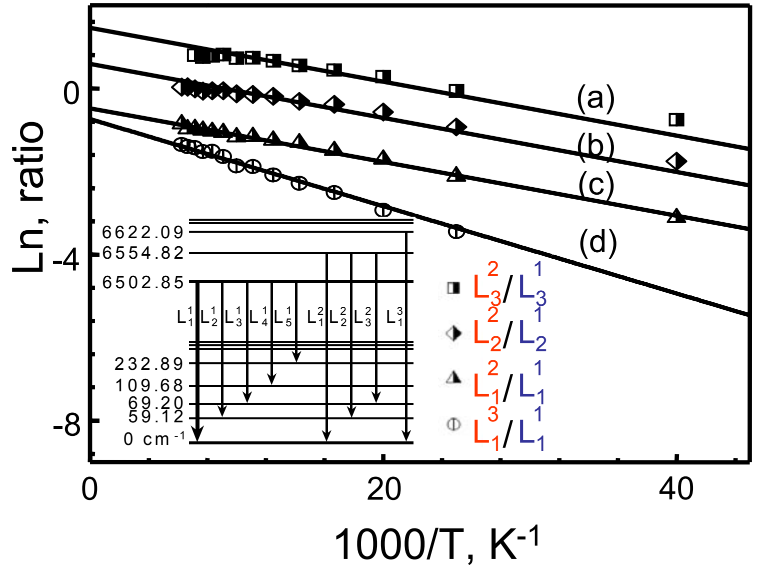

4 All of the main PL lines are accompanied by the “hot” ones that correspond to the transitions from the upper levels of excited $^4I_{13/2}$ multiplet.

Zeeman splitting: main PL line L_1^1

Zeeman splitting observed for the main L^1_1 PL line at 4.2 K in magnetic field of 5.25 T oriented along the crystallographic directions: (a) B||<100>, (b) B||<111> and (c) B||<011 >.

Inset in this figure: angular dependence of the Zeeman effect measured for the L^1_1 line at B = 5.25 T along the (011) crystallographic plane.

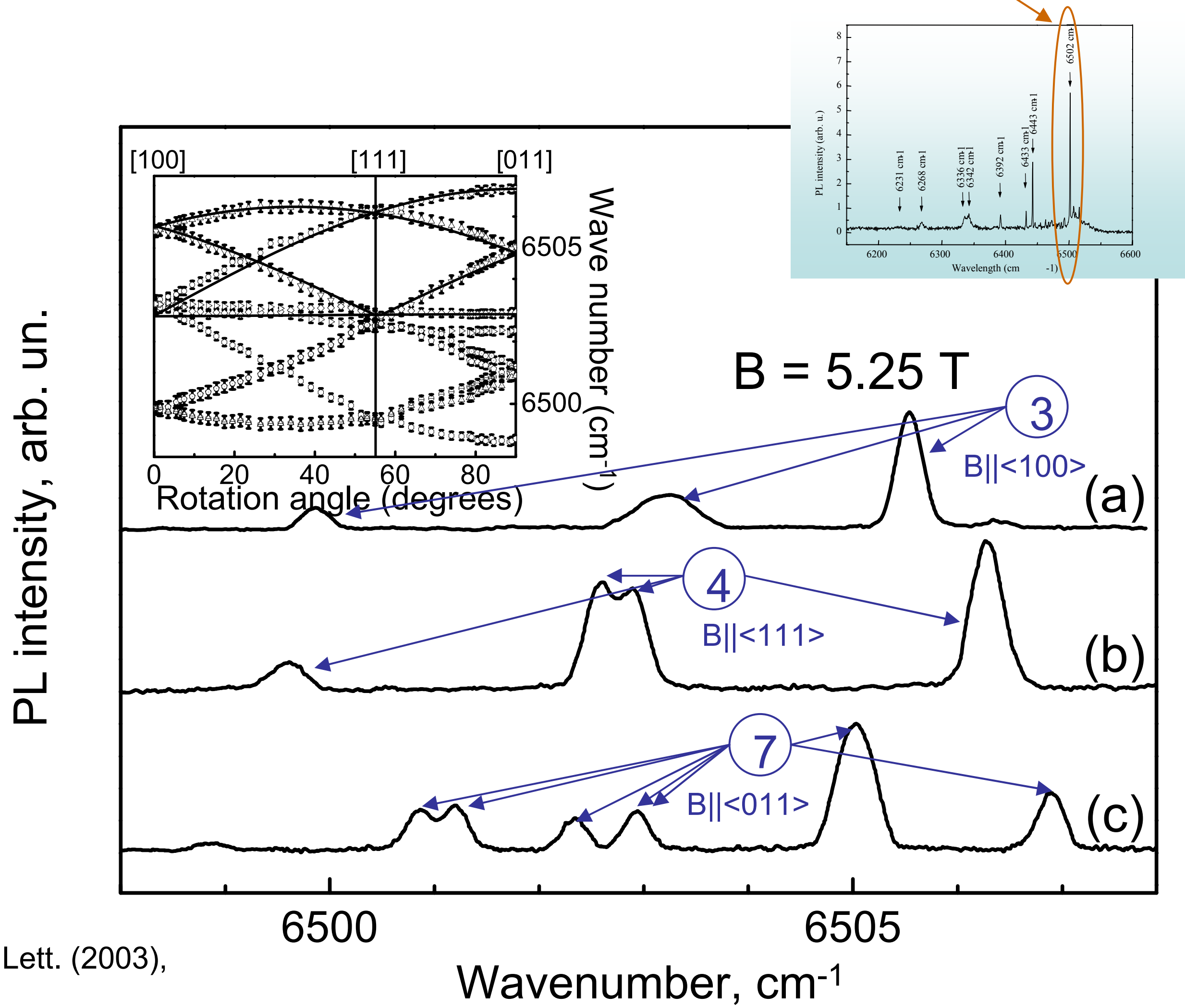

N.Q. Vinh et al., Phys. Rev. Lett. (2003), Phys. Rev. B (2004)

$g^{(1)}$ = [0 ± 0.1; 18.4 ± 0.8; 0 ± 0.1], $G^{(1)}$ = [0 ± 0.1; 15.1 ± 0.8; 0 ± 0.1]

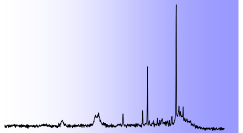

Microscopic structure of the Er-1 centre

- Line L_1^1 - B // <100>: 3 components
- Line L_1^1 - B // <011>: 7 components
- Line L_1^2 - B // <100>: 4 components
- Line L_1^2 - B // <011>: 5 components

Symmetry → Not cubic

Symmetry → Orthorhombic I (C_{2V})

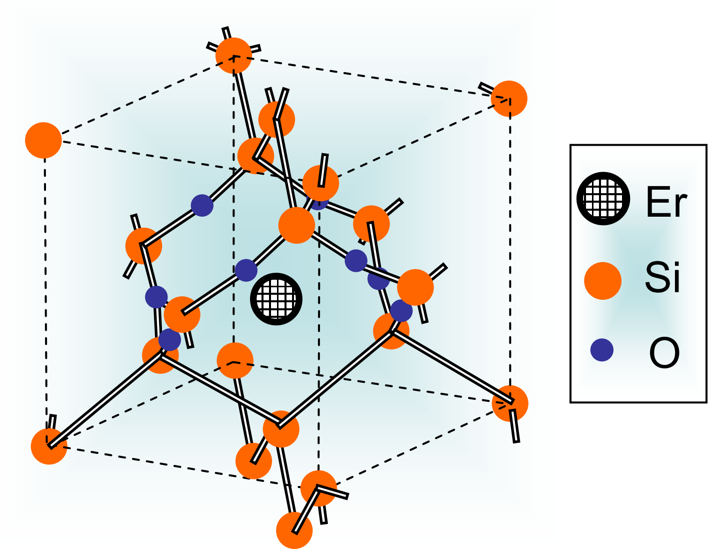

The microscopic structure of Er-1 center consists of an Er^{3+} ion occupying a T_d interstitial site in Si lattice with 8 oxygen atoms in the direct surrounding.

N.Q. Vinh et al., Phys. Rev. Lett. (2003), Phys. Rev. B (2004)

PL response of Si/Si$_{1-x}$Ge$_x$:Er structures

High resolution PL spectra

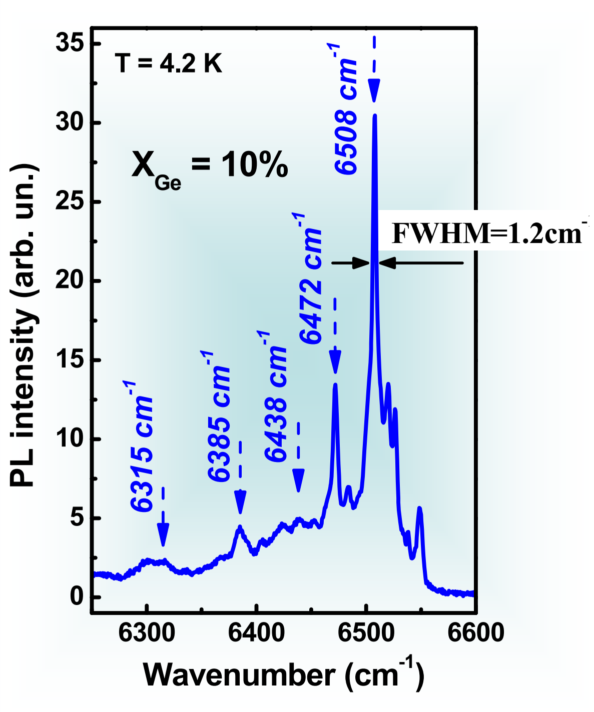

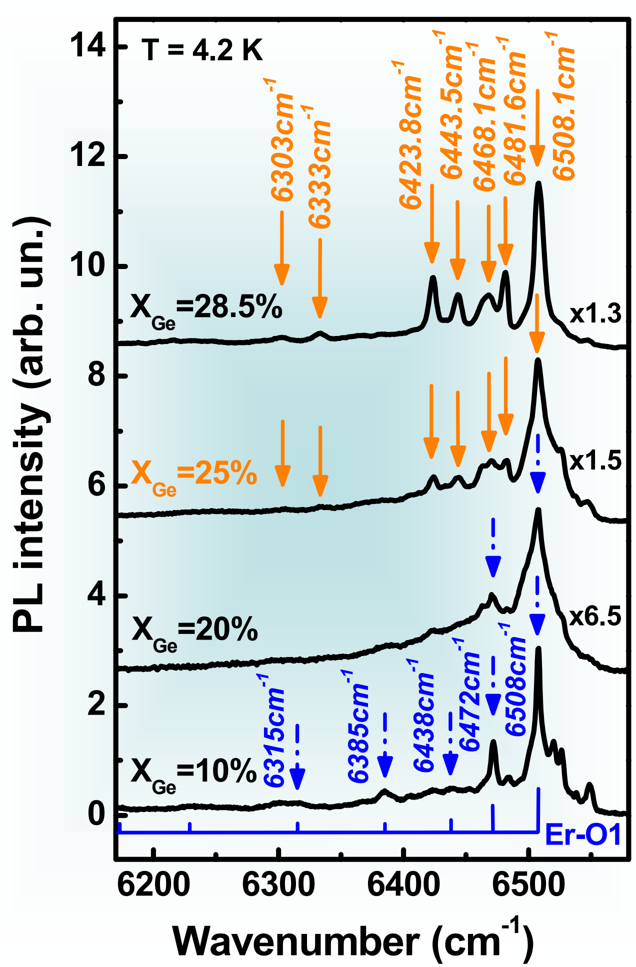

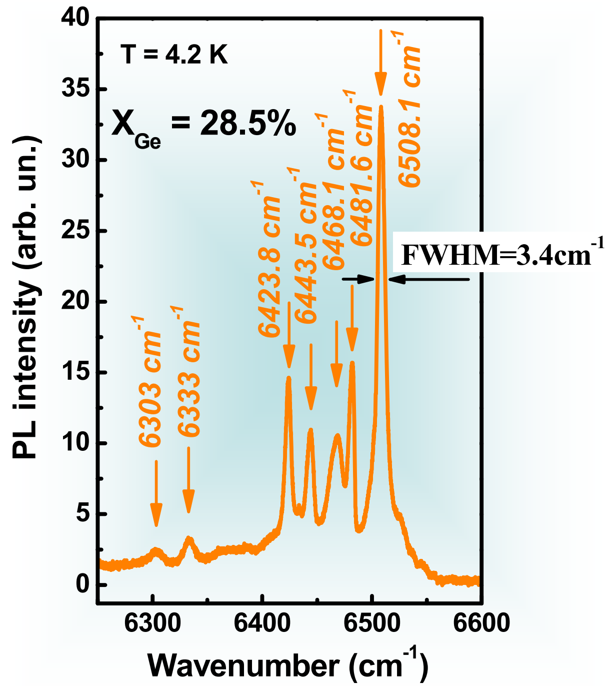

Different type of the optically active Er centers dominate in PL spectra of Si/Si$_{1-x}$Ge$_x$:Er/Si structures depending on the Ge content. One can show that the Er-O related centers similar to those observed in Si:Er layers dominate in the PL response of Si/Si$_{1-x}$Ge$_x$:Er/Si structures with the Ge content < 25%. Novel type of centers, namely Ge-related centers appear in the structures with the Ge content ≥ 25 %.

Optically active Er centers in $Si/Si_{1-x}Ge_x$:Er structures with Ge content ≥ 25%

Center Er-Ge1

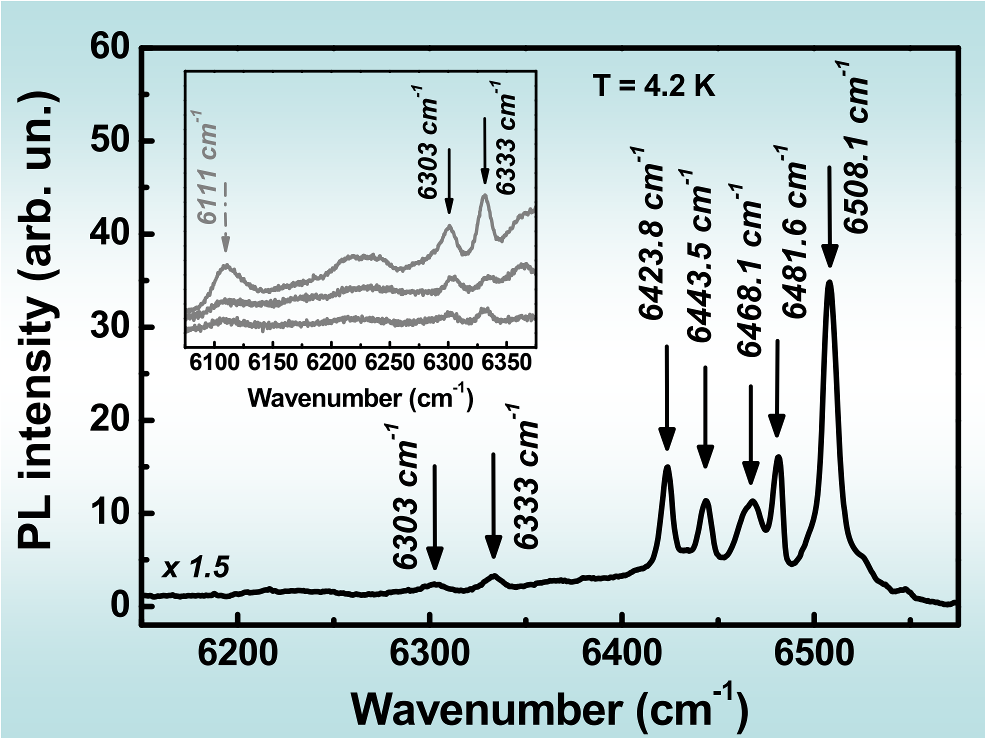

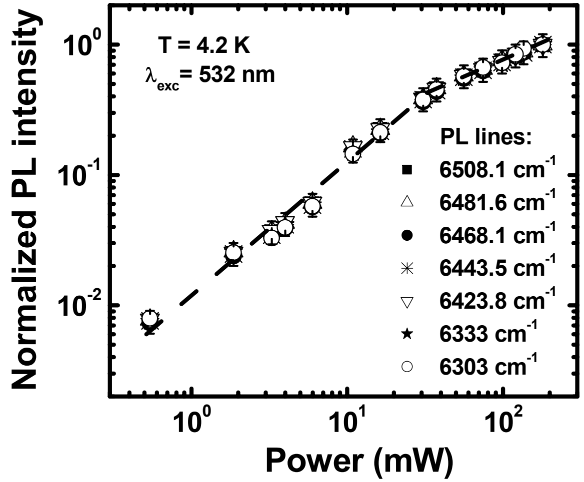

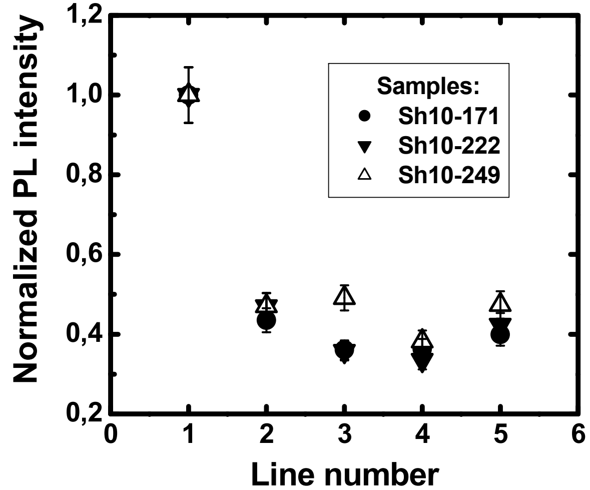

The lines observed behave identically depending on the excitation power and are well reproducible in various samples. This indicates that the lines belong to the same optically active Er center → **center Er-Ge1**.

L.V. Krasilnikova, Semiconductors (2009).

Temperature dependence: appearance of new line series in PL spectra

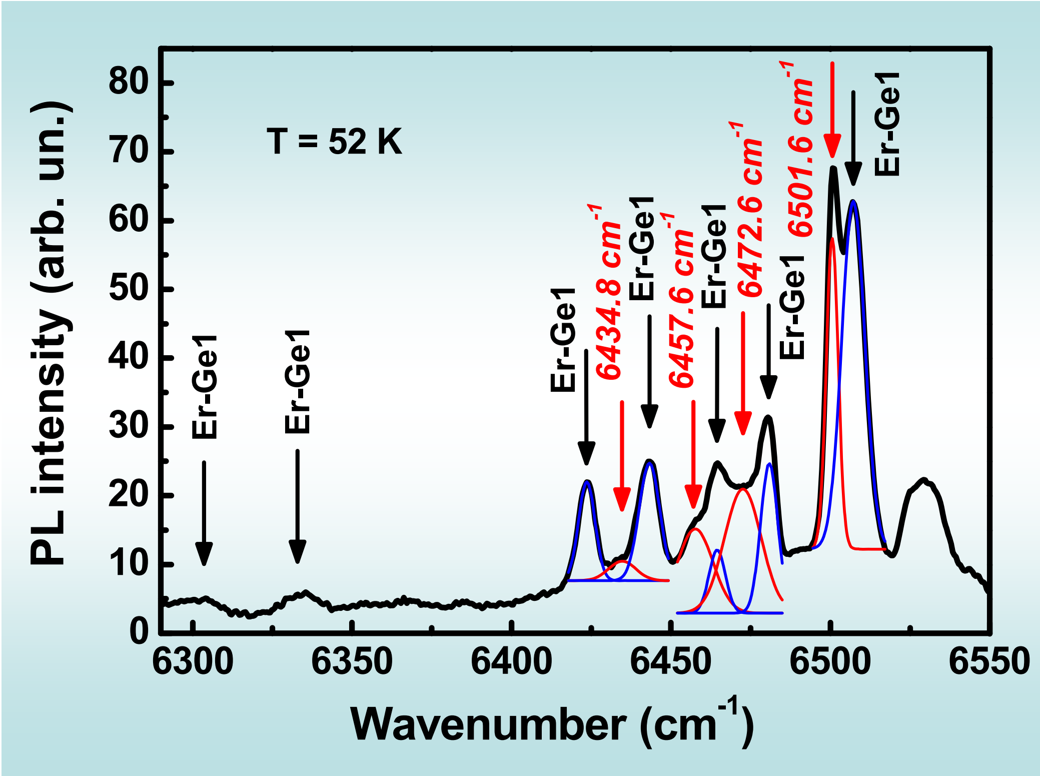

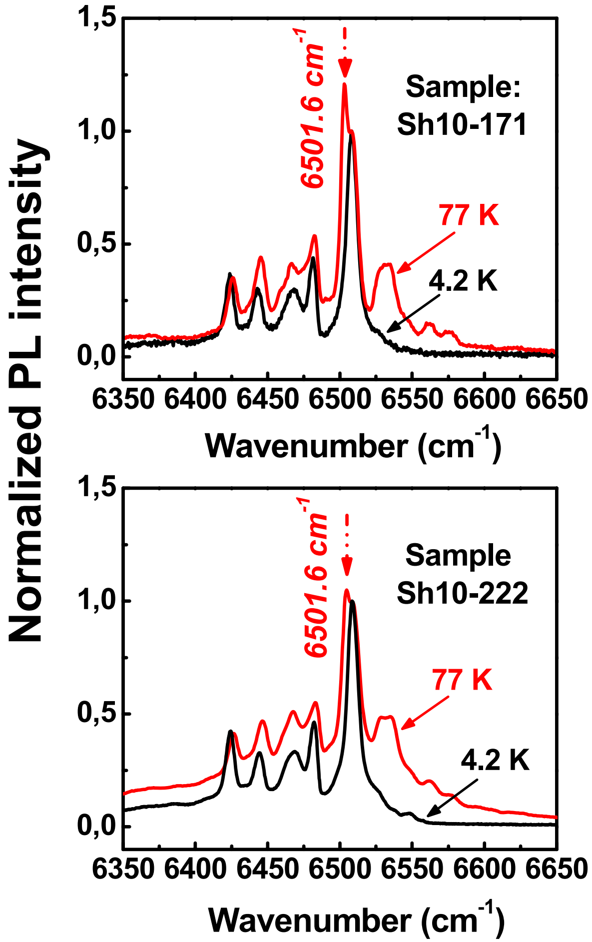

The line intensity of the center Er-Ge1 decreases with the increasing temperature. The Er related PL is not detectable in $Si/Si_{1-X}Ge_X$:Er structures at $T \geq 110$ K. Novel line series appears in PL spectra at elevated temperatures (T > 8K).

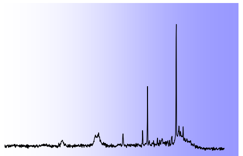

Temperature dependence of PL lines related with Er centers

Deactivation energies and coupling constants describing the temperature quenching of PL lines in the spectra of $Si/Si_{1-x}Ge_x:Er/Si$ structures with Ge content ≥ 25%.

Center	PL line	E_1, meV	C_1	E_2, meV	C_2
Er-Ge1 center	6508.1 cm^{-1}	12.2	1.13	50.1	1278
	6481.6 cm^{-1}	11.1	3.36	50.8	1089
	6468.1 cm^{-1}	11.7	3.59	50.8	1259
	6443.5 cm^{-1}	12.6	2.59	51.8	1138
	6423.8 cm^{-1}	11.3	2.59	51.2	1415
Er-Ge2 center	*6501.6* cm^{-1}	-6.5	4.59	49.1	223
	6472.6 cm^{-1}	-5.2	9.69	48	252
	6457.6 cm^{-1}	-5.9	11.12	48	352
	6434.8 cm^{-1}	-6.27	3.54	48.3	494

Er related centers:

Er-Ge1: E_1 ~ 12 meV, E_2 ~ 51 meV, C_1 ~ 2.65, C_2 ~ 1236;

Er-Ge2: E_1 ~ -6 meV, E_2 ~ 48 meV, C_1 ~ 7.24, C_2 ~ 330.

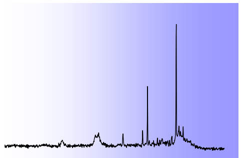

Microscopic structure of Er centers being formed in structures with Ge content ≥ 25%

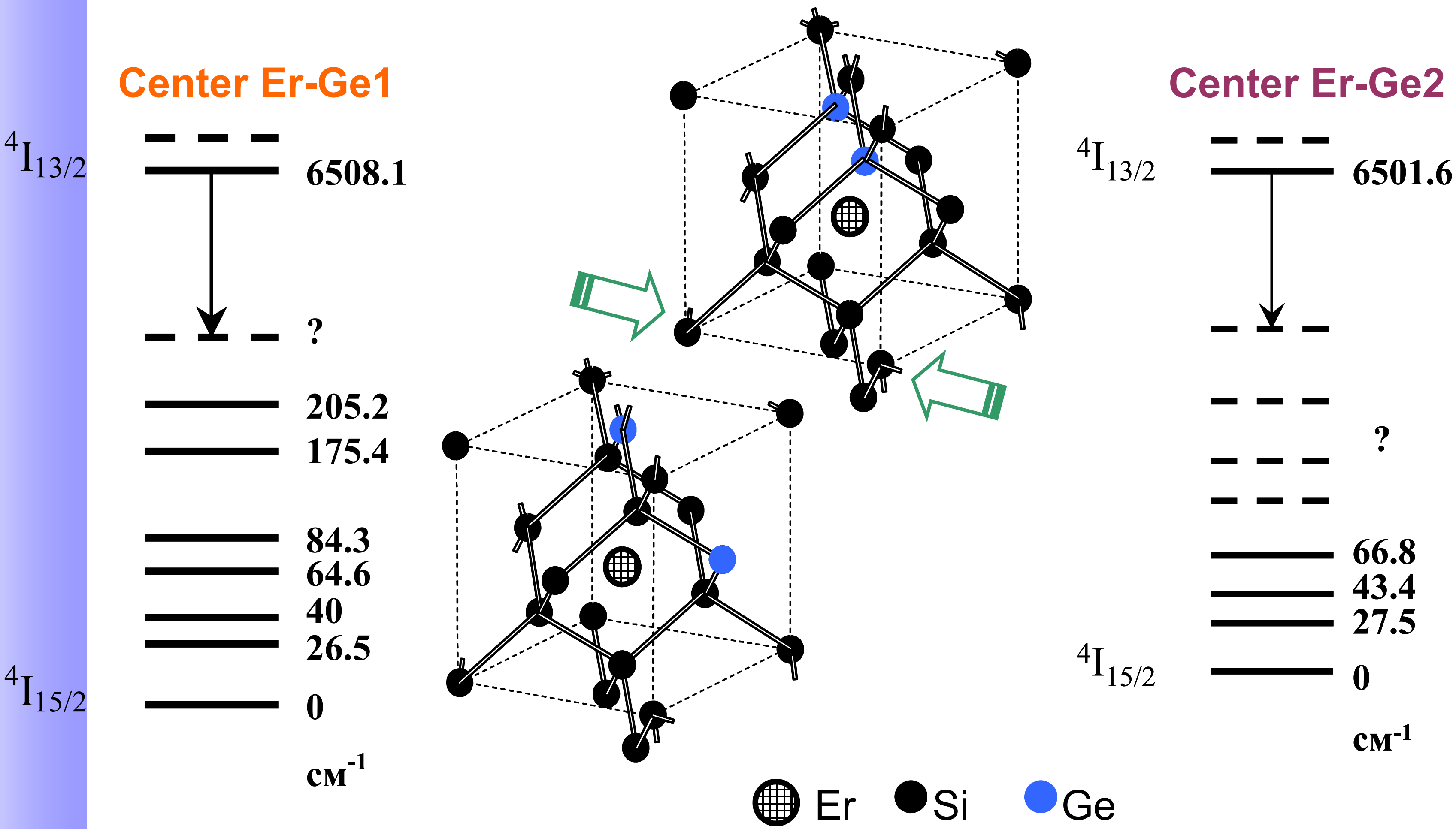

The center Er-Ge1 belongs to the low symmetry Er centers and consists of an Er ion in the interstitial position and at least 2 Ge atoms in the nearest surroundings. The most probable types of symmetry of this center are - C_{2v}, D_{2d}, C_s. The second center belongs to the Er-Ge centers as well. Both centers are differing by their crystal field symmetry. The symmetry variations might be related with the different location of Ge atoms and the presence of strain in $Si_{1-x}Ge_x$ layers.

PL quantum efficiency of Si:Er and SiGe:Er structures produced by the sublimation MBE technique

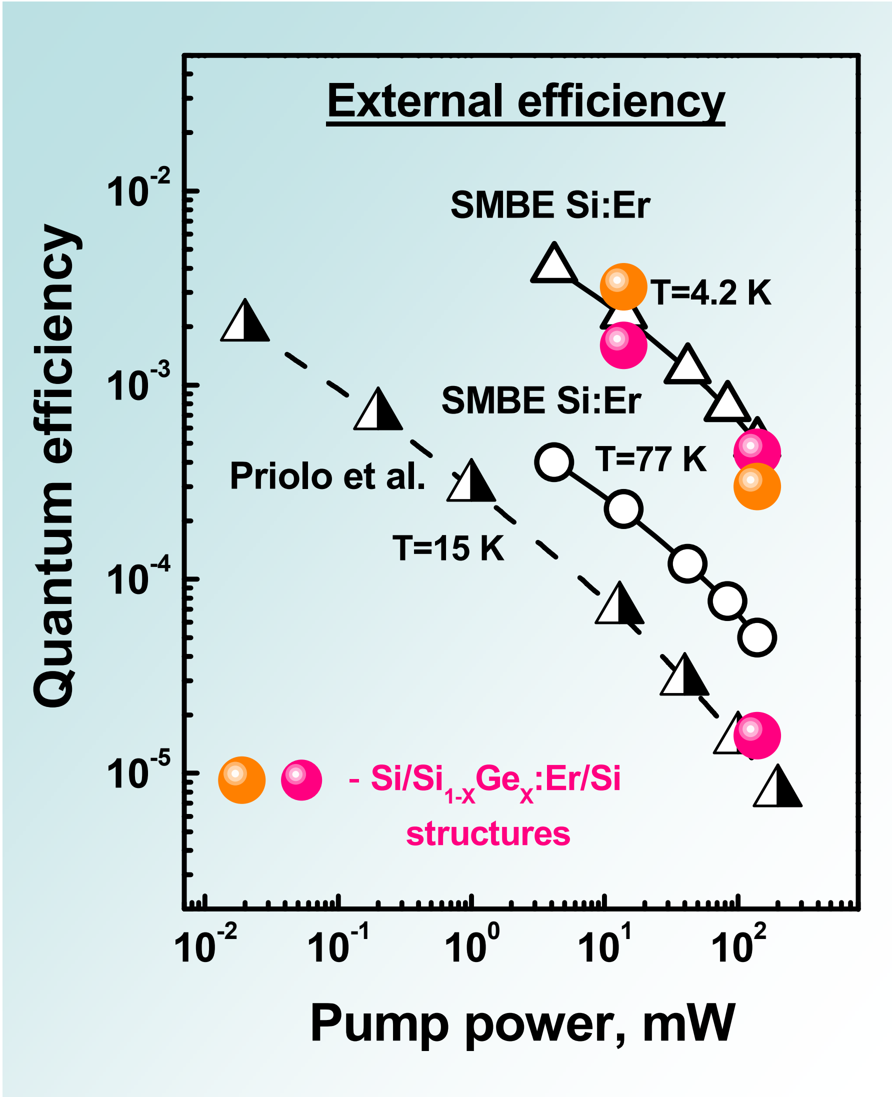

The external quantum efficiency

$\eta_{ext} \approx$ **0.3 - 0.5 % at 4.2 K.**

(P_{pump} = 14 mW)

The internal quantum efficiency

$\eta_i \geq$ **15 % at 4.2 K.**

These values exceeds those obtained for the Er implanted Si structures (data presented by F. Priolo et al., Phys. Rev. B. 57, 4443).

B.A. Andreev et al., Proceed. of ICPS-26 (2003)

M.V. Stepikhova et al., J. of Cryst. Growth (2006),
L. Krasilnikova, et al., Phys. Stat. Sol.(c) (2011).

✓ Light emitting diodes on Si:Er basis

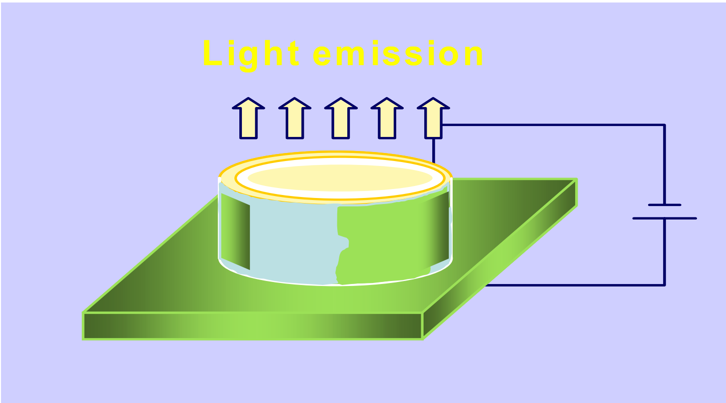

Mechanisms of Er ion excitation in EL regime

FORWARD BIAS REGIME

LT

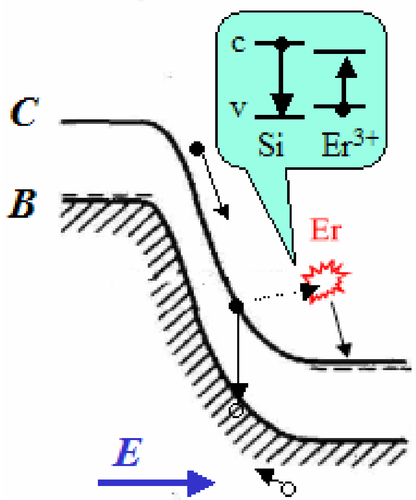

Exciton (e-h) mediated excitation of Er^{3+} ions

REVERSE BIAS REGIME

Junction breakdown:

tunneling

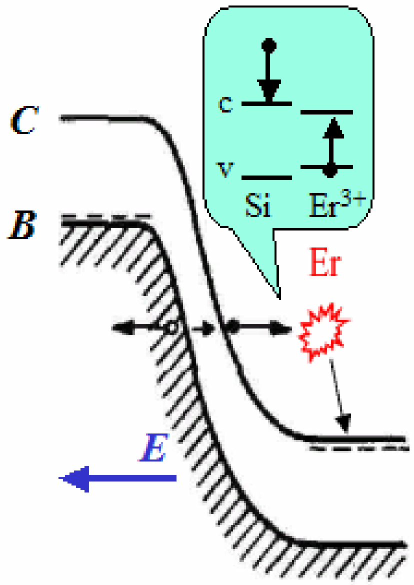

avalanche

RT

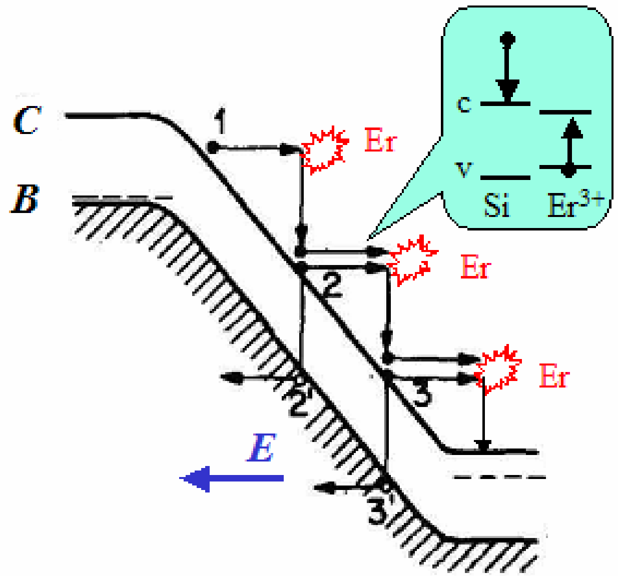

Impact ionization of Er^{3+} ions

History of Er-doped Si LEDs:

(1985) H. Ennen et al., APL **46**, 381 – *forward bias diode, 77 K*;
(1994) F. Priolo et al. APL **64**, 2235 – *tunneling diode, 300 K*;
(1997) N.A. Sobolev et al. APL **71**, 1930 – *avalanche diode, 300 K*;
(1997) C.-X. Du et al. APL **71**, 1023 – *Shottky diode*, *300 K.*

From tunneling to avalanche type diodes on Si:Er basis

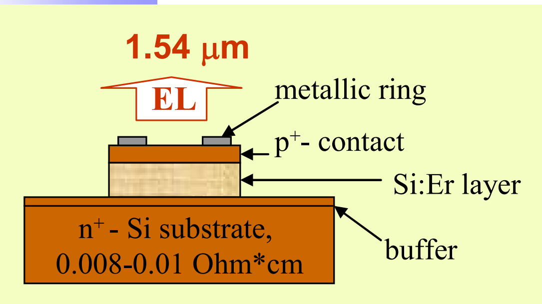

High luminescence efficiency has been obtained for Si:Er LEDs operating in the mixed breakdown regime, where: the effective excitation cross section of Er ions **σ=1.4x10^{-16} cm^2**, lifetime **τ=540 μs**, electroluminescence yield **~ 1 μW**.

Room temperature operations

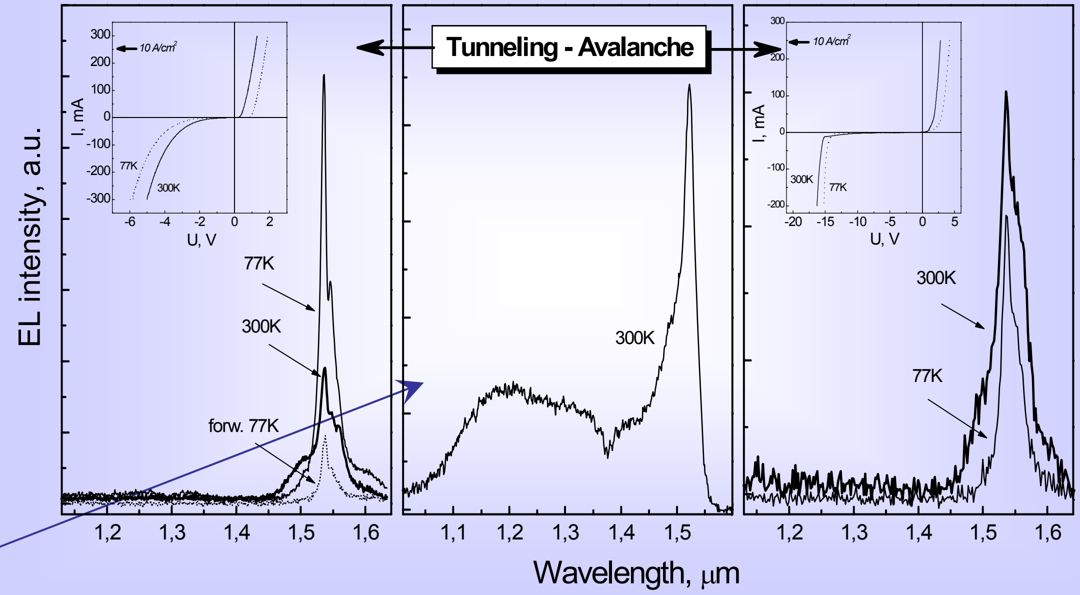

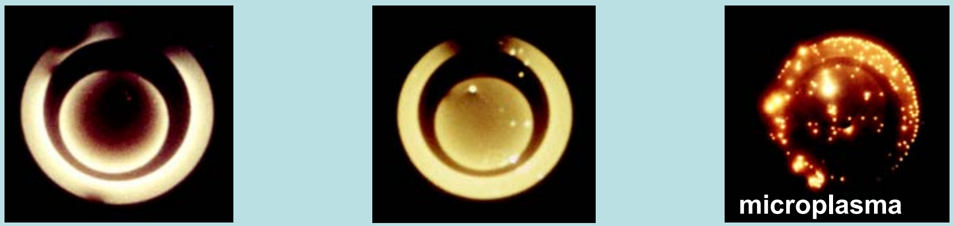

(current pinching)

Breakdown voltage: U_{br} (300K)/ U_{br} (77K)

tunneling	mixed	avalanche
3.9 / 6.0 V	**6.8 / 7.1 V**	**11.1 / 9.6 V**

Z.F. Krasilnik et al. in Towards the First Silicon Laser, NATO Science Series (2003),
V. Shmagin et al., Phys.Sol.St. (2004).

From tunneling to avalanche type diodes on Si:Er basis

High luminescence efficiency was obtained for Si:Er LEDs operating in the mixed breakdown regime. The effective excitation cross section of Er ions in this regime is: **σ=1.4x10^{-16} cm^2**, lifetime **τ=540 µs**, electroluminescence yield **~ 1 µW**.

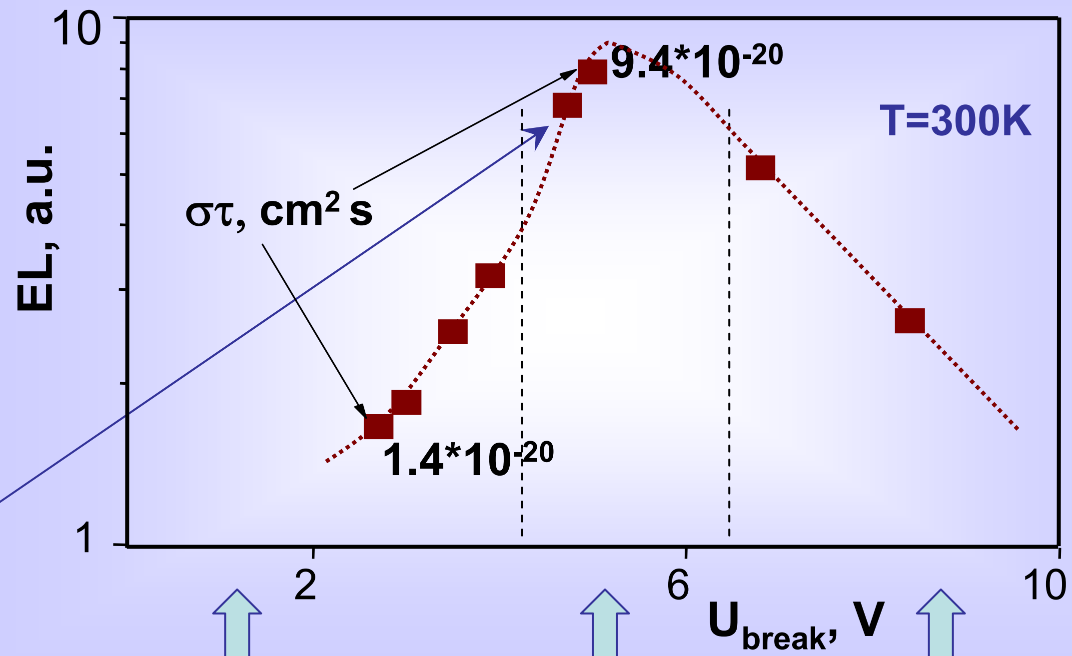

(current pinching)

Breakdown voltage: U_{br} (300K)/ U_{br} (77K)

3.9 / 6.0 V **6.8 / 7.1 V** **11.1 / 9.6 V**

V. Shmagin et al., Phys.Sol.St. (2004)

Concept of the multidiode type structures

The structure produced

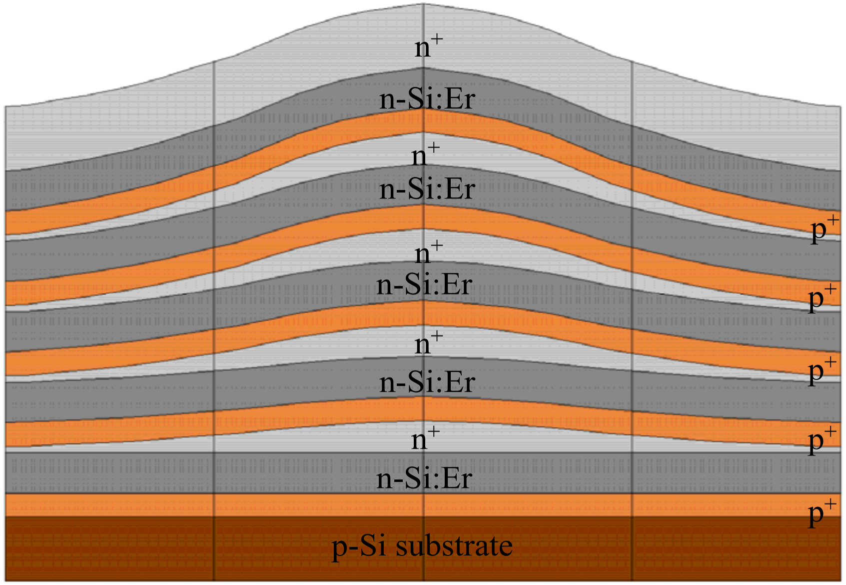

Structure with the different thickness of n^+ layers was grown during the one growth cycle

Structure parameters:

***p*⁺**: Si:B, p ~ $4 \cdot 10^{18}$ cm^{-3}, d = 30 nm,

n : Si:Er, n ~ 10^{16} cm^{-3}, d = 50 nm,

***n*⁺**: Si:P, n ~ $2 \cdot 10^{18}$ cm^{-3}, d = 8÷40 nm,

5 p^+-$n_{Si:Er}$-n^+ periods

M. Stepikhova et al., Patent RU2407109C1 (2009)

Electric field simulations

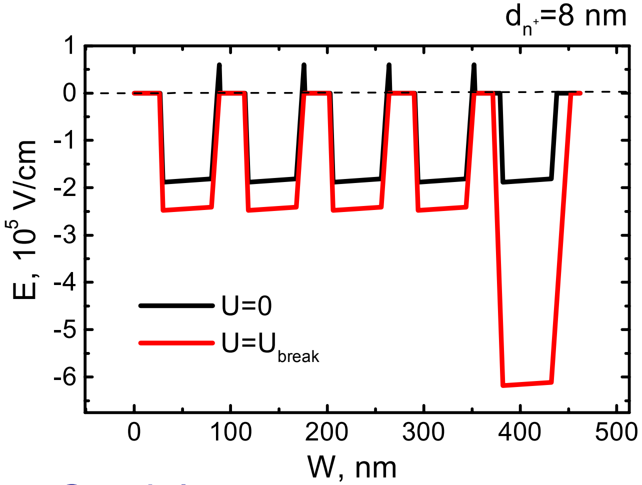

Spatial separation of the diode pairs

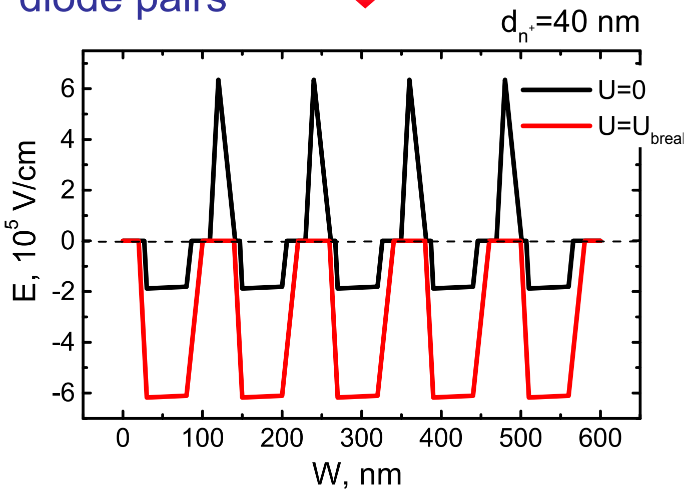

Concept of the multidiode type structures

Current-voltage characteristics

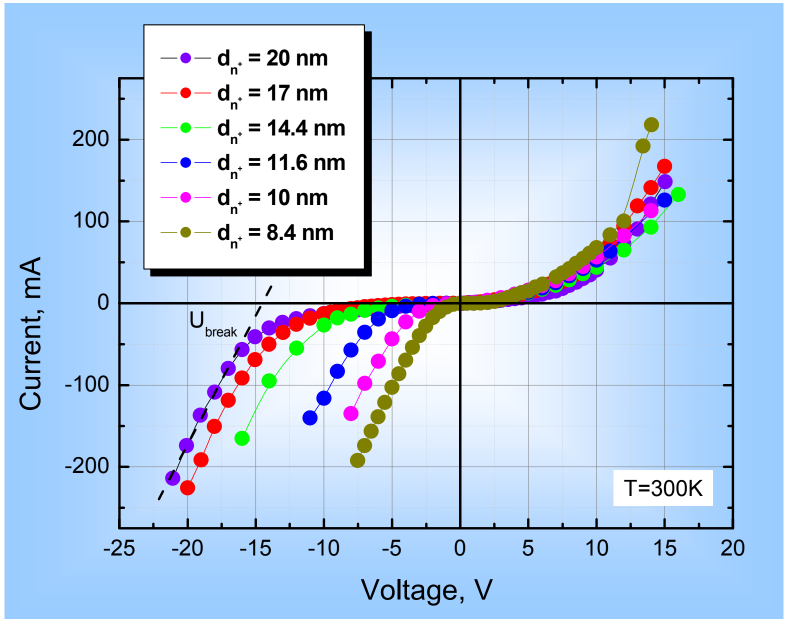

Electroluminescence

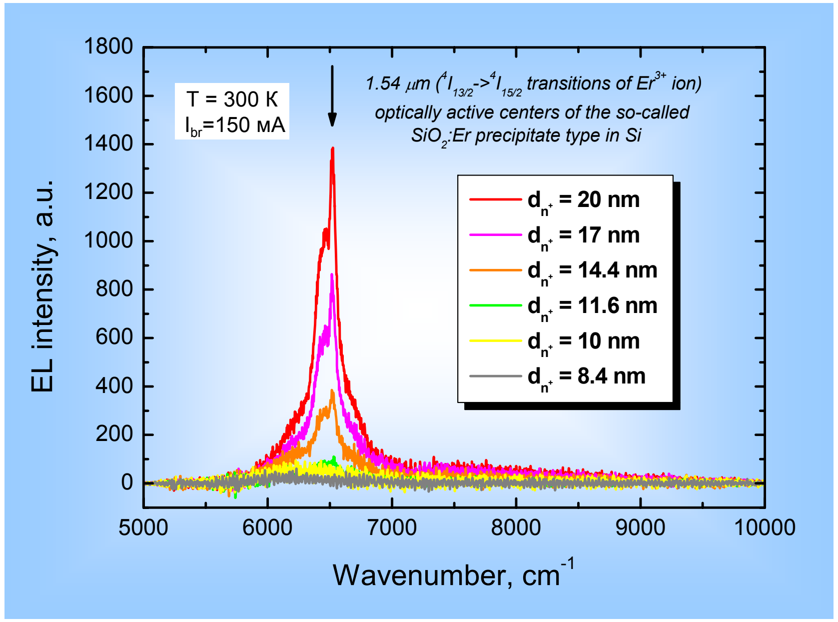

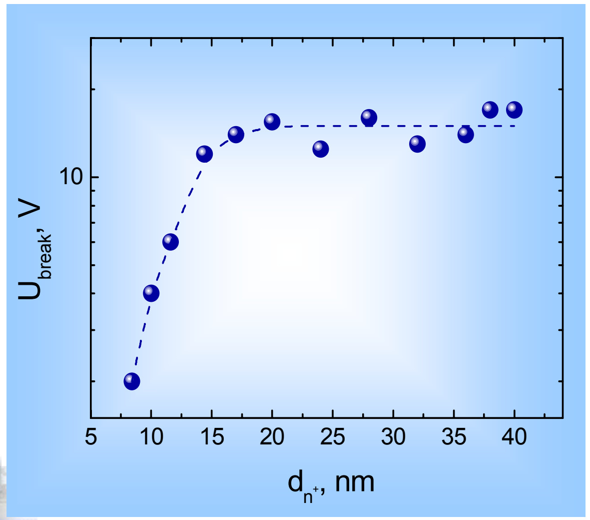

Both the breakdown voltage and the EL intensity show the saturation dependence on the thickness of *n*+ layer.

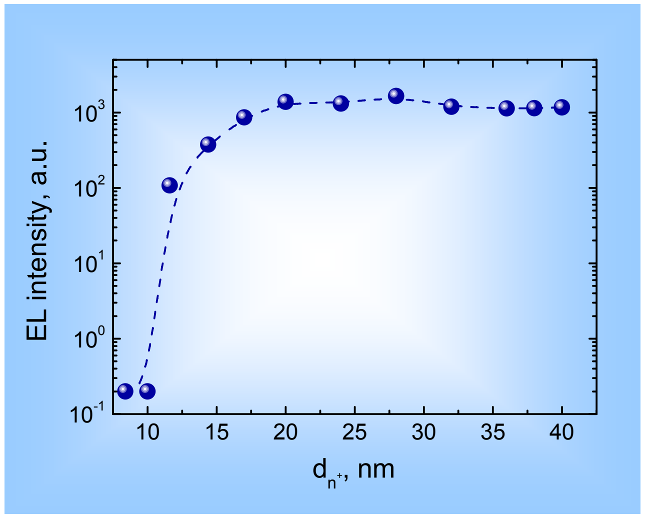

Concept of the multidiode type structures

Comparison of the EL intensities obtained for the «multidiode» and single diode structures

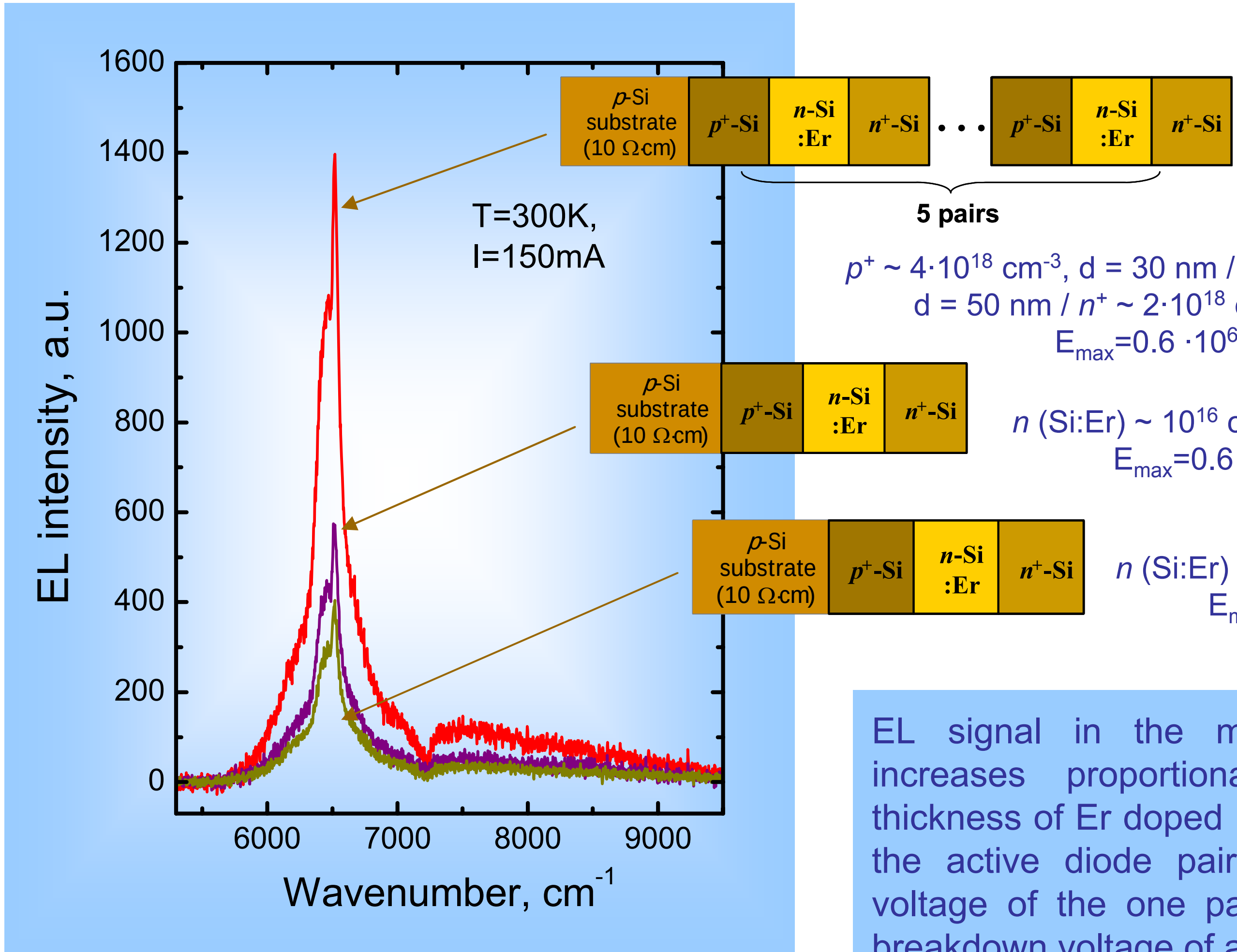

p^+ ~ $4\cdot10^{18}$ cm^{-3}, d = 30 nm / n (Si:Er) ~ 10^{16} cm^{-3}, d = 50 nm / n^+ ~ $2\cdot10^{18}$ cm^{-3}, d = 40 nm; E_{max}=0.6 $\cdot10^6$ V/cm

n (Si:Er) ~ 10^{16} cm^{-3}, d = 120 nm; E_{max}=0.6 $\cdot10^6$ V/cm

n (Si:Er) ~ 10^{16} cm^{-3}, d = 50 nm; E_{max}=1.2 $\cdot10^6$ V/cm

EL signal in the multidiode structure increases proportionally to the total thickness of Er doped layers introduced in the active diode pairs. The breakdown voltage of the one pair is less than the breakdown voltage of a singe diode.

M. Stepikhova et al., Patent RU2407109C1 (2009)

Novel concept of the tunneling transit-time LED

(current pinching)

Tunneling transit-time diode is a way to avoid microplasma breakdown

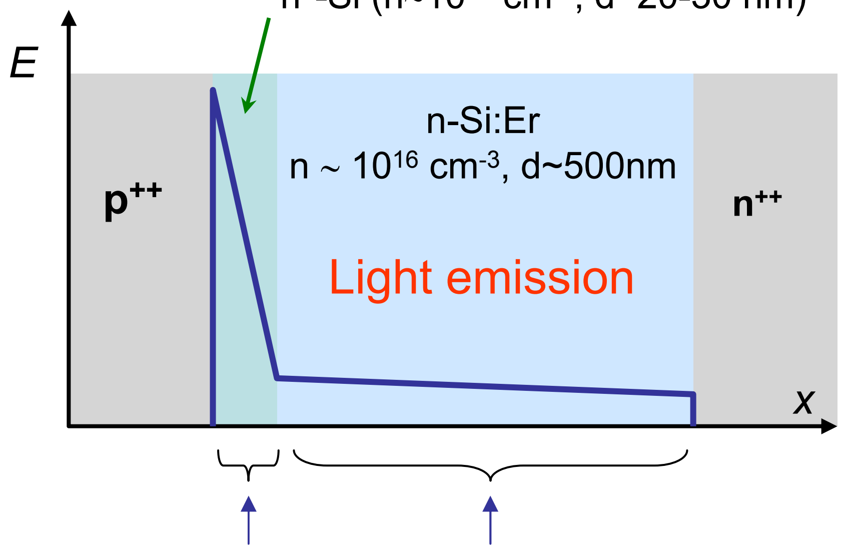

Highly doped narrow region, where the hot electrons are generated. Zenner breakdown of the p-n junction.

Wide, moderately doped transit-time region, where the excitation of Er^{3+} ions takes place.

Potentialities:

Widening of the space charge region.
Increase of the EL intensity and excitation efficiency.

V.B. Shmagin et al., IEEE Journal of Selected Topics in Quantum Electronics (2006)

Novel concept of the tunneling transit-time LED

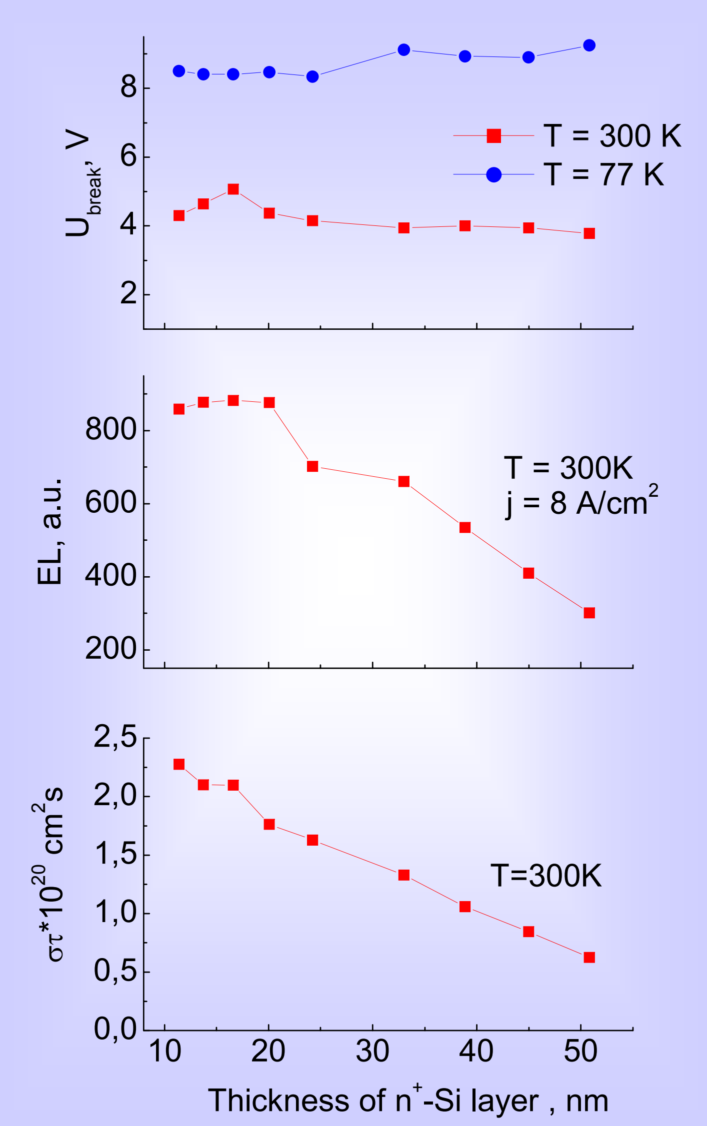

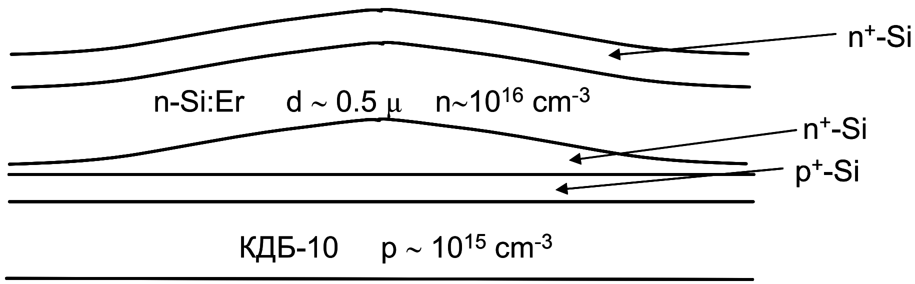

n⁺-Si: d = 10 ÷ 50 nm, n = 2·10¹⁸ cm⁻³

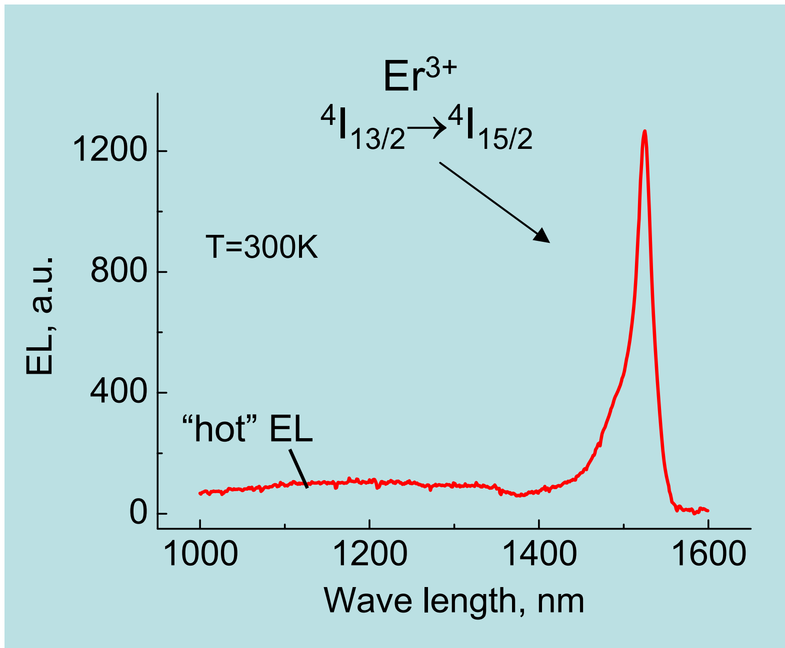

V. Shmagin et al., Semiconductors (2010)

***P* (*λ* = 1.54 μm) ≈ 5 μW (*j* ≈ 20A/cm²),**

$W_{n-Si:Er}$ ≈ 0.5 μm, *T* = 300K

Optically active Er centers being responsible for the LEDs RT operations in reverse bias regime

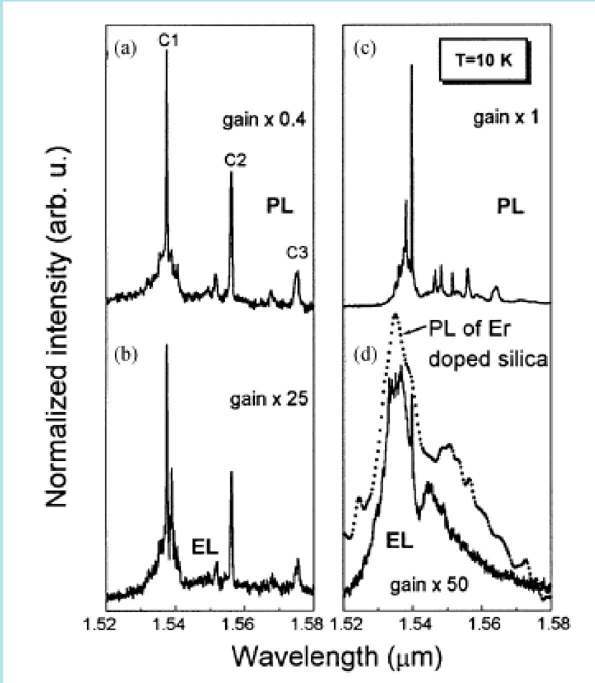

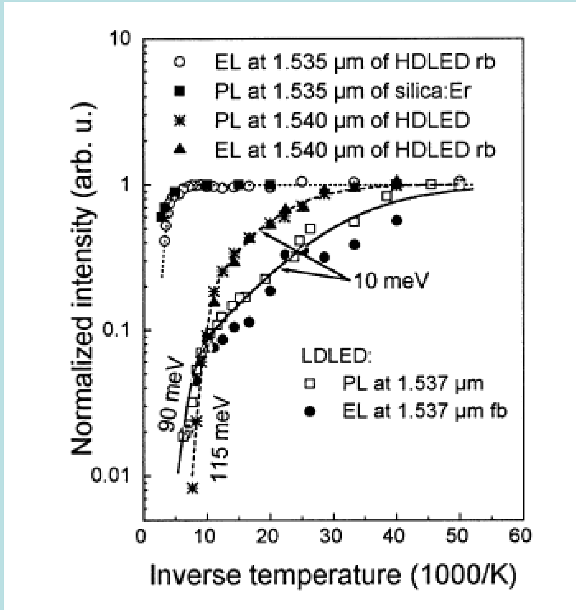

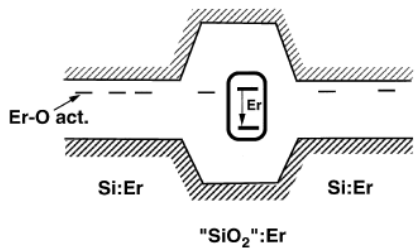

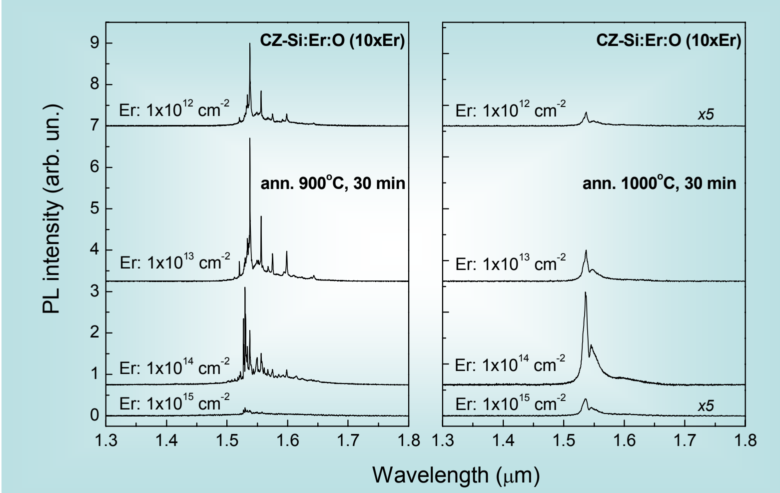

The strong EL signal at room temperature observed in heavily Er and O doped silicon LEDs is related with the so-called SiO_x:Er precipitate type centers.

W. Jantsch, J. of Lumin. (1999), W. Jantsch, Mat. Sci. & Eng. (2001).

✓ Towards the laser realization

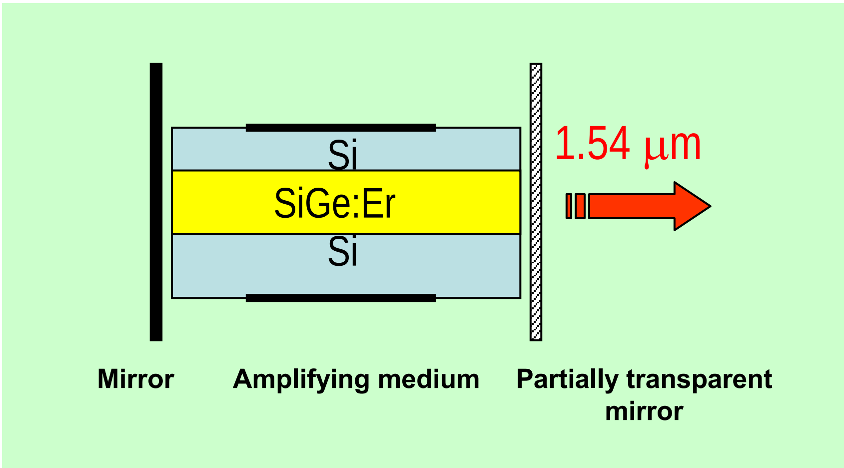

Optical gain in Si:Er structures. Theory.

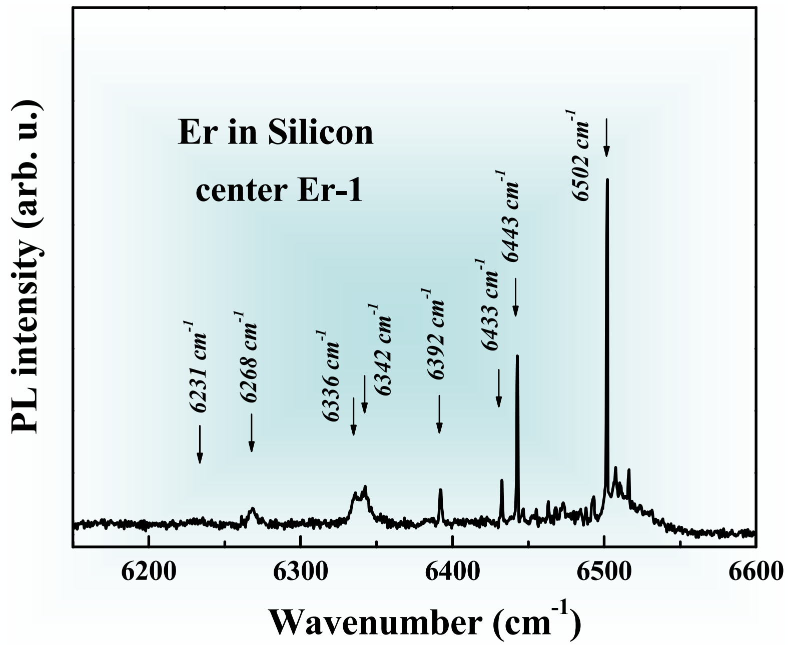

PL decay time:	**τ ~ 1 ms**
Width of PL line:	**$\Delta\nu$ ~ 10 μeV**
Photon absorption:	**$\sigma \approx 10^{-17} \div 10^{-16}$ cm^2**
Free carrier absorption :	**γ ~ 1 cm^{-1}**
Concentration of the optically active Er^{3+} centers	**N_0^E ~ 3×10^{17} cm^{-3}**

$$g = N_0^E \frac{\lambda^4}{4\pi n^2 c\tau\Delta\lambda}$$

FWHM of PL line for the isolated Er-1 center amounts to ~ 10 μeV ⇒ **Optical gain of about <u>30 cm^{-1}</u> should be expected for active Si:Er layers**

Z.F. Krasilnik et al. *in Towards the First Silicon Laser,* NATO Science Series (2003)

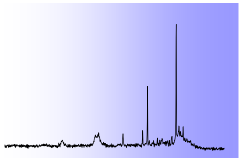

Optical gain in Si:Er structures. Experiment.

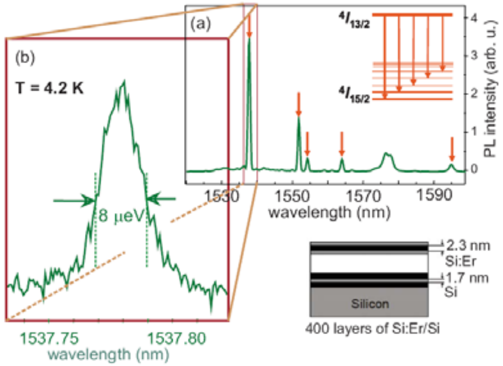

FIG. 2. (Color online) (a) PL spectrum of the Si/Si:Er multinanolayer structure, as measured at T=4.2 K under cw excitation at 532 nm. (b) Detail of the studied Er-1 center related ultranarrow emission line at 1.54 μm. Inset: sketch of the multinanolayer structure.

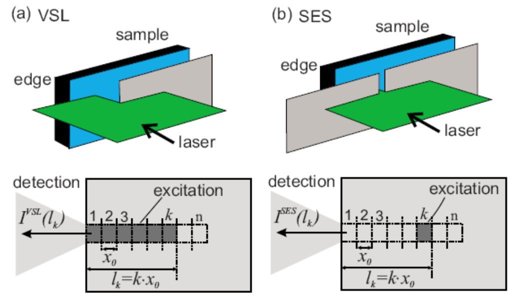

FIG. 1. (Color online) (a) The principle of the VSL and (b) SES techniques. The spot width in the SES is equal to the VSL differential shift step x_0. The emission signal is detected along the laser-exposed stripe area of length $l_k=kx_0$ ($k=0,\ldots,n$), perpendicularly to the excitation beam.

PHYSICAL REVIEW B **81**, 195206 (2010)

Optical gain of the 1.54 μm emission in MBE-grown Si:Er nanolayers

N. N. Ha,* K. Dohnalová,† and T. Gregorkiewicz
Van der Waals-Zeeman Institute, University of Amsterdam, 65 Valckenierstraat, NL-1018 XE Amsterdam, The Netherlands

J. Valenta
Department of Chemical Physics and Optics, Faculty of Mathematics and Physics, Charles University, Ke Karlovu 3, CZ-12116 Prague 2, Czech Republic
(Received 17 September 2009; published 13 May 2010)

We present investigations of the optical gain cross section of 1.54 μm Er-related emission at 4.2 K in Si/Si:Er molecular-beam-epitaxy-grown multinanolayers. This ultranarrow (full width at half maximum below 8 μeV) emission originating from the unique Er-related optical complex, Er-1 center, ensures the best condition to achieve stimulated emission. The experiments were carried out using a combination of the variable stripe length and shifting excitation spot techniques under pulsed and continuous-wave excitations. The comparison of results for both excitation regimes enables to estimate an optical gain within the strong optical losses due to the free carrier absorption. Based on these measurements, the upper limit of the optical gain cross section of 10^{-17} cm^2 and the gain coefficient of 8.8 cm^{-1} are deduced.

Observation of the population inversion of Er ion states in Si/$Si_{1-x}Ge_x$:Er/Si structures

Balance equations:

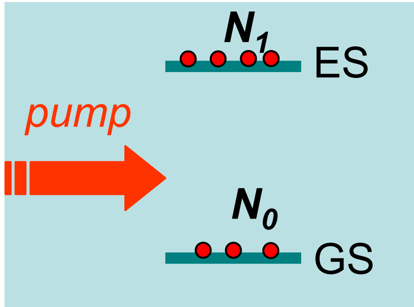

Inversion: $N_1 > N_0$

$$N_{Er} = N_0 + N_1 = const$$

$$\frac{dN_1}{dt} = g(N_{Er} - N_1) - \frac{N_1}{\tau_{decay}}$$

$$g = g(I_{exc}, N_{e-h}, h\nu_{exc}, \ldots)$$

$$\tau_{rise}^{-1} = g + \tau_{decay}^{-1}$$

$$\frac{d}{dt} = 0: \quad \boxed{\frac{N_1}{N_{Er}} = g \times \tau_{rise} = 1 - \tau_{rise} / \tau_{decay}}$$

The relative number of Er ions being in the excited state can be directly determined trough the ratio of PL rise and decay times.

M.V. Stepikhova et al., JETP Letters, 2005
M.V. Stepikhova et al., J. of Cryst. Growth, 2006

Observation of the population inversion of Er ion states in $Si/Si_{1-x}Ge_x:Er/Si$ structures

Experiment:

PL transients were measured under Cu-laser excitation ($h\nu_{exc}$= 2.1, 2.4 eV) with the pump power densities varied form 0.01 to 10 W/cm^2. The signal was dispersed by the 50 cm monocromator and detected with an InGaAs photodiode. All measurements were performed at temperatures of ~10 K in the closed cycle He-cryostat. Spectral resolution of the system – 2nm, time resolution – 0.2 ms.

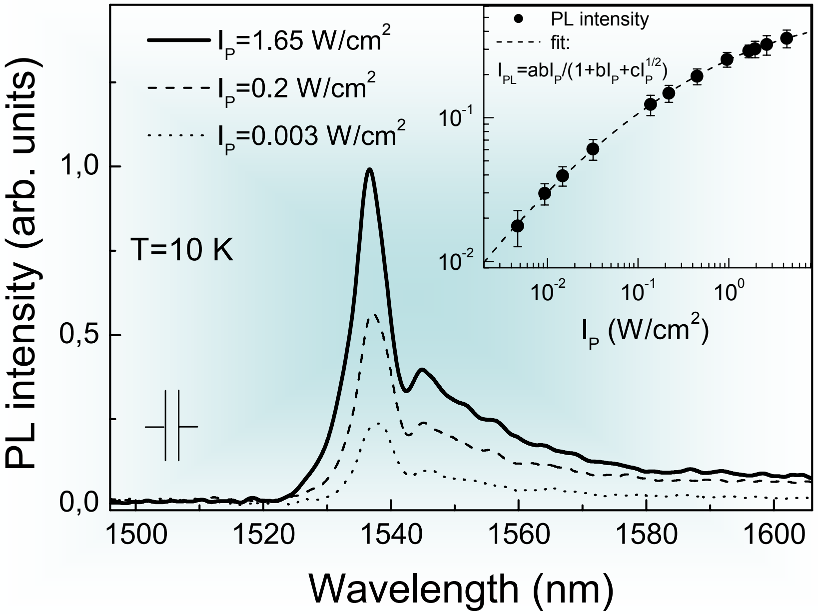

Dependence of the PL intensity on pump power density

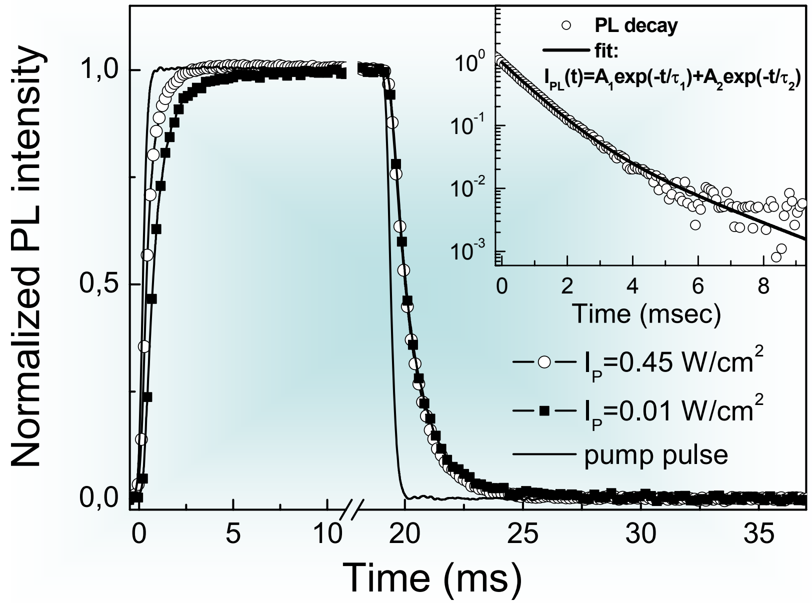

PL transients measured at different pump power densities

Observation of the population inversion of Er ion states in $Si/Si_{1-x}Ge_x:Er/Si$ structures

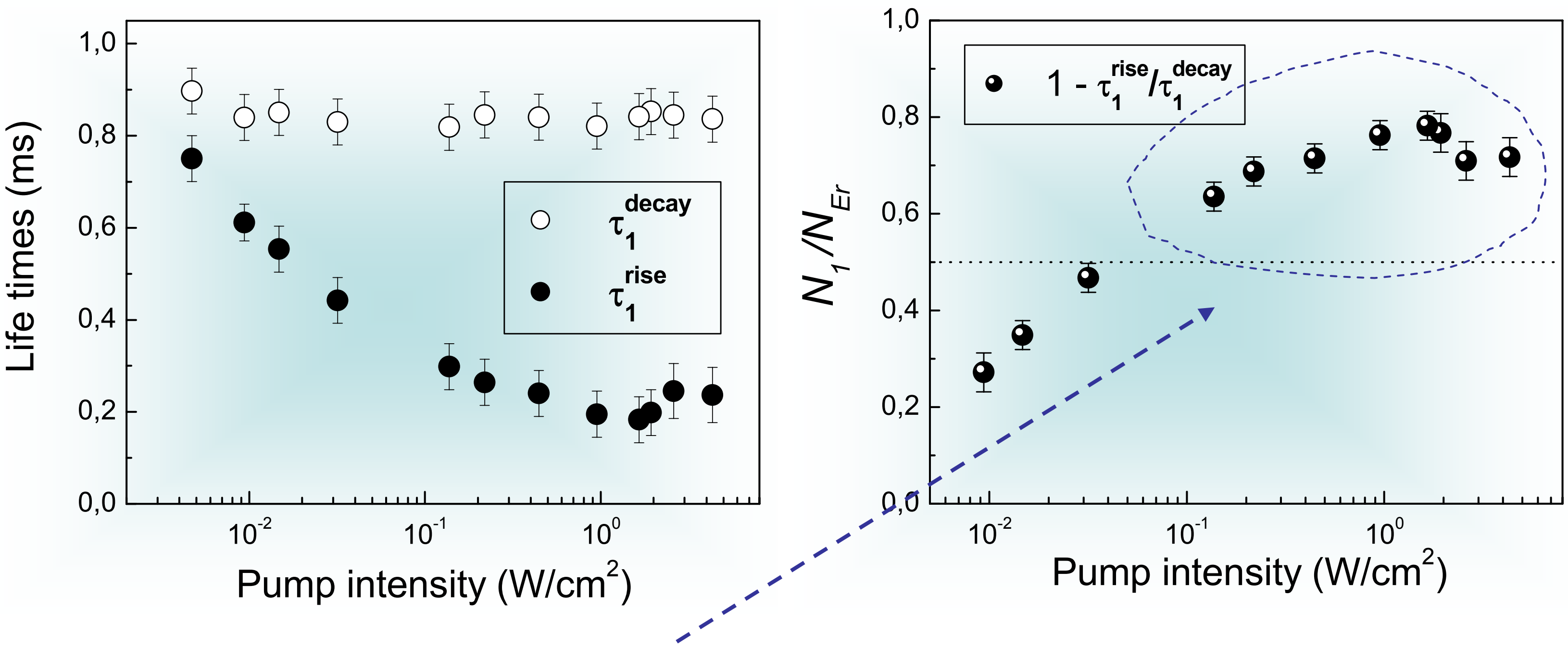

Inversion: $N_1/N_{Er} > ½$, or $N_1/N_0 > 1$

$N_1/N_0 = \tau_{decay}/\tau_{rise} - 1 = 4$

Structure parameters:

Sample	Substrate	Si buffer layer	SiGe:Er layer		Si cup layer	
		d_{buff}, nm	d_{Si-Ge}, nm	x, %	Source	d_{cup}, nm
# 10-156	Si:P - 4.5 Ω·cm (100)	50	1100	28 % RES = -9±10%	Si:P - 2 Ω·cm	220

M. Stepikhova et al., JETP Letters (2005)

Waveguides with an active Er doped layer on Si basis

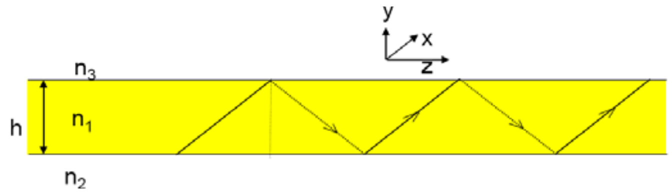

n (Si) = 3.48

n ($Si_{1-x}Ge_x$, x = 10%) = 3.53

n ($Si_{1-x}Ge_x$, x = 30%) = 3.63

n (SiO_2) = 1.5

$Si/Si_{1-x}Ge_x$:Er/Si waveguides

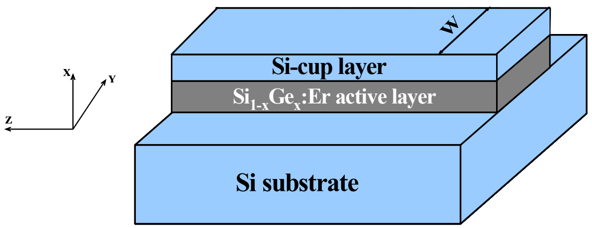

x_{Ge} = 28 %, W = 50 мкм,
$d_{Si1-xGex:Er}$ = 1.1 мкм, d_{Si-cup} = 0.22 мкм

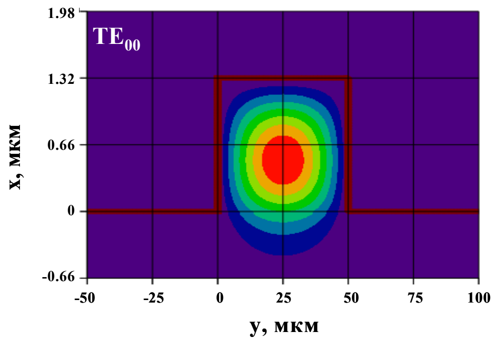

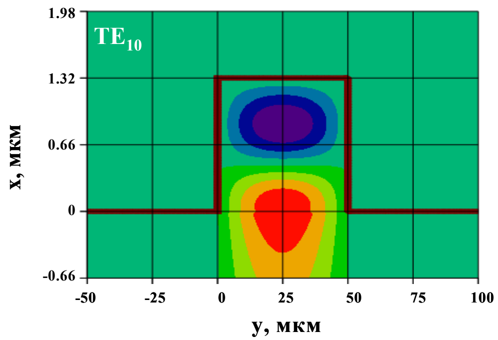

SOI/Si:Er waveguides

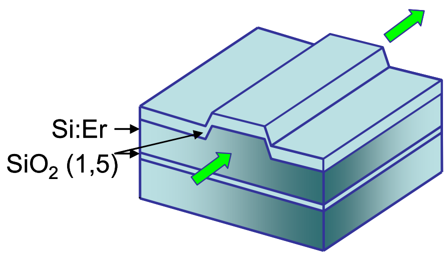

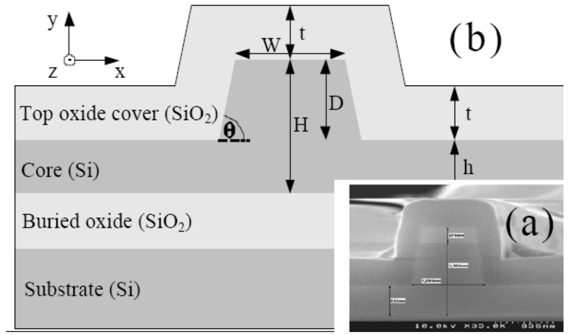

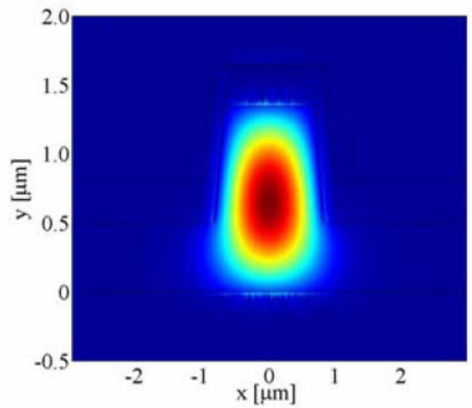

Laser cavities

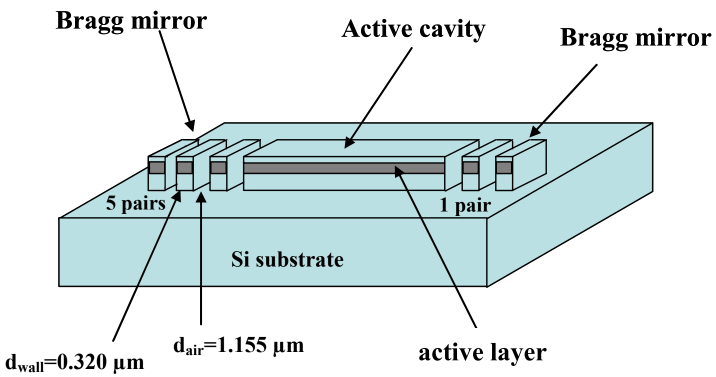

Bragg mirrors:

$d_{Si\text{-}wall}$ = 320 nm
d_{air} = 1155 nm
number of Si/air pairs:
N = 1 → R = 0.9191
N = 5 → R = 1.

Active cavity:

Γ = 1,
losses ~ 1 cm^{-1},
gain = 2 – 10 cm^{-1}.

Laser threshold condition:

$$\beta = \alpha(a) + \frac{1-\Gamma}{\Gamma}\alpha(c) + \alpha(m)$$

gain (β); **losses in an active layer** ($\alpha(a)$); **losses in confinement layers** ($\alpha(c)$); **mirror losses** ($\alpha(m)$)

$$\alpha(m) = \frac{1}{2L}\ln\left(\frac{1}{R_1 R_2}\right)$$

cavity length *L* > 0.1 mm

SOI/Si:Er cavities

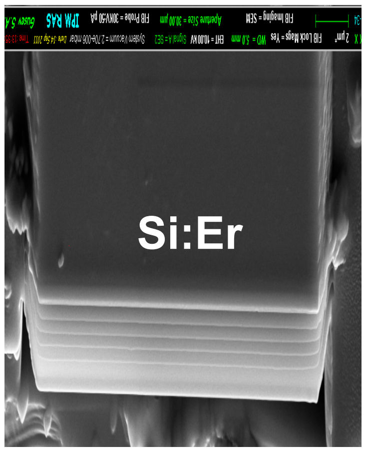

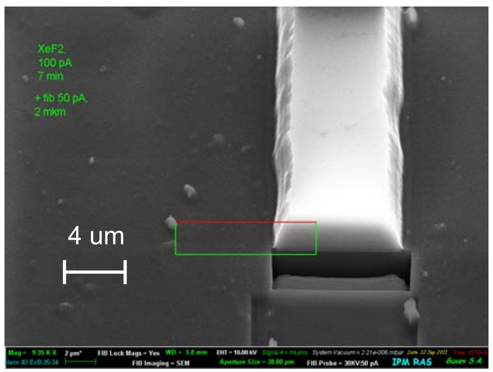

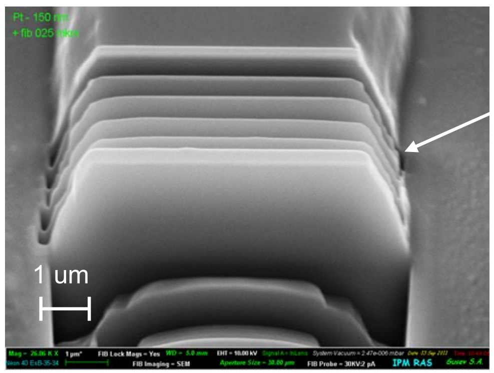

FIB etching

Z.F. Krasilnik et al., St. Petersburg, 2012

Laser cavities

Simulations for $Si_{0.7}Ge_{0.3}$ disk resonator

(radius *a* = 18 μm, height *h* = 0.22 μm)

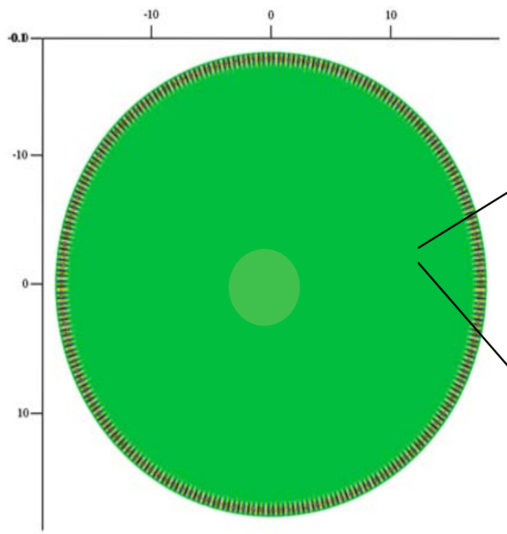

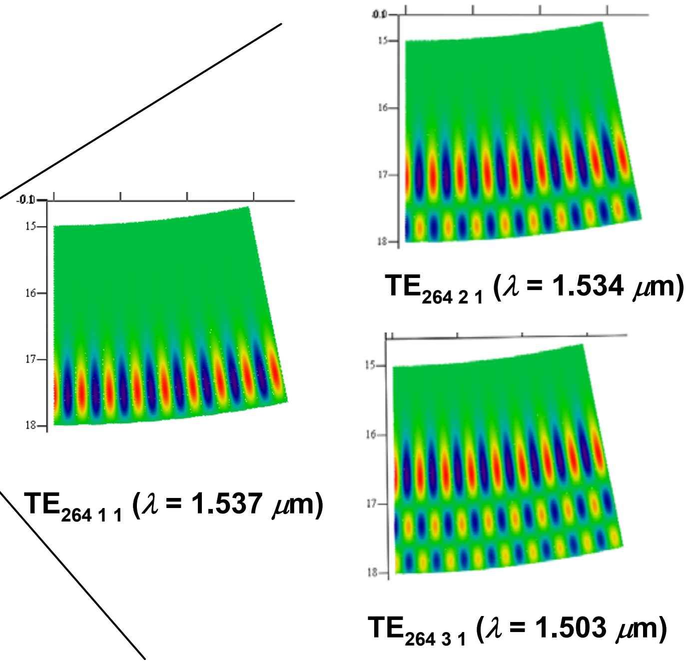

Disk resonator made of $Si_{0.7}Ge_{0.3}$:Er

(radius *a* = 18 μm, height $d_{SiGe:Er}$ = 2 μm)

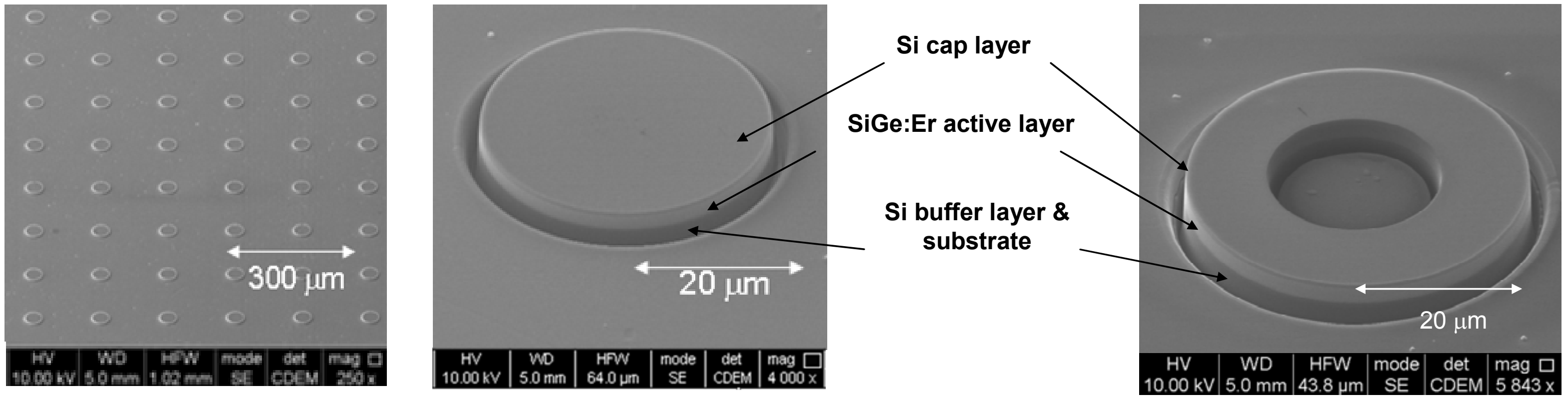

N. Yurasova et al., J. Lumin. (2012), Z.F. Krasilnik et al., St. Petersburg, 2012

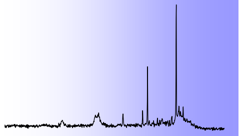

Conclusions

- Applying the optical doping with the Er impurity we are able to realize effective light-emitting Si and SiGe structures operating at the wavelength of 1.54 µm. The internal quantum efficiency of the photoluminescence for these structures reaches the value of 20% at 4.2 K.

- The light-emitting diodes with the output power of 5 µW that operate at the room temperature were realized on this basis.

- There are the prerequisites that testify to the ability for a laser realization on the basis of Er doped Si and SiGe structures.

Nearest future → laser realization

Questions?

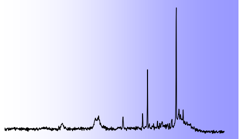

APPLIED PHYSICS LETTERS VOLUME 83, NUMBER 5 4 AUGUST 2003

Fiber-coupled erbium microlasers on a chip

Lan Yang,[a] D. K. Armani, and K. J. Vahala[b]
Department of Applied Physics, California Institute of Technology, Pasadena, California 91125

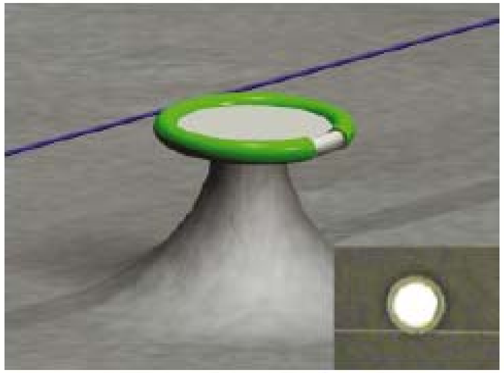

FIG. 1. (Color) Illustration showing a microchip laser consisting of an erbium-doped sol-gel thin film applied to a microtoroid. Also shown is a fiber taper used for both pump coupling and laser emission extraction. The inset is a photomicrograph of the top view of an erbium microtoroid laser coupled by a fiber taper.

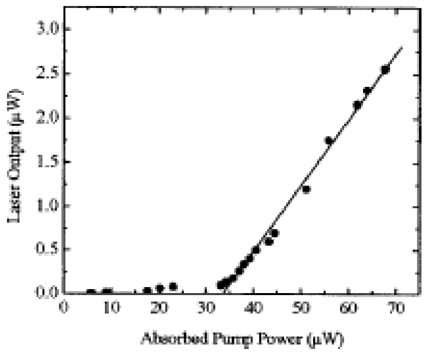

FIG. 4. Measured laser output power plotted vs absorbed pump power for a microtoroid laser with a diameter of 80 μm.

APPLIED PHYSICS LETTERS VOLUME 84, NUMBER 7 16 FEBRUARY 2004

Ultralow-threshold erbium-implanted toroidal microlaser on silicon

A. Polman[a]
Department of Applied Physics, California Institute of Technology, Pasadena, California 91125 and FOM-Institute AMOLF, Kruislaan 407, 1098 SJ Amsterdam, The Netherlands
B. Min
Department of Applied Physics, California Institute of Technology, Pasadena, California 91125
J. Kalkman
FOM-Institute AMOLF, Kruislaan 407, 1098 SJ Amsterdam, The Netherlands
T. J. Kippenberg and K. J. Vahala[b]
Department of Applied Physics, California Institute of Technology, Pasadena, California 91125

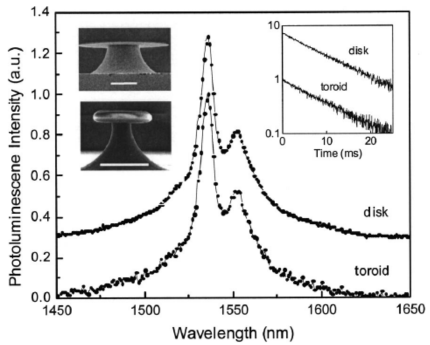

FIG. 1. Photoluminescence spectra of Er-implanted microresonators before and after laser annealing (the spectrum for the disk is shifted vertically for clarity). The right inset shows photoluminescence decay traces measured at λ=1535 nm for both a disk and a toroid. The left insets show scanning electron microscopy images of a microresonator disk and toroid. Scale bars are both 43 μm.

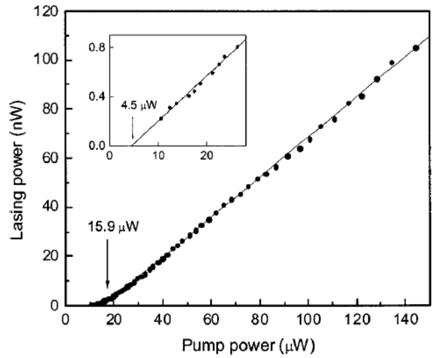

FIG. 3. Unidirectional lasing power as a function of launched power for a 32 μm diameter Er-implanted microtoroid. The lasing threshold is 15.9 μW. λ_{pump}=1465 nm, λ_{lasing}=1558 nm. The inset shows a measurement made on the best resonator, showing a pump threshold of 4.5 μW.

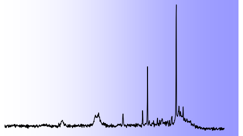

Quantum efficiency of Si:Er-based light emitting diodes

$$\eta_{int} = \sigma_{eff} \cdot \Phi_{Er} \cdot \frac{\tau}{\tau_{rad}} \approx 1 \cdot 10^{3}$$

Ion-implanted structures

	Intern. quant. effic.	Er excitation cross section	Excited Er lifetime	Conditions	
F	10^{-1}	$3 \cdot 10^{-15}$ cm^2	2 ms	PL, T=15 K, $P_{pump}=10^{-5}$W, $\Phi_{Er}=3 \cdot 10^{13}$ cm^{-2}	F. Priolo et al., PRB 57, 4443 (1998)
F	$1.5 \cdot 10^{-5}$ (forward bias)	$3 \cdot 10^{-15}$ cm^2	$2 \cdot 10^{-4}$ ms	T=300 K, $\Phi_{Er}=1 \cdot 10^{13}$ cm^{-2}	F. Priolo et al., PRB 57, 4443 (1998)
R	10^{-4} (reverse bias)	$6 \cdot 10^{-17}$ cm^2	0.1 ms	T=300 K, $\Phi_{Er}=4 \cdot 10^{13}$ cm^{-2}	S. Coffa et al., APL 69, 2077 (1996)
R	$5 \cdot 10^{-4}$ (reverse bias)	$1 \cdot 10^{-16}$ cm^2		T=300 K	S. Libertino et al., Mater.Science in Semicond.Process. 3, 375 (2000)

MBE structures *(IPM RAS)*

F	$4 \cdot 10^{-2}$	$6 \cdot 10^{-16}$ cm^2	1,1 ms	PL, T=77 K, $P_{pump}=4 \cdot 10^{-3}$ W	S. Gastev et al., Semiconductors, 37,1100 (2003) .
R	10^{-3} (reverse bias)	$1.4 \cdot 10^{-16}$ cm^2	0.54 ms	T=300 K, $\Phi_{Er}=3 \cdot 10^{13}$ cm^{-2}, $j \leq 1$A/cm^2	D. Remizov et al., Phys. Solid State 47, 98 (2005)

High and ultrahigh Q laser cavities

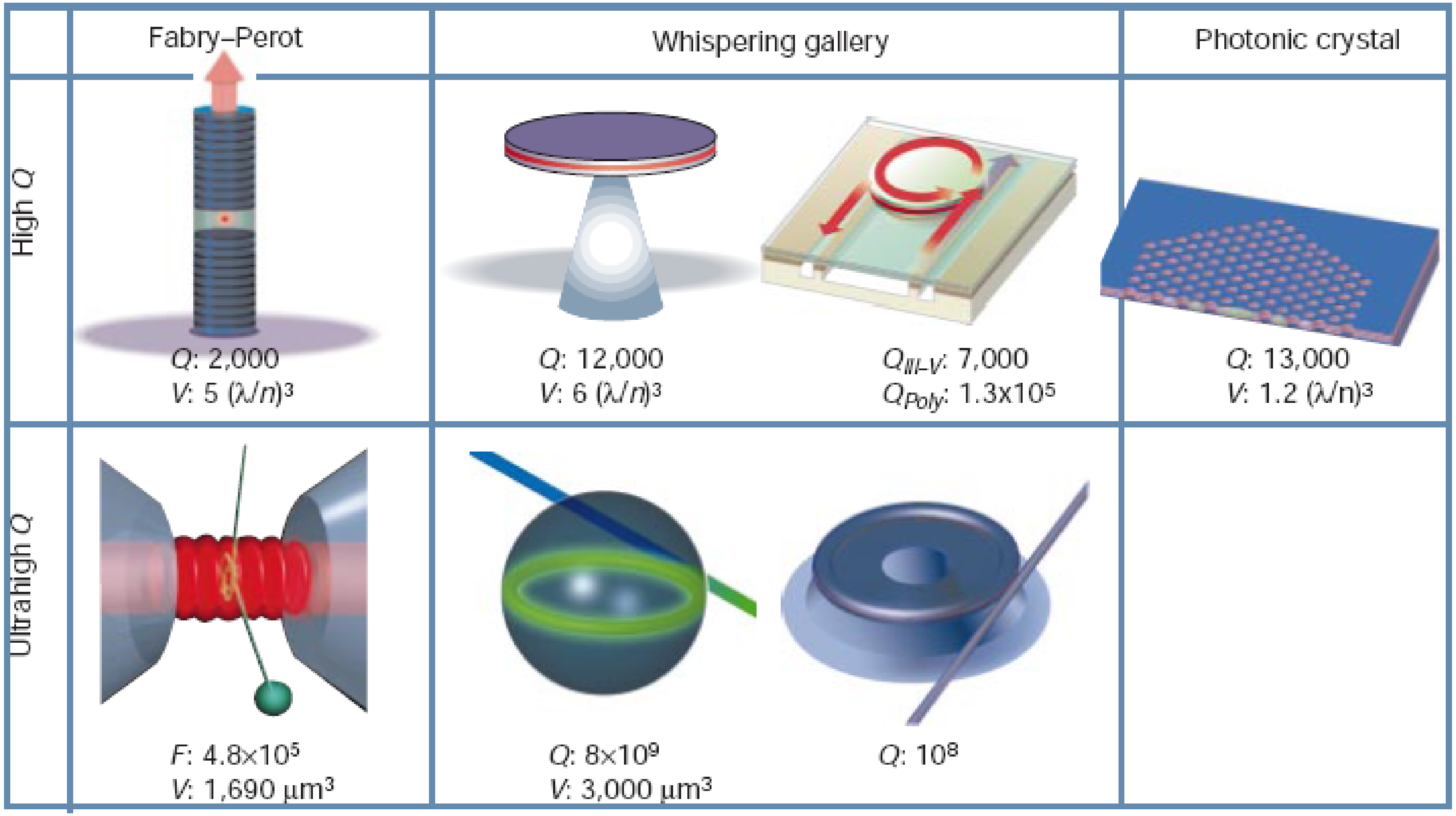

*K.J. Vahala // Nature **424**, 839 (2003)*

Optically active Er centers in Si matrixes.
Er implanted Si.

Er implantation:

ion energies : 320keV, 600keV (at room temperature) and 2 MeV (at 350°C)
doses: 10^{12}- 10^{15} cm^{-2} (Er concentrations 10^{17}- 10^{20} cm^{-3})

Subsequent annealing procedures:

600 °C – solid state epitaxy;
600°C + **900**°C;
one step annealing at **600** ÷ **1100°C** (in N_2 atmosphere)

Optically active Er-centers distinguished in Er-implanted Si

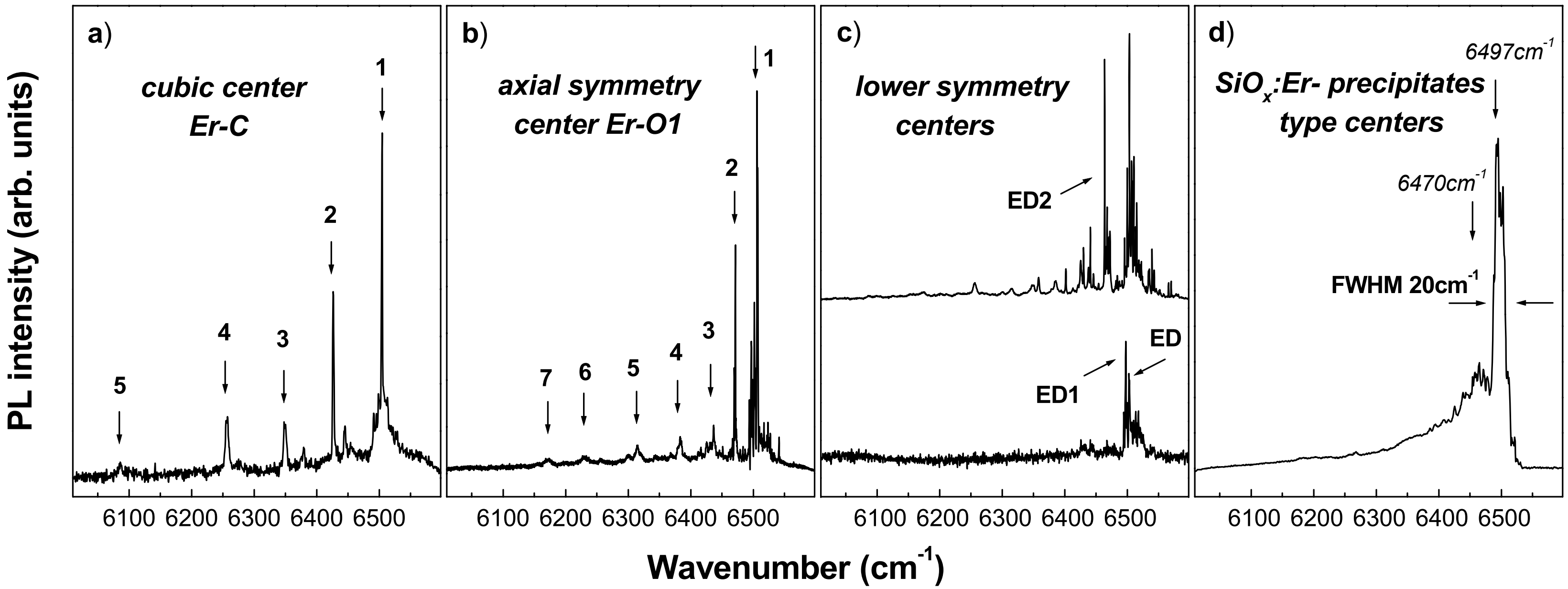

PL line pattern is a fingerprint of an Er center

M.V. Stepikhova et al., PhD thesis

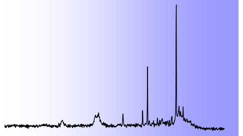

Parameters of $Si/Si_{1-x}Ge_x$:Er structures grown by the sublimation MBE in germane gas atmosphere

Sample parameters:

n-Si substrate /n-Si buffer/ n-$Si_{1-X}Ge_X$:Er /n-Si cap

$Si_{1-X}Ge_X$:Er layers:

$d_{SiGe:Er}$ = 0.01÷2.5 μm,
Ge content ≤ 35%,
RES = 0÷100%,
[Er] = $(0.1÷5)\cdot10^{18}$ cm^{-3},
[O] = $(2÷20)\cdot10^{18}$ cm^{-3}

X-ray diffraction and SIMS data

Sample #10-145
X_{Ge}=23%, RES=65%, $d_{SiGe:Er}$=0.15μm

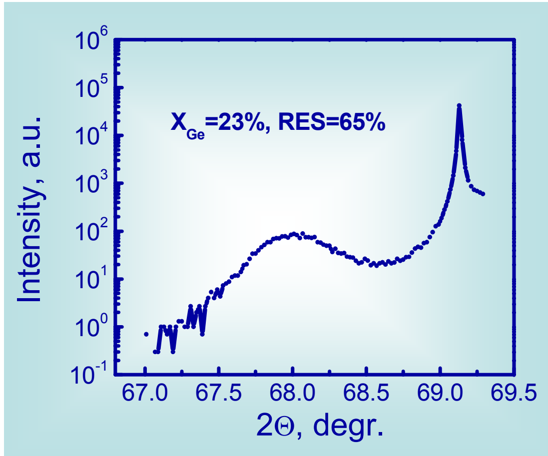

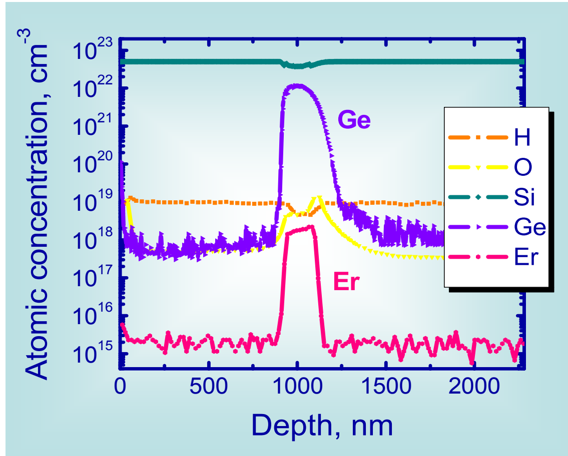

Sample #10-156
X_{Ge}=28%, RES=-9±10%, $d_{SiGe:Er}$=1.1μm

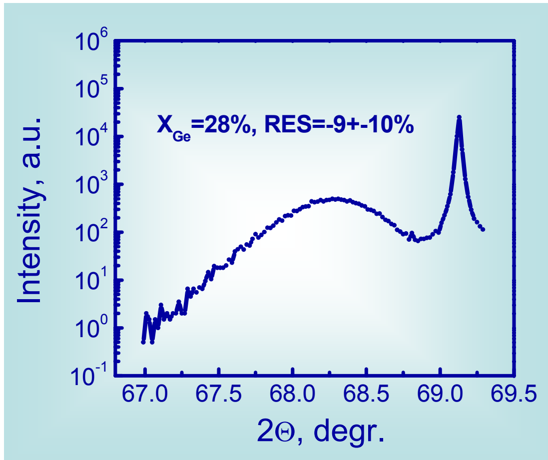

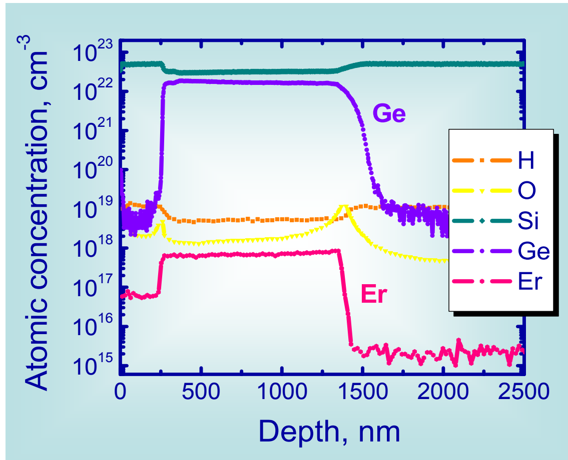

Si/$Si_{1-x}Ge_x$:Er structures grown by the sublimation MBE in germane gas atmosphere

TEM cross sectional images

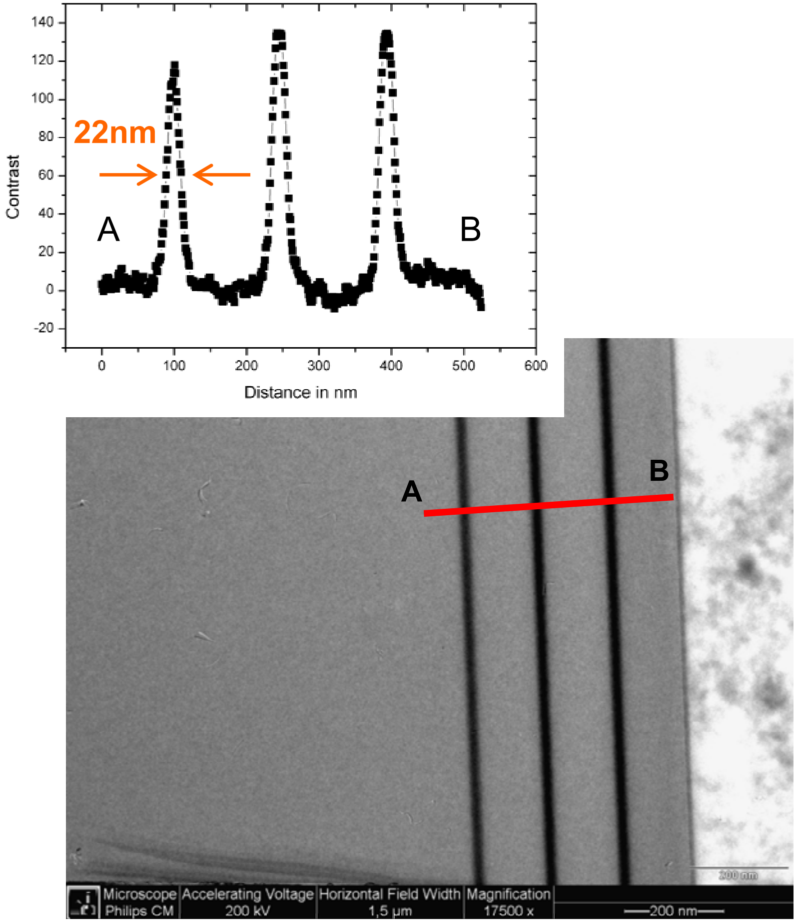

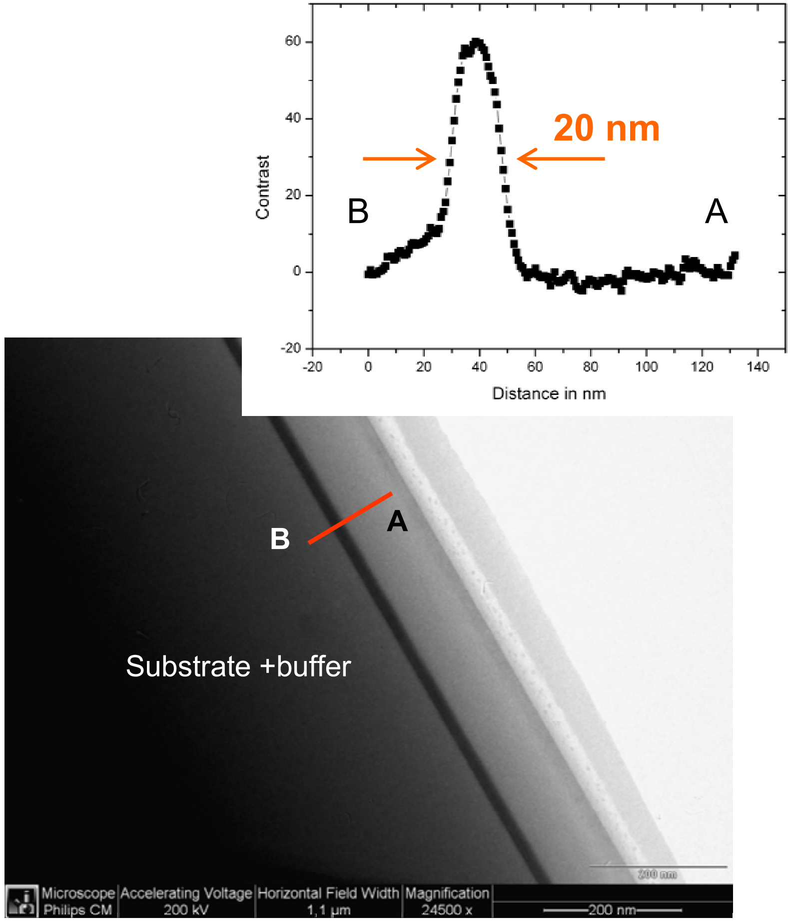

Measured by N. Zakharov, P. Werner, Max-Planck Institute of Microstructure Physics, Halle (Saale), Germany.

✓ Electro-optical storage on Si:Er basis

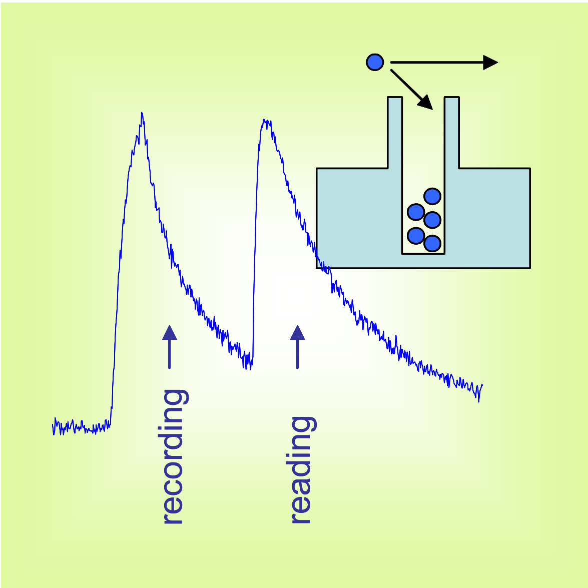

Electro-optical storage

Erasing
forward bias pulse,
or light pulse (λ < 1.06 μm)

Recording
100 ms at zero bias

Reading
reverse bias pulse

Erasing
low reverse bias pulse

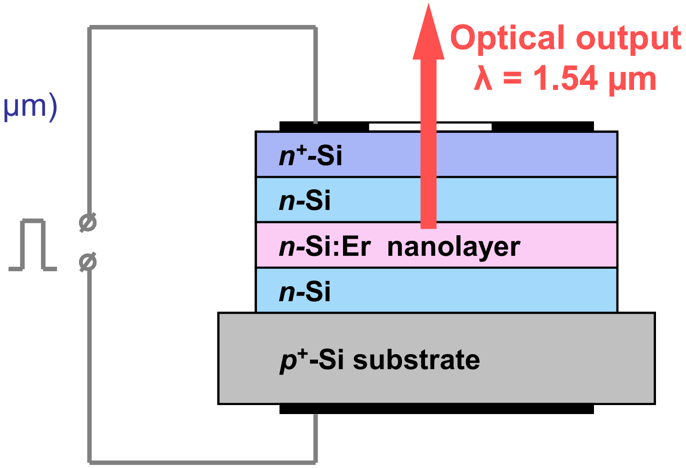

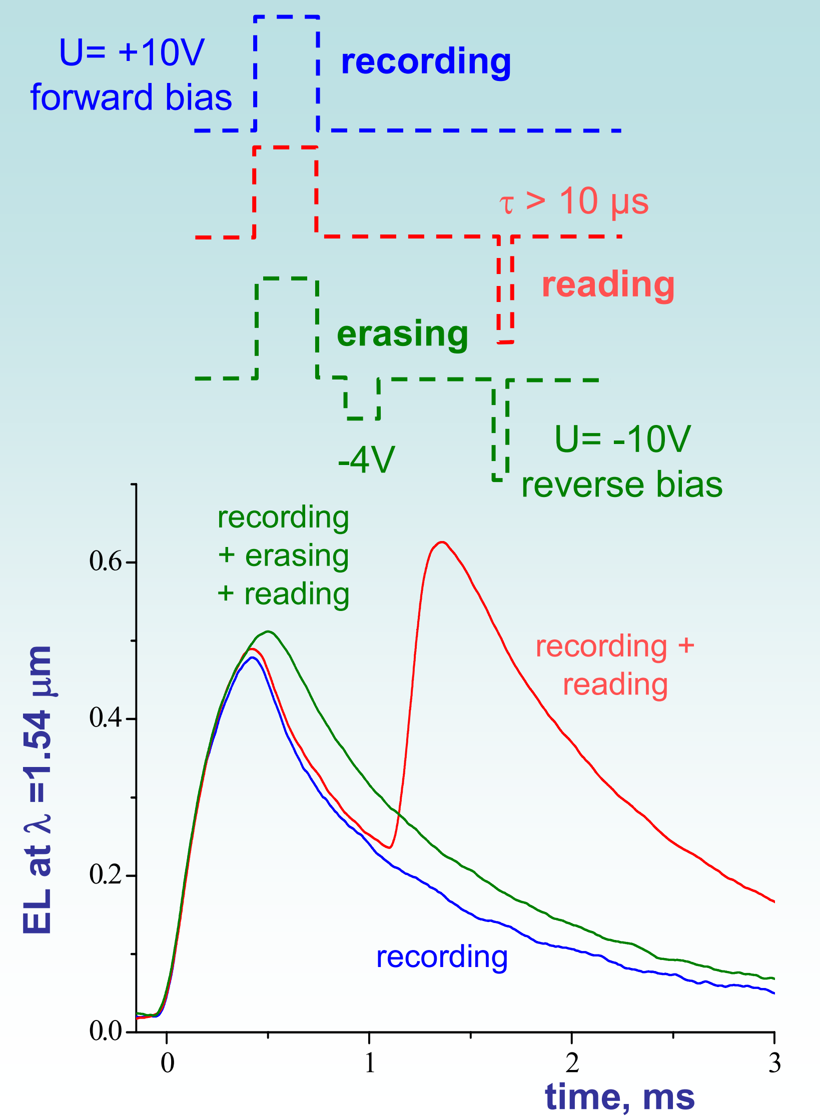

Structure parameters:

$n^+ = 6*10^{18}$ cm^{-3}
n = $2*10^{15}$ cm^{-3} , d = 10 mkm
Si:Er active layer, n ~ 10^{16} cm^{-3} , d = 70 nm
n = $2*10^{15}$ cm^{-3}, d = 1 mkm
substrate, $p^+ = 10^{17}$cm^{-3}

B.A. Andreev et al. Appl. Phys. Lett. (2006).
D.I. Kryzhkov et al. PCT Patent 2007/082329 (2007).

Electro-optical storage: principle of operation

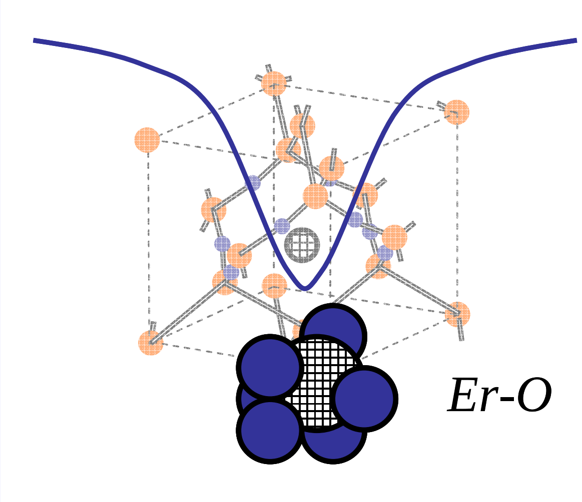

Er-O complex in Si matrix.

Such complex can result in the formation of some potential well in the Si band gap.

reading / erasing

Electrons localized in the potential well can be released by the application of an electric field. Free electrons will be accelerated by the electric field and after their energy reaches the value of 0.8 eV they will excite erbium ions.

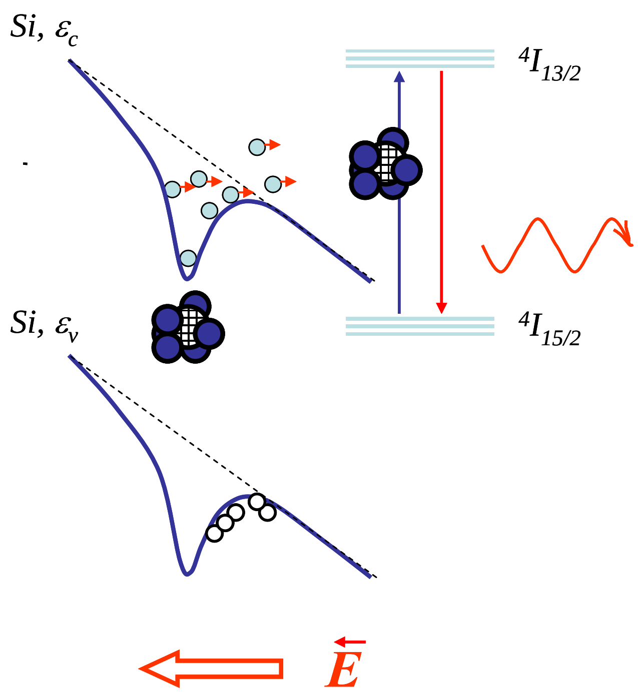

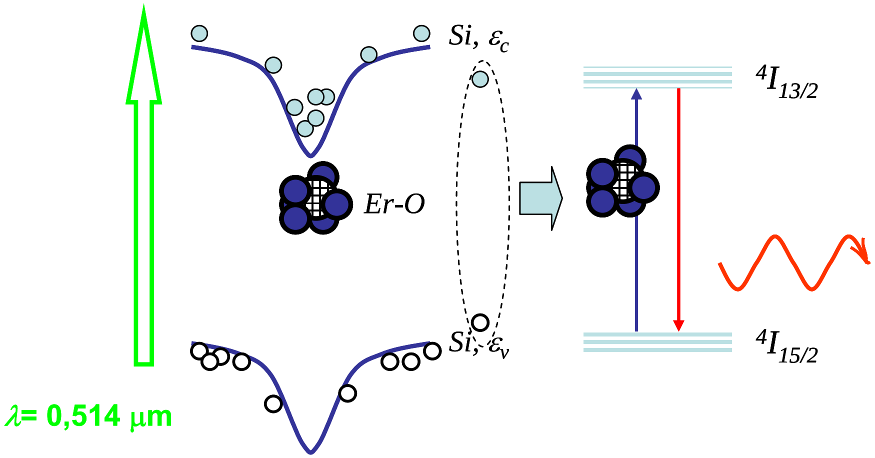

recording

A part of the e-h pairs generated by an argon laser can form the excitons and excite Er ions, whereas the another part can be trapped into the potential well in the band gap.

Optical confinement in a planar waveguide with the active $Si_{1-x}Ge_x$:Er layer

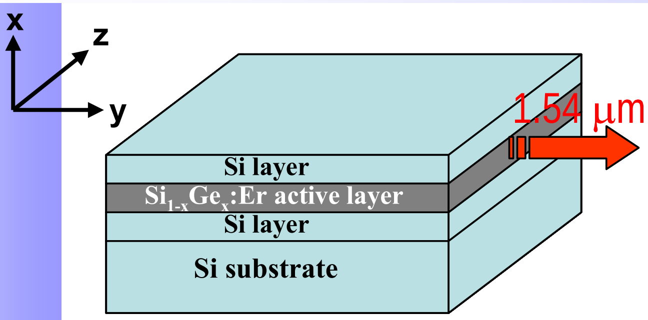

$$\nabla^2 \boldsymbol{E} + k^2 n_j \boldsymbol{E} = 0$$

$$\nabla^2 \boldsymbol{H} + k^2 n_j \boldsymbol{H} = 0$$

$$\Gamma = \frac{\int_0^d |E_y(x)|^2 dx}{\int_{-\infty}^{+\infty} |E_y(x)|^2 dx}$$

Optical mode distribution:

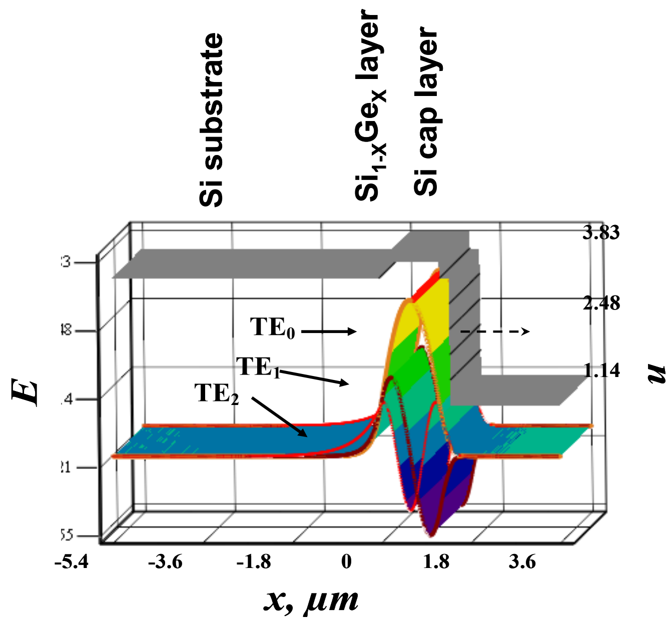

Si/$Si_{1-x}Ge_x$/Si structure: x_{Ge} = 60 %, $d_{SiGe:Er}$ = 1.2 µm, $d_{Si\text{-}cap}$ = 0.2 µm

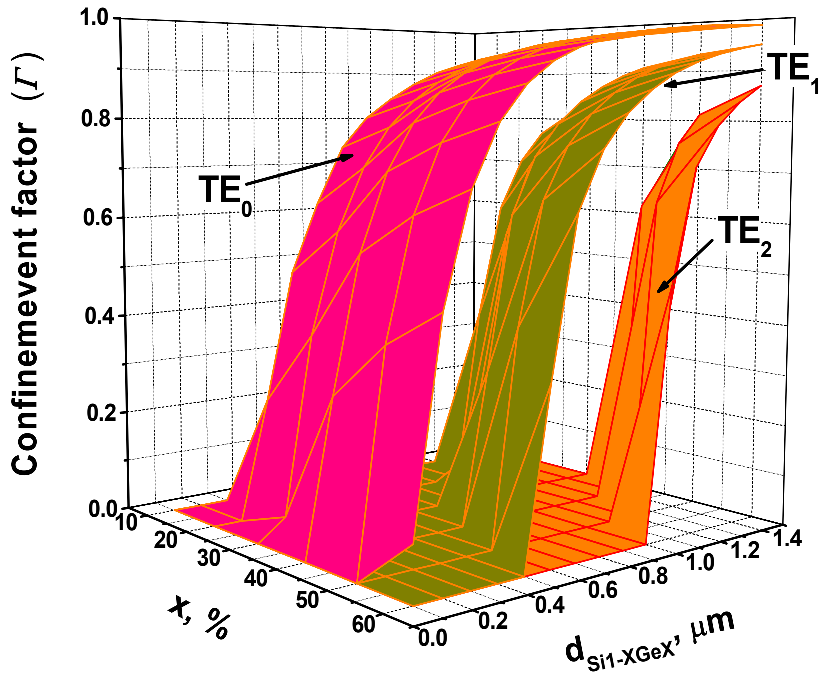

Depending on the Ge content refraction index of $Si_{1-x}Ge_x$ layers can be varied in high extend enabling the strong localization of the optical modes.

Optical confinement factor $\Gamma \rightarrow 0.98$

Z.F. Krasilnik et al., J. Mater. Res. (2006).

Ион Er^{3+}: уровни энергии и оптические переходы в 4f оболочке

Свободный ион Er^{3+}

$4d^{10}4f^{11}5s^{2}5p^{6}$

Energy levels for free Er^{3+} ion

	cm^{-1}	µm
$^4I_{15/2}$	0.0	0.0
$^4I_{13/2}$	6485	1.542
$^4I_{11/2}$	10123	0.988
$^4I_{9/2}$	12345	0.810
$^4F_{9/2}$	15182	0.659
$^4S_{3/2}$	18299	0.547
$^2H_{11/2}$	19010	0.526
$^4F_{7/2}$	20494	0.488
$^4F_{5/2}$	22181	0.451
$^4F_{3/2}$	22453	0.445

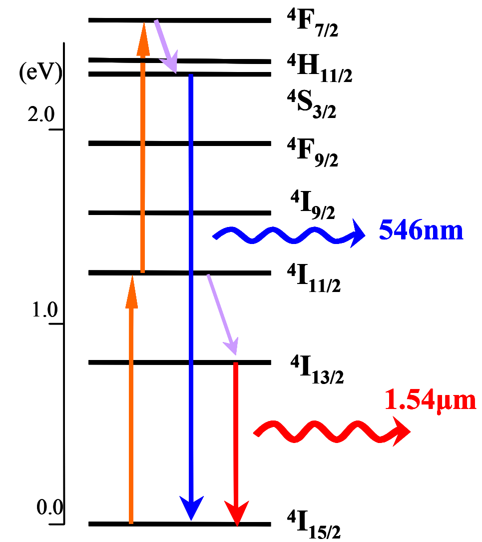

Ион Er^{3+} в кристаллическом поле

Расщепление мультиплетов иона Er^{3+} в кристаллическом поле